ABSTRACT

REDUCTION OF THE EDGE DIFFRACTION OF A CIRCULAR GROUND PLANE BY USING RESISTIVE EDGE LOADING

by

Rose Waikuen Wang

Chairman: Valdis V. Liepa

In many antenna measurements, a large flat circular conducting ground plane is a basic part of the measurement structure. To minimize the effects of edge diffraction, it is desirable to use as large a ground plane as possible. But in many instances this is not feasible due to the constraints imposed by structural limitations, such as mounting the antenna on a tower, or rotating the antenna on a pedestal to perform antenna pattern measurements. A large ground plane can also be cumbersome to use in laboratory where space is limited.

The task here is to develop a finite size ground plane for an antenna whose electromagnetic characteristics resemble those on an infinite ground plane, that is, the antenna impedance and the radiation patterns approach those on an infinite ground plane. The basic problem is to reduce the ground plane edge diffraction effects over a wide range of frequencies.

Specifically, the problem addressed is that of a monopole located at the center of a circular ground plane whose edges are extended using resistive sheet material. The antenna impedance, radiation patterns, and currents on the ground plane are studied.

The problem is formulated using the body of revolution technique and then solved numerically using the method of moments. Quantities studied for cases with and without resistive loading are the antenna impedances, the currents on the monopole and on the ground plane, and the far field patterns.

To verify the computations, a monopole antenna was built and evaluated with both metal and resistive ground planes. The resistive material was made by spraying resistive paints of different conductivities onto a non-conductive material base to obtain the desired resistance variation. Since the resistivity of the sprayed sheet can not be accurately predetermined, non-destructive methods are devised to measure local resistivity at both DC and microwave frequencies.

REDUCTION OF THE EDGE DIFFRACTION OF A CIRCULAR GROUND PLANE BY USING RESISTIVE EDGE LOADING

by

Rose Waikuen Wang

A dissertation submitted in partial fulfillment
of the requirements for the degree of
Doctor of Philosophy
(Electrical Engineering)
in The University of Michigan
1985

Doctoral Committee:

Associated Professor Valdis V. Liepa, Chairman
Professor William J. Anderson
Professor Chiao-Min Chu
Professor Chen-To Tai
Senior Research Scientist Dipak L. Sengupta

ACKNOWLEDGEMENTS

The author wishes to express her gratitude to all the members of her Doctoral Committee for their helpful comments and constructive criticisms. She is especially indebted to her Chairman, Professor Valdis V. Liepa, for his invaluable guidance and encouragement. Appreciation also goes to Mr. Larry Champney for his help with the experimental work.

Finally, the author wishes to thank her family for their encouragement, understanding and support during the course of this work.

TABLE OF CONTENTS

Page

LIST OF TABLES

LIST OF FIGURES

Figure		Page

LIST OF APPENDICES

CHAPTER I. INTRODUCTION

1.1 Background

In most antenna measurements, a highly conducting flat ground plane is a basic part of the measurement structure. Experimental work by Meier and Summers [1] indicates that a small ground plane may have appreciable effects on the measurements. It is often desirable to reduce and eliminate as much as possible the effects associated with the edges of a finite size ground plane and thus obtain the impedance and radiation characteristics of the antenna that would approach those when an infinite ground plane or a large ground plane is used.

The input impedance of a monopole at the center of a metallic circular ground plane has been studied experimentally by Meier and Summers [1]. Theoretically the problem was studied first by Bardeen [2]. He considered the problem of an antenna placed vertically at the center of a circular ground plane and obtained an integral equation for currents on the ground plane. However, he did not solve the equation except for the case when a ground plane is small in comparison with the wavelength.

Leitner and Spence [3] obtained a solution for this problem in the form of spheroidal functions. Unfortunately, however, the series converges very slowly for large radii ground planes, and thus, for the practical case of a ground plane greater than ten wavelengths in diameter, this approach is limited to general applications.

Storer [4,5] has solved the same problem using the variation method, and so did Fikioris [6]. Although, they both use a method that involves considerable complexity, no complete solution is applicable to ground planes of both small and large diameters.

Theoretical comparison by Thiele and Newhouse [7,8] using the geometrical theory of diffraction, showed good agreement with experiments for both the circular ground plane and an octagonal one. However, as the number of sides increases, their method for the octagonal ground plane would not converge to the circular ground plane case and results based on this approach would be in error. Green [9] used a different analysis for the variation of input impedance of the monopole above a circular ground plane as a function of ground plane radius. For his method, the experimental value of the average input impedance had to be used and this was added to the calculated variations.

Awadalla [10-12] made use of the fictitious edge current and the principle of magnetic ring current. His result is in good agreement with experiments for ground planes down to 0.6λ in diameter. When the same technique is applied to a radiation pattern, it is found that agreement is fairly good for large diameters, but poor when the diameters are small.

Recently, Griffin [13] reported on the experimental study of a monopole on a circular ground plane with microwave absorbent material placed around the perimeter of the ground plane. His experiment was based on only one grade of absorbent material, the same as that used to line anechoic chambers. Since the wedge-shaped microwave absorbent material foam on the ground plane near the wedges attenuates the outward travelling wave as the electric field and the current pass through, the reflected components, if such still remain, are also attenuated. In the edge treatment study presented here, a tapered resistive sheet is used instead, where the edge itself is made into an absorbing structure by changing uniformly the resistivity from zero ohms per square to a large value (approximately 1000 ohms per square) at the outer edge.

1.2 Outline of the Work

The task presented here is to develop a finite size ground plane whose electromagnetic characteristics on its surface and in the far field are approximate to those of an infinite size ground plane when excited by a monopole at the center. Specifically, the problem studied here is that of a monopole located at the center of a circular ground plane with resistive edge loading. The effect of such edge treatment on the impedance and the radiation patterns of the antenna are of special interest.

The problem is solved numerically by applying the method of moments to a suitable integral equation formulated for the surface of revolution. A computer program was developed to solve the currents on the monopole and the ground plane, for the antenna impedance, and for the far field patterns. The resistive sheet boundary condition is included and by choosing appropriate resistivity variation, the edge diffraction can be reduced over a wide range of frequencies. Using resistive paints, resistive sheet material was made whose resistivity can be varied by controlling the layers of paint applied and the choice of the conductivity of the paint. The antenna was then constructed and measurements were performed.

The concept of the resistive boundary condition and its inclusion in the formulation [14-17] is discussed in the remaining section of this chapter. Chapter II is devoted to a representation of the E-field equations and the method of moments technique. Chapter III deals with the body of revolution technique in conjunction with the method of moments. Integral equations are derived and adapted for numerical assessment. The making of the resistive sheets and their resistivity measurements are discussed in Chapter IV. Chapter V deals with experimental studies in which a model is built and measurements are made for the antenna impedance and the far field patterns. The numerical (computed) results for the current distribution and the antenna impedance as a function of frequency, antenna geometry, etc. are presented in Chapter VI along with some experimental data. A summary and the conclusions are provided in Chapter VII.

1.3 The Resistive Sheet Boundary Condition

A resistive sheet is characterized by three unique properties. It is infinitesimally thin, carries only the electric currents, and these are proportional only to the tangential component of the (total) electric field. Mathematically, a resistive sheet is characterized by a parameter R_s as follows

$$R_s = \lim_{\substack{\Delta \to 0 \\ \sigma \to \infty}} \frac{1}{\sigma \Delta} \tag{1.1}$$

where

R_s is the sheet resistivity (ohms/square)

σ is the conductivity of the material

Δ is the thickness of the material.

As Δ approaches to zero, σ will be increased in such a manner that R_s is finite and non-zero in the limit. The result is an idealized (infinitely thin) electric sheet whose electromagnetic properties are specified by the single measurable quantity R_s. This definition is applicable to a non-magnetic, conductive material whose thickness is small compared to the wavelength λ and the penetration depth δ .

The boundary conditions for an electrically resistive sheet of resistivity R_s are

$$\hat{n} \times (\bar{E}^{+} - \bar{E}^{-}) = 0 \tag{1.2}$$

$$\hat{n} \times (\bar{H}^{+} - \bar{H}^{-}) = \bar{J} \tag{1.3}$$

$$\hat{n} \times (\hat{n} \times \bar{E}^{\pm}) = - R_s \bar{J} \tag{1.4}$$

where

$\hat{n}$ is a normal unit vector from the sheet

$\bar{J}$ is the (total) electric current supported by the sheet.

Next, let

$$\bar{E}_t^i = \hat{t} E_t^i \tag{1.5}$$

$$\bar{J}_t = \hat{t} J_t \tag{1.6}$$

where

$\hat{t}$ is tangential unit vector in the sheet.

From Eq.(1.4) the resistive boundary condition on one side of the sheet becomes

$$E_t(\bar{R}) = R_s(\bar{R})J_t(\bar{R}) \tag{1.7}$$

$$E_t(\bar{R}) = E_t^i(\bar{R}) + E_t^s(\bar{R}) \tag{1.8}$$

$$E_t^i(\bar{R}) = R_s(\bar{R})J_t(\bar{R}) - E_t^s(\bar{R}) \tag{1.9}$$

where

E_t is the total electric field in the $\hat{t}$ direction

E_t^i is the incident field in the $\hat{t}$ direction

E_t^s is the scattered field in the $\hat{t}$ direction, and

J_t is the total current in the $\hat{t}$ direction.

Equation (1.9) expresses both the incident field and the scattered field in terms of resistivity R_s which need not be constant but can vary with the distance $\bar{R}$ in the sheet.

CHAPTER II. THEORETICAL BACKGROUND

2.1 Representation of the Electromagnetic Fields

The total electromagnetic field can be represented as the sum of scattered and incident fields. A time harmonic field with $e^{j\omega t}$ time variation suppressed is assumed, where $j = \sqrt{-1}$ and ω is the angular frequency. With the aid of electric and magnetic scalar potentials [33], the scattered field can be expressed by

$$\bar{E}^{s}(\bar{R}) = -j\omega\, \bar{A}(\bar{R}) - \nabla\Phi(\bar{R}) - \frac{1}{\varepsilon}\, \nabla \times \bar{A}^{*}(\bar{R}) \tag{2.1}$$

$$\bar{H}^{s}(\bar{R}) = -j\omega\, \bar{A}^{*}(\bar{R}) - \nabla\Phi^{*}(\bar{R}) + \frac{1}{\mu}\, \nabla \times \bar{A}(\bar{R}) \tag{2.2}$$

where the vector and scalar potentials are defined as

$$\bar{A}(\bar{R}) = \mu \iint_{s} \bar{J}(\bar{R}')G(\bar{R},\bar{R}')\, ds' \tag{2.3}$$

$$\bar{A}^{*}(\bar{R}) = \varepsilon \iint_{s} \bar{J}^{*}(\bar{R}')G(\bar{R},\bar{R}')\, ds' \tag{2.4}$$

$$\Phi(\bar{R}) = \frac{1}{\varepsilon} \iint_{s} \rho_{e}(\bar{R}')G(\bar{R},\bar{R}')\, ds' \tag{2.5}$$

$$\Phi^{*}(\bar{R}) = \frac{1}{\varepsilon} \iint_{s} \rho_{m}(\bar{R}')G(\bar{R},\bar{R}')\, ds' \tag{2.6}$$

and, they contain the free space Green's function

$$G(\bar{R},\bar{R}') = \frac{e^{-jkR}}{4\pi R} \tag{2.7}$$

where

$$R = \bar{R} - \bar{R}' = [\, r^2 + r'^2 - 2rr'\cos(\phi-\phi') + (z-z')\,]^{\frac{1}{2}}$$

The quantities ρ_e and ρ_m are the electric and the magnetic charge densities, respectively, and, are related to the surface currents through the continuity equation

$$\rho(\bar{R}') = \frac{j}{\omega}\,[\nabla\cdot\bar{J}(\bar{R}')] \tag{2.8}$$

2.2 The Method of Moments

2.2.1 General Procedure

The method of moments [18,19] is a numerical technique devised to solve the deterministic equation

$$L(f) = g \tag{2.9}$$

where L is a linear operator, g is known, and f is to be determined. Let f be expanded into a series of functions, f_1, f_2, f_3, f_4... in the domain of L as

$$f = \sum_n \alpha_n f_n \tag{2.10}$$

where the α_n are constants and the f_n are called expansion functions or basis functions. For exact solutions of f, Eq.(2.10) would be an infinite summation and the f_n would be required a complete set of basis functions. For approximate solutions, Eq.(2.10) is usually a finite summation. Substituting Eq.(2.10) into Eq.(2.9) and using the linearity property of L, one gets

$$\sum_n \alpha_n L(f_n) = g \tag{2.11}$$

A set of weighting functions or testing functions, $\{w_1, w_2, w_3 ..\}$ is then defined in the range of operator L. The inner product of Eq.(2.11) is taken with each w_m , the result is

$$\sum_n \alpha_n \langle w_m, Lf_n \rangle = \langle w_m, g \rangle \qquad m=1,2,3.... \tag{2.12}$$

This set of equations can be written in a matrix form as

$$[l_{mn}][\alpha_n] = [g_m] \tag{2.13}$$

where

$$[l_{mn}] = \begin{bmatrix} \langle w_1, Lf_1 \rangle & \langle w_1, Lf_2 \rangle & \cdots \\ \langle w_2, Lf_1 \rangle & \langle w_2, Lf_2 \rangle & \cdots \\ \cdots & \cdots & \cdots \\ \cdots & \cdots & \cdots \end{bmatrix} \tag{2.14}$$

$$[\alpha_n] = \begin{bmatrix} \alpha_1 \\ \alpha_2 \\ \cdot\cdot \\ \cdot\cdot \end{bmatrix} \tag{2.15}$$

$$[g_m] = \begin{bmatrix} \langle w_1, g \rangle \\ \langle w_2, g \rangle \\ \cdot\ \cdot\ \cdot\ \cdot \\ \cdot\ \cdot\ \cdot\ \cdot \end{bmatrix} \tag{2.16}$$

If the matrix $[l_{mn}]$ is non-singular, its inverse $[l_{nm}^{-1}]$ exists. The α_n are then given by

$$[\alpha_n] = [l_{nm}^{-1}]\ [g_m] \tag{2.17}$$

and the solution for f is given by Eq.(2.10). For a concise expression of the result, the transposed matrix of f is defined as

$$[\tilde{f}] = [\ f_1,\ f_2,\ f_3.\ .\ .\ .\ .\ ] \tag{2.18}$$

and, Eq.(2.10) can be written in matrix forms as

$$f = [\tilde{f}]\ [\alpha_n]$$

$$= [\tilde{f}]\ [l_{nm}^{-1}]\ [g_m] \tag{2.19}$$

This solution may be exact or approximate, depending upon the choice of f_n and w_n. The particular choice $f_n = w_n$ is known as the Galerkin's method (see Kantorovich and Krylov [20], Jones [21,22]) and is most often used in application of the method of moments to electromagnetic problems.

2.2.2 Point Matching

The integration involved in the evaluation of $l_{mn} = < w_m , Lf_n >$ in Eq.(2.14) is difficult to perform for problems of practical interest. A simple way to obtain approximate solutions is to require that Eq.(2.11) be satisfied at discrete points in the region of interest. This procedure is called the point-matching method, which is equivalent to using the Dirac Delta Functions as the testing functions.

2.2.3 Subsectional Bases

The method of subsections involves the use of basis function f_n, each of which exists only in a subsection in the domains of f. Then, each α_n of the expansion function in Eq.(2.10) affects the approximation of f only over a subsection of the region of interest. This procedures often simplifies the generation of the matrix $[l_{mn}]$. Thus, it is convenient in our computation to use point matching in conjunction with subsectional bases method.

2.3 Application of the Method of Moments to Solve the E-Field Equations

The problem is formulated as follows. Let $\bar{E}^i$ denote the impressed or the incident field and $\bar{E}^s$ the scattered field due to the currents and charges on the body. Then the total field $\bar{E}$ is the sum of the incident and the scattered fields, that is to say

$$\bar{E} = \bar{E}^i + \bar{E}^s \tag{2.20}$$

For a conducting surface S (R=0), the boundary condition requires that the total tangential component of $\bar{E}$ vanishes on S. Hence

$$\bar{E}^i_{tan} = - \bar{E}^s_{tan} \tag{2.21}$$

In the format of method of momemts, Eq.(2.21) can also be written as

$$L(\bar{J}) = \bar{E}^i_{tan} \tag{2.22}$$

From Eq.(2.1)

$$L(\bar{J}) = (j\omega\bar{A} + \nabla\Phi)_{tan} \tag{2.23}$$

which follows from Eq.(2.1) and Eq.(2.21).

In Eq.(2.23), L is an integro-differential operator and a subscript "tan" denotes the tangential component on S.

A solution of Eq.(2.22) gives the surface current J on S.

Next, let the inner product of two arbitrary tangential vectors on S be defined by

$$< \overline{F} \, , \, \overline{G} > = \iint_S \overline{F} \cdot \overline{G} \, ds \qquad (2.24)$$

A set of expansion functions $\{\overline{J}_j\}$ is next defined for the expansion of currents on S by

$$\overline{J} = \sum_j I_j \, \overline{J}_j \qquad (2.25)$$

where I_j are constants to be determined. Because of the linearity property of L, when Eq.(2.25) is substituted into Eq.(2.22), it becomes

$$\sum_j I_j \, L(\overline{J}_j) = \overline{E}^{i}_{tan} \qquad (2.26)$$

A set of testing function $\{W_i\}$ is defined, and an inner product of Eq.(2.26) with each W_i is taken. This results in

$$\sum_j I_j <\overline{W}_i , \, L\overline{J}_j> = <\overline{W}_i , \, \overline{E}^{i}_{tan}> \qquad i=1,2,3.... \qquad (2.27)$$

For convenience and shorter representation, definitions from the circuit theory are introduced and the network matrices are defined as

$$[Z] = [\langle \overline{W}_i, L\overline{J}_j \rangle] \tag{2.28}$$

$$[V] = [\langle \overline{W}_i, \overline{E}^{i}_{tan} \rangle] \tag{2.29}$$

$$[I] = [I_i] \tag{2.30}$$

Eq.(2.27) then becomes

$$[Z]\ [I] = [V] \tag{2.31}$$

The excitation matrix [V] is obtained from Eq.(2.29). It is either an incident field as in the case of scattering problems or a local source coordinate as in the case of radiation problems.

In the radiation problem considered here, the term $\langle \overline{W}_i, \overline{E}^{i}_{tan} \rangle$ in Eq.(2.29) is replaced by V_i/d, where V_i is the locally generated voltage applied over a small gap centered at point i and d is the gap width.

Now [Z] can be considered as a generalized impedance matrix. The impedance elements of Eq.(2.28) are explicitly given by

$$Z_{ij} = \iint_S \overline{W}_i \cdot (j\omega A_j + \nabla \Phi_j)\ ds' \tag{2.32}$$

which follows from equations (2.23) and (2.24).

Applying the Divergence theorem to the vector $\overline{W}_i\Phi$ on the surface, the following results

$$\iint_S \nabla\Phi \cdot \overline{W}_i \, ds' = -\iint_S \Phi\nabla \cdot \overline{W}_i \, ds' \tag{2.33}$$

and Eq.(2.32) can now be written as

$$Z_{ij} = \iint_S (j\omega \, \overline{W}_i \cdot \overline{A}_j - \Phi_j\nabla \cdot \overline{W}_i) \, ds' \tag{2.34}$$

Because the gradient of Φ has been eliminated in Eq.(2.32), Eq.(2.34) is now in a more convenient form for numerical evaluation.

CHAPTER III. BODY OF REVOLUTION TECHNIQUES

3.1 Introduction

In this section, the formulation of the integral equations and the application of method of moments to the proposed problem are discussed using the body of revolution techniques.

The body of revolution (BOR) geometry is the characteristic of many physical structures, such as rockets, missiles, satellites, raindrops and many types of biological cells. This method has the advantage of enabling one to apply the method of moments to three-dimensional structures which are fairly large with respect to the wavelength, yet requires only a fraction of the unknowns to be determined, as compared to a general three-dimensional method of moments formulation.

Several authors have presented the techniques for treating problems involving radiation and scattering by perfectly conducting BOR. Andreasen [23], and, Mautz and Harrington [24 through 27] have employed the electric field integral equation (EFIE), whereas, Oshiro, Mitzner [28] and Uslenghi [29] have used the magnetic field integral equation (MFIE). Several extensions and refinements of the basic techniques of these authors have also been developed.

Recently, Glisson and Wilton [30,31] presented techniques which appear to have alleviated some difficulties previously encountered by others in the treatment of perfectly conducting and dielectric bodies of revolution. Their techniques are being adapted here.

A special case of a body of revolution is a surface of revolution (SOR). Here, instead of determining the currents and charges throughout a body, they are determined on the surface only. The resistive sheet boundary conditions can thus be applied to the surface of revolution geometry, which may be closed (such as a spherical shell) or open (such as a coffee cup).

Any line S revolving about the z axis will generate a surface of revolution geometry. Thus an antenna geometry of a monopole located at the center of the circular ground plane can be generated as a surface of revolution as shown in Fig.(3.1). Using the method of moments, the currents on the antenna and on the ground plane, the input impedance, and the far field patterns can be computed.

3.2 Application of the Method of Moments (MOM)

3.2.1 Evaluation of the MOM Impedance Matrix

Consider a surface S generated by revolving a line about the z axis. The coordinate system is shown in Fig.(3.1). Here ρ,ϕ,z are the usual cylindrical coordinate variables, and, t is the length variable along the

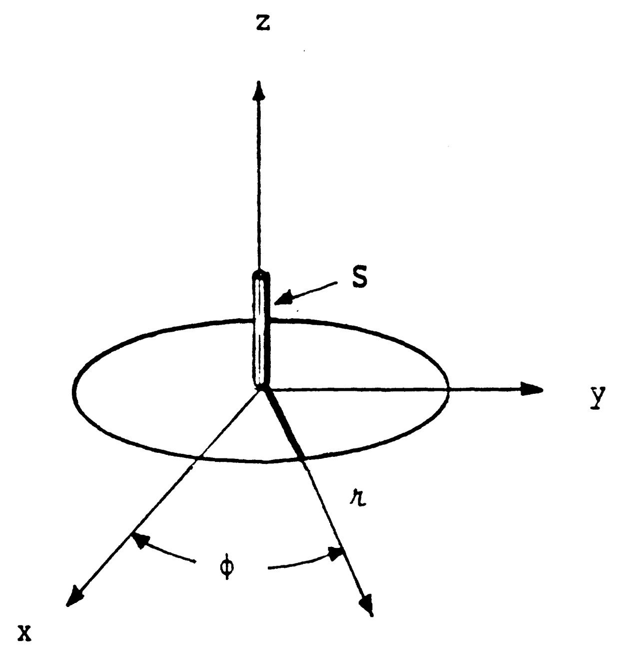

Fig. 3.1 A line S Rotated about the Z-Axis Generates a Monopole Antenna on the Circular Ground Plane.

generating curve S. In general, the independent set of expansion functions of the $\bar{J}(t,\phi)$ on S [30] are defined as

$$\bar{J}(t) = \hat{t} \sum_{n=1}^{N} (r_n J_t^n) P_1^n(t') + \hat{\phi} \sum_{n=1}^{N+1} J_\phi P_2^n(t') \qquad (3.1)$$

where

$$P_1^n(t') = \begin{cases} 1, & t_{n-\frac{1}{2}} \leqq t' \leqq t_{n+\frac{1}{2}} \\ 0, & \text{Otherwise} \end{cases} \qquad (3.2)$$

$$P_2^n(t') = \begin{cases} 1, & t_{n-1} \leqq t' \leqq t_n \\ 0, & \text{Otherwise} \end{cases} \qquad (3.3)$$

For the problem studied here, there is no ϕ dependence, and hence the second term in Eq.(3.1) involving J_ϕ vanishes. The charge distribution is obtained from the derivatives of J_t with respect to t (c.f. Eq.(2.8)) and these can be approximated by

$$\frac{d}{dt} [\bar{J}_t(t')] = \sum_{n=1}^{N+1} \frac{\bar{J}_t^n - \bar{J}_t^{n-1}}{t_n - t_{n-1}} P_2^n(t') \qquad (3.4)$$

where

$$|t_n - t_{n-1}| = \Delta t_n = [(r_n - r_{n-1})^2 + (z_n - z_{n-1})^2]^{\frac{1}{2}} \qquad (3.5)$$

It is assumed that at the edges, the current J_t is zero, that is

$$\bar{J}_t^{o} \equiv \bar{J}_t^{N+1} \equiv 0 \tag{3.6}$$

Since each t_n is common to two linear adjoining segments, it is convenient to approximate the incident field and the vector potential by their values at $t_n = t$, Fig.(3.2). Integration of Eq.(3.2) in the variable t yields

$$\int_t P_1^q(t)\ \hat{t}\cdot\bar{U}(t)dt = \int_{t_{q-\frac{1}{2}}}^{t_q} \hat{t}\cdot\bar{U}(t)dt + \int_{t_q}^{t_{q+\frac{1}{2}}} \hat{t}\cdot\bar{U}(t)dt$$

$$= \frac{1}{2}\left(\Delta t_q \hat{t}_{q-\frac{1}{2}} + \Delta t_{q+1}\hat{t}_{q+\frac{1}{2}}\right)\bar{U}(t_q) \tag{3.7}$$

where $\bar{U}$ is the vector quantity tested and $\hat{t}_{q-\frac{1}{2}}$ is the unit vector describing the orientation of linear segments containing the points t_{q-1} and t_q .

The testing functions are defined as

$$W_1(t) = \delta_1(t) \tag{3.8}$$

$$W_2(t) = \delta_2(t) \tag{3.9}$$

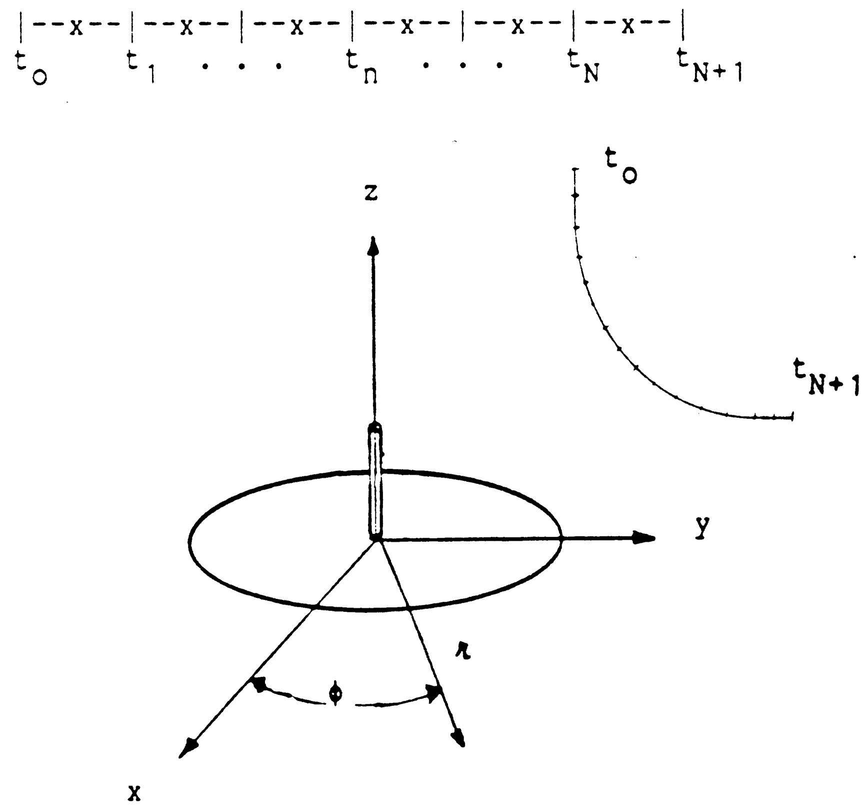

Fig. 3.2 Approximating of Generating Arc by Linear Segments for Strip of Revolution.

where

$$\delta_1(t) = \begin{cases} 1 , & t = t_q \\ 0 , & \text{otherwise} \end{cases} \tag{3.10}$$

$$\delta_2(t) = \begin{cases} 1 , & t = t_{q-\frac{1}{2}} \\ 0 , & \text{otherwise} \end{cases} \tag{3.11}$$

Substituting Eqs.(2.4), (2.8) and (2.33) into Eq.(2.34), one gets

$$Z_{ij} = \iint_S ds' \iint_S ds [j\omega \overline{W}_i \cdot \overline{J}_j + \frac{1}{j\omega\varepsilon} (\nabla \cdot \overline{W}_i)(\nabla \cdot \overline{J}_j)] \frac{e^{-jkR}}{4\pi R} \tag{3.12}$$

Note, for body of revolution, in general

$$\iint_S ds = \int_0^N dt \int_0^{2\pi} \rho(t) \, d\phi \tag{3.13}$$

An orthogonal triad of unit vectors ($\hat{n}$, $\hat{\phi}$, $\hat{t}$) can be associated with each coordinate point ($\hat{t}$, $\hat{\phi}$) where $\hat{n}$, $\hat{\phi}$, $\hat{t}$ are defined as follows:

$$\hat{n} = \cos\gamma \cos\phi \, \hat{x} + \cos\gamma \sin\phi \, \hat{y} - \sin\gamma \, \hat{z} \tag{3.14}$$

$$\hat{\phi} = - \sin\phi \, \hat{x} + \cos\phi \, \hat{y} \tag{3.15}$$

$$\hat{t} = \sin\gamma \cos\phi \, \hat{x} + \sin\gamma \sin\phi \, \hat{y} + \cos\gamma \, \hat{z} \tag{3.16}$$

where γ is the angle between the tangent to the generating curve t and the z axis, defined to be positive if t points away from the z axis and negative if t points towards the z axis. In this coordinate system, the surface divergence becomes

$$\nabla \cdot \bar{J} = \frac{1}{\rho} \frac{\partial}{\partial t}(\rho J_t) + \frac{1}{\rho} \frac{\partial}{\partial \phi}(J_\phi) \tag{3.17}$$

and R becomes

$$R = \{\rho^2 + \rho'^2 - 2\rho\rho' \cos(\phi-\phi') + (z-z')^2\}^{\frac{1}{2}} \tag{3.18}$$

To obtain the $\bar{W} \cdot \bar{J}$ term in Eq.(3.12), one writes

$$\bar{W}_i \cdot \bar{J}_j = \hat{u}_p \cdot \hat{u}_q \tag{3.19}$$

where p and q represent the permutation of t and ϕ. The unit vector dot products, in terms of body coordinates $(\hat{n}, \hat{\phi}, \hat{t})$ are

$$\hat{u}_{t'} \cdot \hat{u}_t = \sin\gamma \sin\gamma' \cos(\phi-\phi') + \cos\gamma \cos\gamma' \tag{3.20}$$

$$\hat{u}_{t'} \cdot \hat{u}_\phi = -\sin\gamma' \sin(\phi-\phi') \tag{3.21}$$

$$\hat{u}_{\phi'} \cdot \hat{u}_t = \sin\gamma \sin(\phi-\phi') \tag{3.22}$$

$$\hat{u}_{\phi'} \cdot \hat{u}_{\phi} = \cos(\phi-\phi') \tag{3.23}$$

For a resistive surface in operator form Eq.(1.9) becomes

$$\bar{E}_t^i = Z_{ij}\,[\bar{J}_t(\bar{R}')] + R_s(\bar{R}')\,\bar{J}_t(\bar{R}') \tag{3.24}$$

where

$$\begin{aligned}\bar{E}_t^i = \;& jkZ_o \iint_s \bar{J}(\bar{R}')\,G(\bar{R},\bar{R}')\,ds' \\ & - \frac{jZ_o}{k}\,\frac{\partial}{\partial t}\iint_s \frac{1}{\rho'}\,\frac{\partial}{\partial t'}(\rho'\,\bar{J}(\bar{R}'))\,G(\bar{R},\bar{R}')\,ds' \\ & + R_s(\bar{R}')\,\bar{J}_t(\bar{R}')\end{aligned} \tag{3.25}$$

It is desirable to express all the quantities of Eq.(3.25) in terms of local arc coordinates ($\hat{t}$, $\hat{\phi}$) on the body surface. Thus, Eq.(3.25) is written

$$\begin{aligned}\bar{E}_t^i = \;& jkZ_o \iint_s \bar{J}_t[\sin\gamma\sin\gamma'\cos(\phi-\phi')+\cos\gamma\cos\gamma']G\,ds' \\ & - \frac{jZ_o}{k}\,\frac{\partial}{\partial t}\iint_s \frac{1}{\rho'}\,\frac{\partial}{\partial t'}(\rho'\,\bar{J}_t)\,G\,ds' \\ & + R_s(\bar{R}')\,\bar{J}_t(\bar{R}')\end{aligned} \tag{3.26}$$

where

$$G(\bar{R},\bar{R}') = \frac{e^{-jkR}}{4\pi R} \qquad (3.27)$$

and

$$R = \bar{R} - \bar{R}' = [\, r^2 + r'^2 - 2rr'\cos(\phi-\phi') + (z-z')]^{1/2}$$

After some manipulation of Eq.(3.26), the impedance matrix such as Eq.(3.24) can be written as

$$\begin{aligned}
Z_{ij} = R_j &+ \frac{jkZ_o}{4\pi} \sin\gamma_i \; \chi_s(\Delta t_j,\gamma_j)[K_1(t_{i-1/2},\, t_i;\, t_j)] \\
&+ \frac{jkZ_o}{4\pi} \sin\gamma_{i+1} \; \chi_s(\Delta t_j,\gamma_j)[K_1(t_i,\, t_{i+1/2};\, t_j)] \\
&+ \frac{kZ_o}{4\pi} \cos\gamma_i \; \chi_c(\Delta t_j,\gamma_j)[K(t_{i-1/2},\, t_i;\, t_j)] \\
&+ \frac{kZ_o}{4\pi} \cos\gamma_{i+1} \; \chi_c(\Delta t_j,\gamma_j)[K(t_i,\, t_{i+1/2};\, t_j)] \\
&+ \frac{Z_o}{4\pi k\Delta t_i} [K(t_{i-1},\, t_i;\, t_{j+1/2}) - K(t_{i-1},\, t_i;\, t_{j-1/2})] \\
&- \frac{Z_o}{4\pi k\Delta t_{i+1}} [K(t_i,\, t_{i+1};\, t_{j+1/2}) - K(t_i,\, t_{i+1};\, t_{j-1/2})]
\end{aligned} \qquad (3.28)$$

where

$$K_1(t_1,\, t_2;\, t_j) = \int_{t_1}^{t_2} G_1(t_j,t')\, dt' \qquad (3.29)$$

$$K\,(t_1,\, t_2;\, t_j) = \int_{t_1}^{t_2} G_o(t_j, t')\, dt' \tag{3.30}$$

$$G_1 = \int_{-\pi}^{\pi} \frac{e^{-jkR}}{R} \cos(\phi-\phi')\, d\phi' \tag{3.31}$$

$$G_o = \int_{-\pi}^{\pi} \frac{e^{-jkR}}{R}\, d\phi' \tag{3.32}$$

$$\chi_s(\Delta t_j, \gamma_j) = (\Delta t_{j+1} \sin\gamma_{j+1} + \Delta t_j \sin\gamma_j)/2 \tag{3.33}$$

$$\chi_c(\Delta t_j, \gamma_j) = (\Delta t_{j+1} \cos\gamma_{j+1} + \Delta t_j \cos\gamma_j)/2 \tag{3.34}$$

and i is the field point index

j is the source point index.

The matrix $[Z]_{ij}$ is the required MOM matrix to be evaluated. There are eight integrals to be evaluated in Eq.(3.28), which are basically the integration of the Green's functions for a given source and observation points. These integrals are defined in Eq.(3.29) and Eq.(3.30). Having the impedance matrix $[Z]_{ij}$ and given the excitation matrix [V], the current matrix [I] can be computed using the Gaussian elimination method. The current computed can then be used to evaluate the antenna impedance and the far field patterns.

3.2.2 Evaluation of the Antenna Impedance

The input impedance, Z_{in}, of an antenna is the impedance presented by the antenna at its terminals.

In computation for the currents on the antenna one volt (rms) is applied across the gap and the impedance is determined from the equation

$$V_{in} = I_{in} Z_{in} \tag{3.35}$$

The current I_{in} is defined as the total current at the input gap and is related to the current density J_t by

$$I_{in} = 2 \pi \textit{r} J_t \tag{3.36}$$

Thus, the input impedance of the monopole antenna is

$$Z_{in} = \frac{V_{in}}{2 \pi \textit{r} J_t} \tag{3.37}$$

3.2.3 Evaluation of the Far Field

The scattered far field is an integral over the surface currents and can be written in the form

$$\bar{E}^s = A \iint_s \bar{J}(\bar{R}') \frac{e^{-jkR}}{R} ds' \tag{3.38}$$

where

A is a constant

and

$$R = |\overline{R} - \overline{R}'|$$

is the distance between a surface point R' and the far field observation point R.

If the body is finite so that R is much greater than any of the body dimensions, then

$$\overline{E}^s = \frac{Ae^{-jkR}}{R} \iint_s \overline{J}(\overline{R}')\, e^{-jk\hat{R}\cdot\overline{R}'} ds' \tag{3.39}$$

In terms of local arc coordinates ($\hat{t}$, $\hat{\phi}$) on the body surface, the dot products applicable to Eq.(3.12) are given by

$$\hat{u}_t \cdot \hat{u}_\theta = \cos\theta\sin\gamma\cos\phi - \sin\theta\cos\gamma \tag{3.40}$$

$$\hat{u}_\phi \cdot \hat{u}_\theta = -\cos\theta\sin\phi \tag{3.41}$$

Then Eq.(3.39) becomes

$$\overline{E}_t^s = \frac{A}{R} \iint_s \overline{J}_t[\cos\theta\sin\gamma\cos\phi - \sin\theta\cos\gamma] e^{jk(r\sin\theta\cos\phi + z\cos\theta)} ds' \tag{3.42}$$

Using the integral representation for the Bessel function

$$J_m(r) = \frac{j^m}{2} \int_0^{2\pi} e^{-jr\cos\phi}\, e^{-jm\phi}\, d\phi \tag{3.43}$$

one can analytically evaluate the ϕ integration in Eq.(3.43), which results in

$$\bar{E}_t^s = \frac{A}{R} \int \rho \bar{J}_t e^{jkz\cos\theta}[\, j\cos\theta\sin\gamma J_1 - \sin\theta\cos\gamma J_o] \, dt' \tag{3.44}$$

where

$J_m = J_m(k\rho\sin\theta)$

and J_o = the Bessel function of 1st kind, 0th order

J_1 = the Bessel function of 1st kind, 1st order.

After the currents are evaluated using the method of moments and the body of revolution technique, it is a relatively straightforward task to compute the far field patterns from Eq.(3.44).

Rewriting Eq.(3.38) in matrix form and dotting with $\hat{u}$ to obtain a (scalar) transverse component, one gets the following

$$\bar{E}^s \cdot \hat{u} = -A' \frac{j\omega\mu}{4\pi R} e^{-jkR}[Z][I] \tag{3.45}$$

where

$$[Z]_n = 2\pi j \int \rho\delta_n(t) e^{jkz\cos\theta}[\cos\theta\sin\gamma\, J_1 + j\sin\theta\cos\gamma J_0] \, dt' \tag{3.46}$$

In Eq.(3.45), A' is a constant and $\delta_n(t)$ are delta functions defined in Eqs.(3.10), (3.11).

After some manipulation, the impedance matrix can be written as

$$[Z]_n = 2\pi\ [jJ_1\cos\theta\chi_s - J_o\ \sin\theta\chi_c]\ e^{jkz\cos\theta} \tag{3.47}$$

where

$$\chi_s(\Delta t_n, \gamma_n) = (\Delta t_{n+1}\sin\gamma_{n+1} + \Delta t_n\ \sin\gamma_n)/2$$

$$\chi_c(\Delta t_n, \gamma_n) = (\Delta t_{n+1}\cos\gamma_{n+1} + \Delta t_n\ \cos\gamma_n)/2$$

with n being the source segment index.

Equation (3.47) requires essentially the evaluation of the zeroth-order and the first-order Bessel functions of the first kind. Since the unknown current distribution [I] is found by solving the MOM impedance matrix $[Z]_{ij}$ of Eq.(3.28), the far field patterns can be evaluated using Eq.(3.45) where $[Z]_n$ is obtained from Eq.(3.46).

CHAPTER IV. RESISTIVE MATERIALS AND MEASUREMENTS

4.1 Introduction

The effects of edge diffraction can usually be reduced by adding absorbent materials around the edge, corrugating the edge or a combination of both. The latter would probably be more effective. Tapered resistive sheets are studied here primarily because the approach is new and it shows a lot of promise. Since the resistive sheets are not readily available and usually have to be custom made for a particular application, techniques are developed to make them in the laboratory, which consists of spraying resistive paints on plastic or other types of nonconducting base materials. The conductivity of the paint can be varied by mixing different paints in various proportions. The resistivity of the sheet can be controlled by the paint used and the layers of the paint applied. In this chapter, the making of resistive sheets is discussed. The properties of different types of paints are tabulated. The results of mixing different paints (by weight) and the effects on the sheet resistivity are plotted. Methods are devised to measure the resistivities of the sheets at DC and at microwave frequencies to determine if the resistivity of the sheets remains constant over the frequency range of interest.

4.2 Resistive Materials

Thin resistive materials can be made by spraying resistive paints on plastic or paper material (Kimura [32]). The resistive paints contain finely processed carbon particles plus a bonding resin and solvent. The resistivity of the finished product can be controlled by selecting appropriate ratios of different types of paints to be mixed (Fig.(4.4) through Fig.(4.6)), the number and thickness of the coatings applied (Fig.(4.1) and Fig.(4.2)), and the drying time (type of solvent and temperature) as well as the type of the base material (Fig.(4.3)).

For our study, lacquer base paints were chosen because they are easier to mix and can be redissolved even after drying. Also, lacquer thinner is readily available and can be used to clean the spraying equipment.

The paints used were Electrodag®109, 110, 415 and 502. Their properties are summarized in Table (4.1). These paints can be directly applied by brush, dip or spray methods. The latter requires dilution with solvent. An air-brush was used to produce smooth and uniform coatings (c.f. Fig.(4.7)). To obtain the required spray consistency and eventual sheet material resistivity requires a lot of patience and practice. Paint thickness, air pressure,

---

Electrodag® is the trademark of Acheson Colloid Company, Port Huron, Michigan. 48060

Paint Type	Pigment	Density	Solvent	Resistance* Ohms/sq.
Electrodag 109	Graphite	1.025 Kg/ℓ	Lacquer thinner	Less than 30
Electrodag 110	Graphite	0.98 Kg/ℓ	Lacquer thinner	1.5-2.5K
Electrodag 415	Silver	1.7 Kg/ℓ	Lacquer thinner	Less than 0.1
Electrodag 502	Graphite	0.82 Kg/ℓ	Lacquer thinner	Less than 250

*0.001 inch Coating

Table 4.1 The Properties of Paints Used.

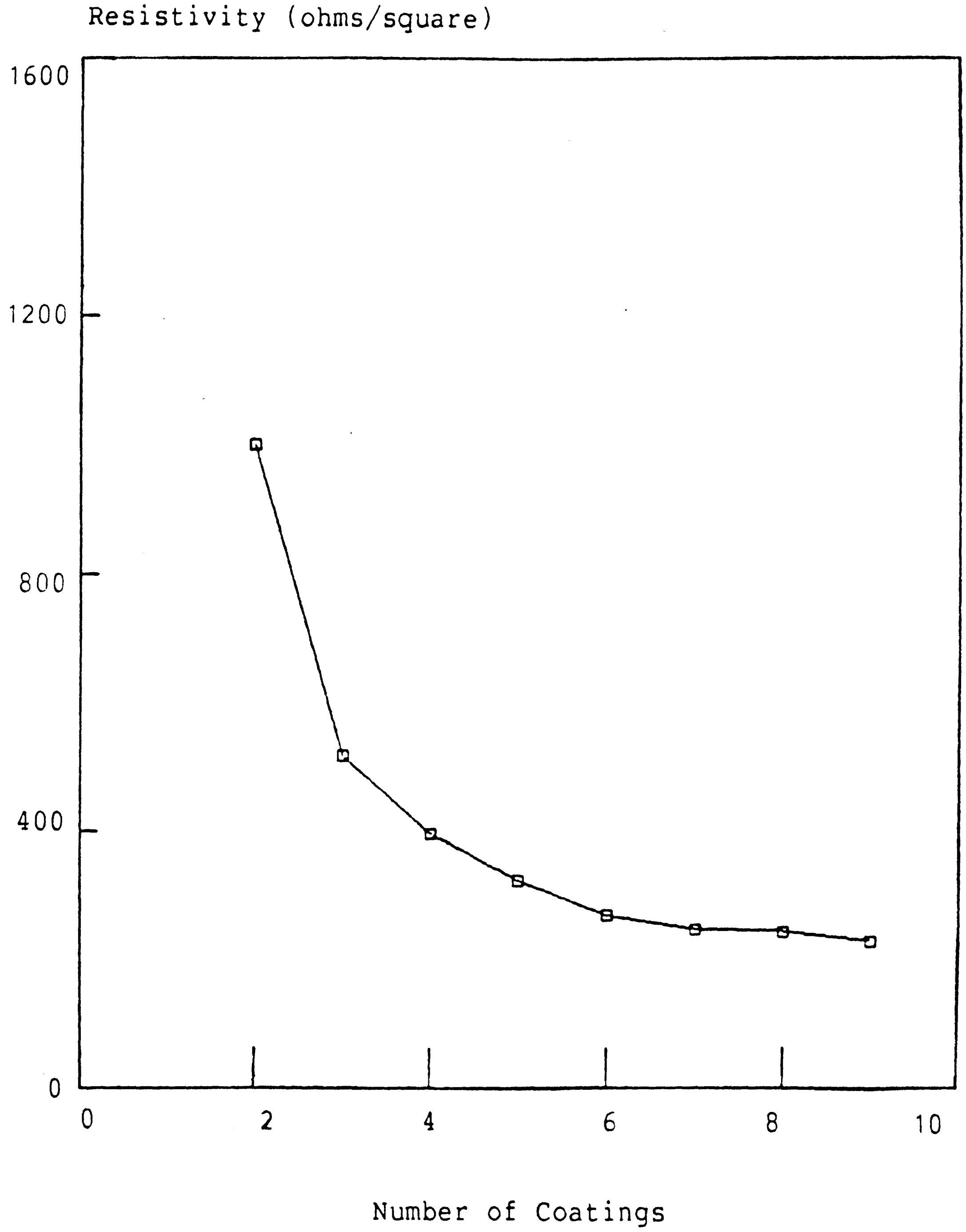

Fig. 4.1 Resistivity vs. Number of Coatings of Electrodag 110; Paper Base.

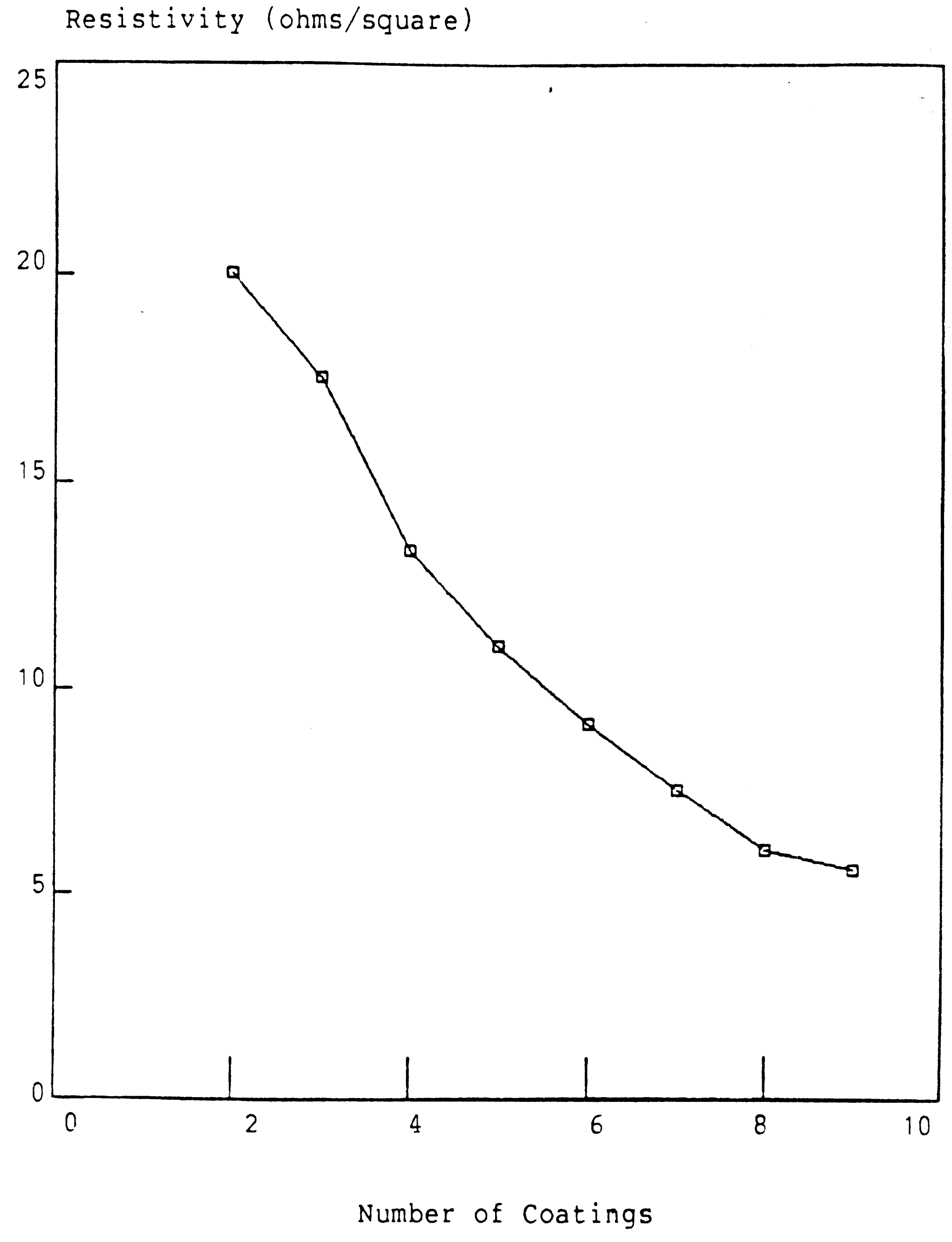

Fig. 4.2 Resistivity vs. Number of Coatings of Electrodag 109; Paper Base.

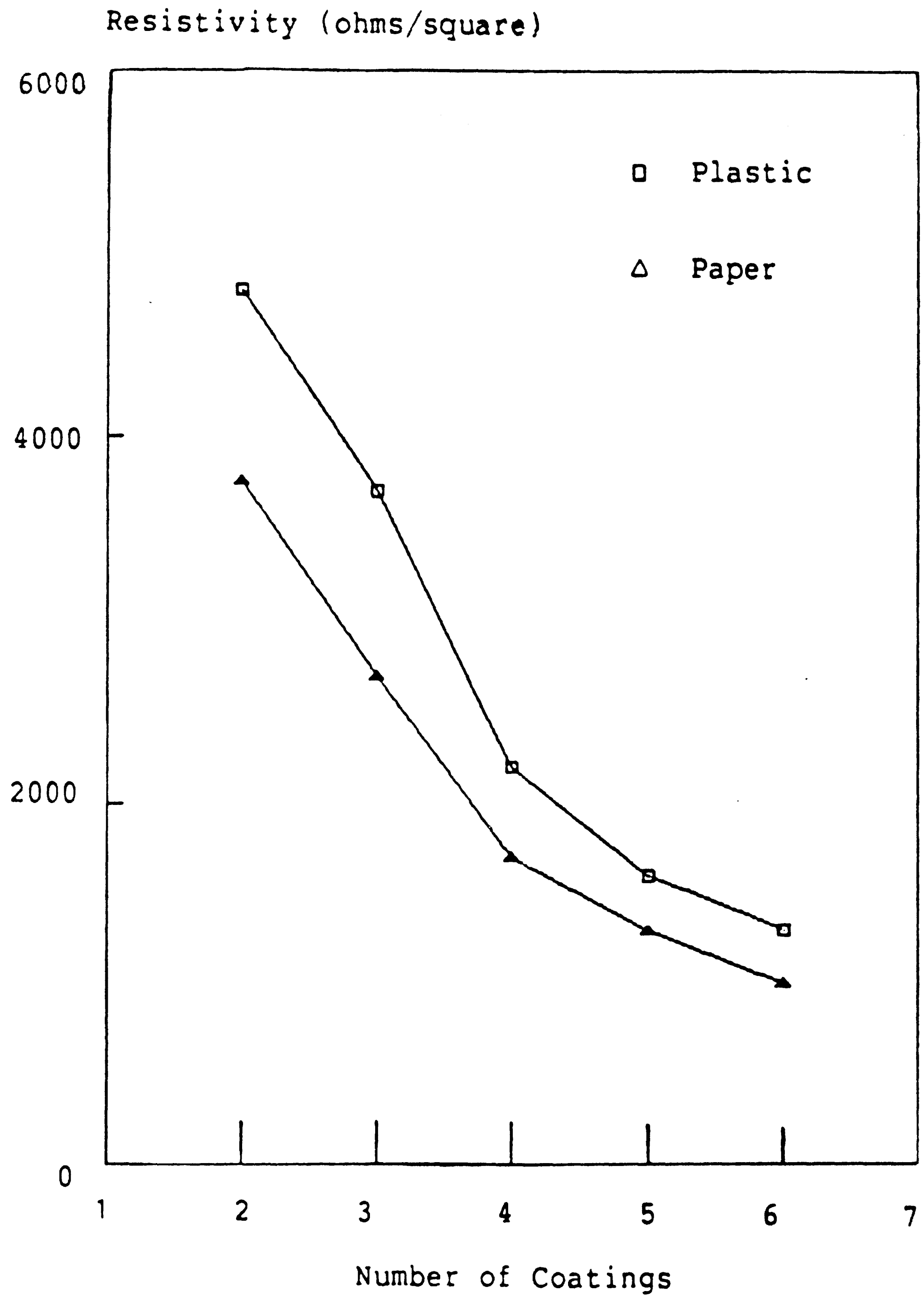

Fig. 4.3 Effect of Base Material on Resistivity; Electrodag 502.

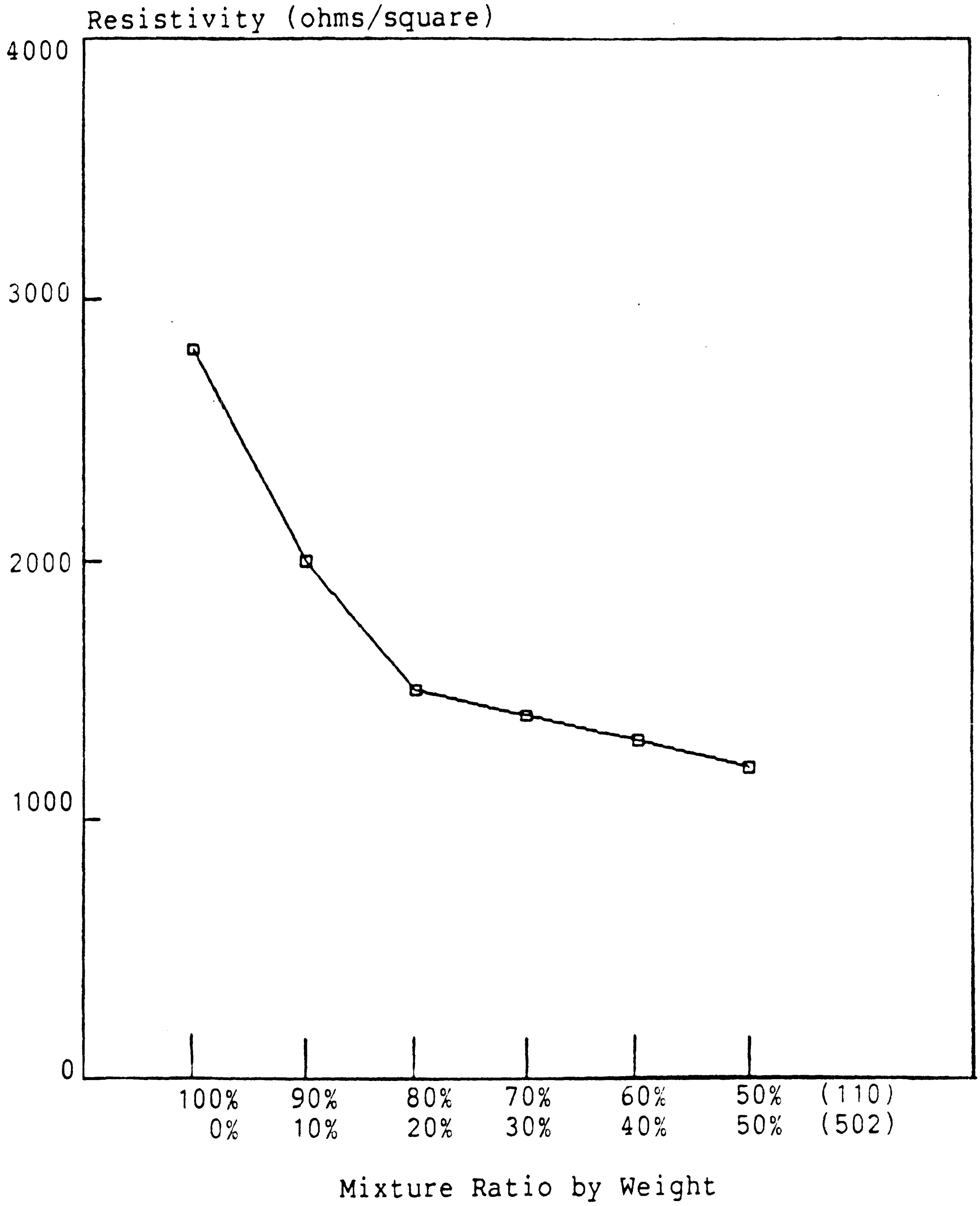

Fig. 4.4 Resistivity vs. Mixture Ratio of Electrodag 110 & 502; Plastic Base, 2 coats.

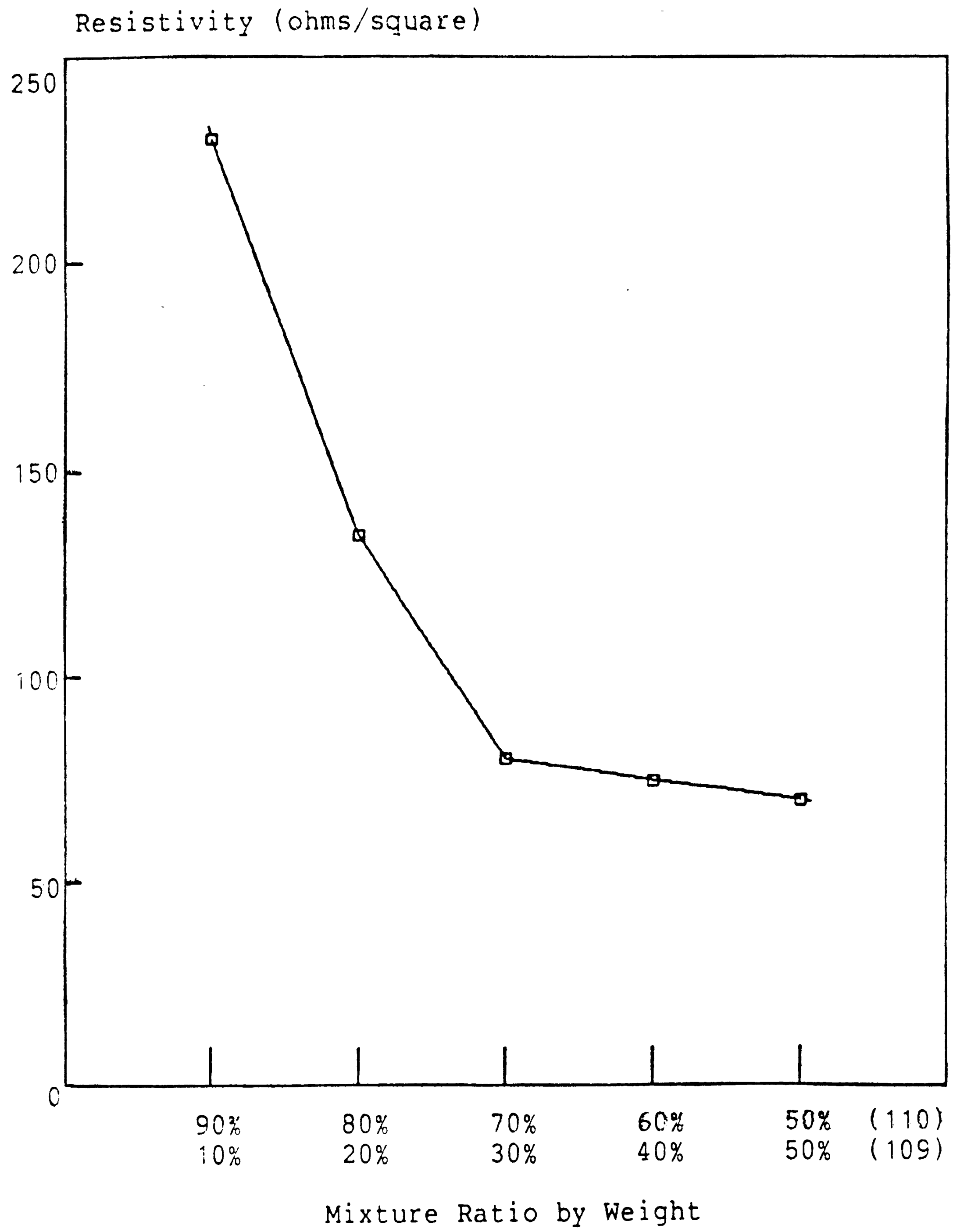

Fig. 4.5 Resistivity vs. Mixture Ratio of Electrodag 110 & 109; Plastic Base, 2 coats.

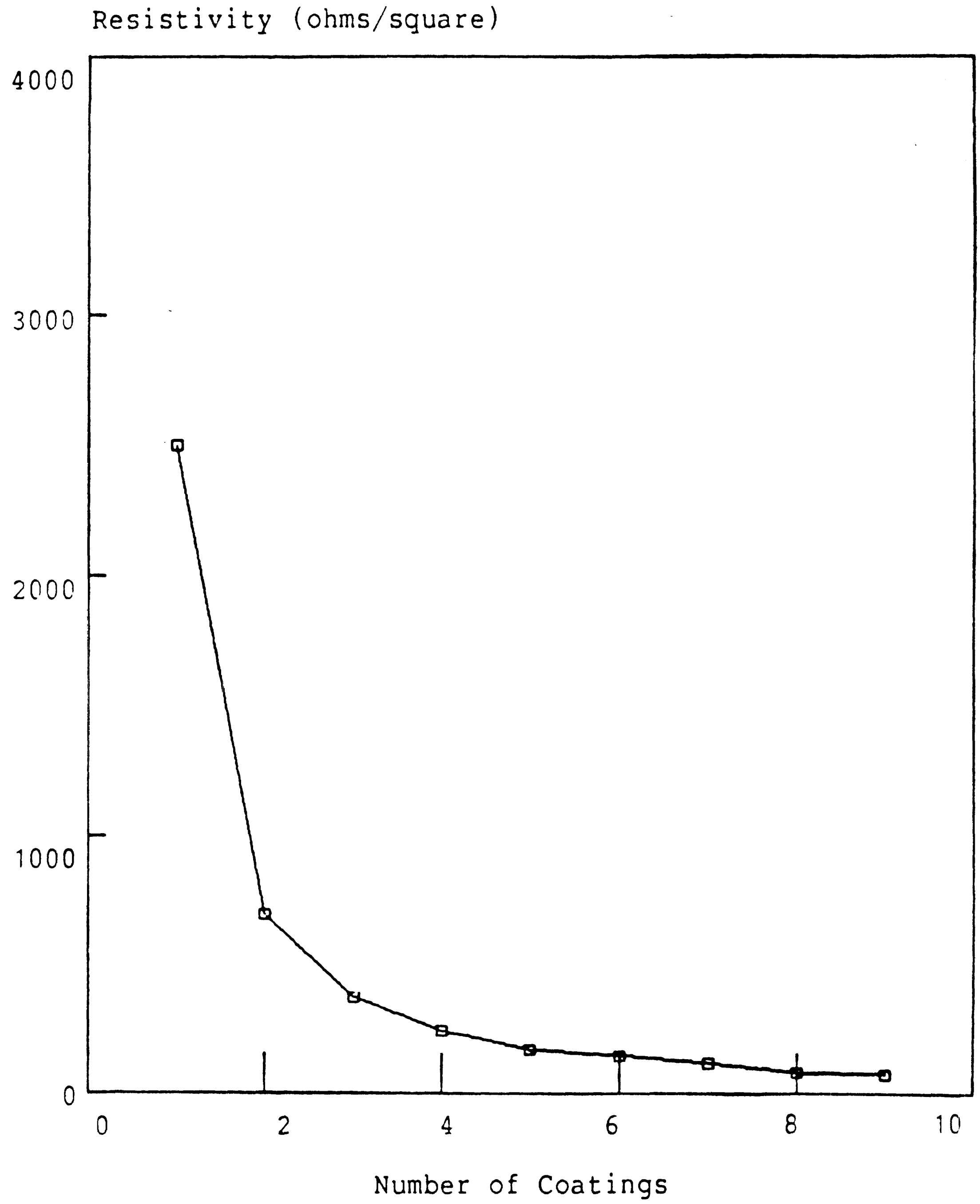

Fig. 4.6 Resistivity vs. Number of Coatings of Electrodag 109 & 502 (1:4 Ratio by weight); Plastic Base.

the spraying distance from the brush to the sample, and the speed-of-hand motion all have significant effect on the final resistivity.

Thus, by a combination of the paints and the coatings applied, the resistivity of the material can be controlled. For the actual ground plane model, where resistivities were needed to vary from 0 to 1000 ohms/square, Electrodag 109 was first used primarily because of its low resistivity, then a mixture of Electrodag 109 and 502 (ratio of 1:4, mixed by weight) was applied, see Table (5.1).

In practice, it is simpler to measure liquids by volume, such as with a 10 cc syringe that was used. With the paints accurately weighed (they all came in the quart cans) and their densities calculated, the exact ratio for mixing by volume was obtained for the given ratio by weight. After the paints were mixed, a lacquer thinner was added to faciliate the spraying process with the air-brush.

Depending on the drying time of different paints, it usually takes at least three to four days for the paints to be completely dried and stablized to obtain accurate resistivity measurements.

4.3 Measurement of the Resistivity of the Sample

The resistance of the painted sample can be measured at DC and microwave frequencies. There are several

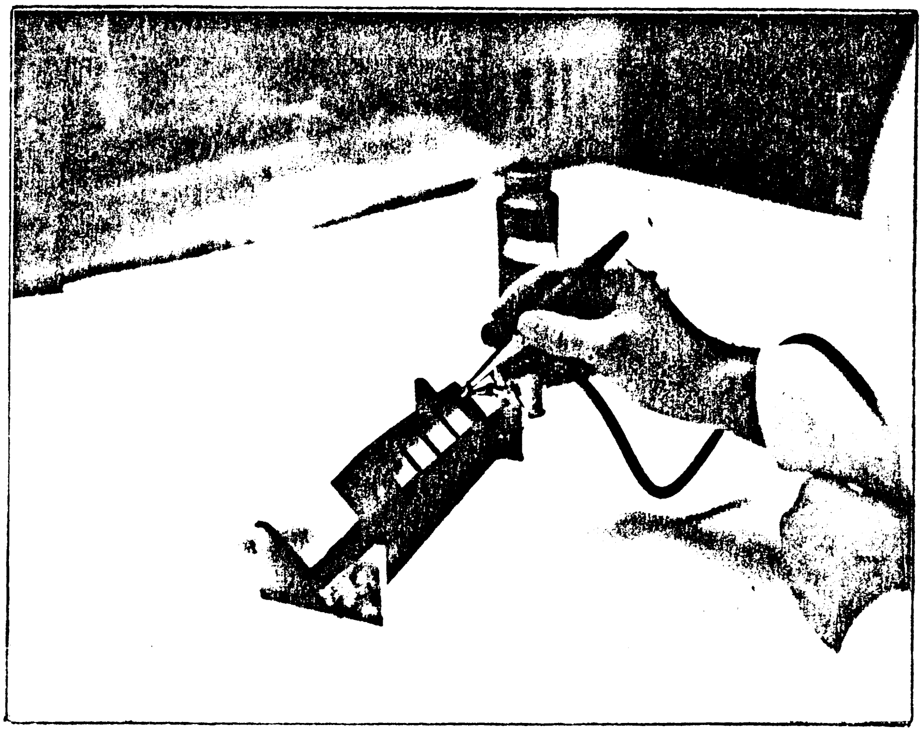

Fig. 4.7 Spraying of Test Samples Using an Air-Brush Method.

ways of making DC measurements. The most common approach (direct method) is to use a rectangular sample painted with silver electrodes on opposite sides, and measure the resistance with a multimeter (ohmmeter). A two-wire line is the other DC method used. A more accurate measurement of the effective resistivity can be obtained at frequency of operation using an open-ended coaxial sample holder and a network analyzer.

4.3.1 DC Measurements

(a) Direct Method

A resistive sample is cut into rectangular patches, then the opposite edges painted with silver paint (Electrodag 415) to provide the edge electrodes. After drying, the resistance of the sample is measured by an ohmmeter as shown in Fig.(4.8). The resistance R_m (ohms) and the sheet resistivity R_s (ohms/sq.) of the sample are related by

$$R_s = \frac{n}{N} R_m \tag{4.1}$$

or

$$R_s = \frac{W}{\ell} R_m \tag{4.2}$$

where

N = number of square cells in series

n = number of square cells in parallel

W = width of the sample

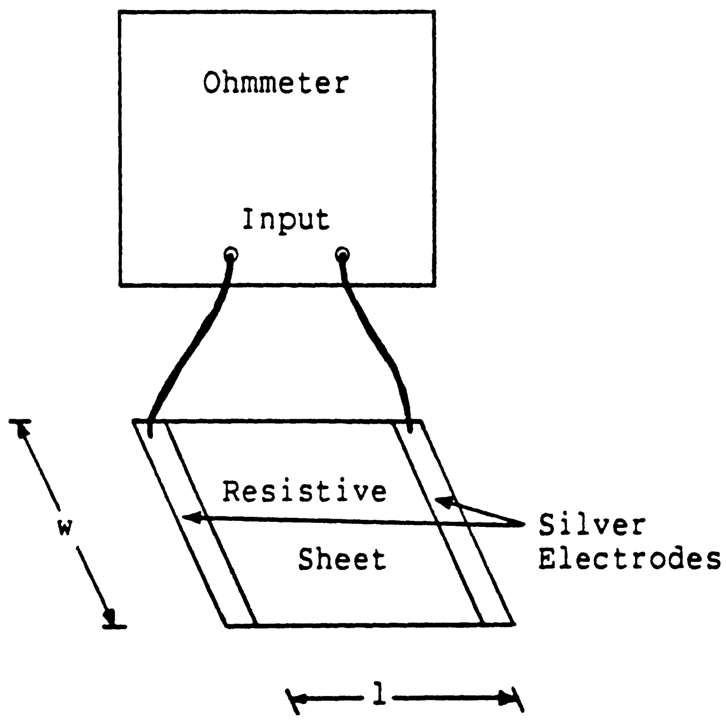

Fig. 4.8 DC Measurement of Sample Using Direct Method.

ℓ = length of the sample

(b) Coaxial Transmission Lines and Two-Wire Lines

The resistivity of a resistive sheet can also be measured by using a coaxial line or two-wire line geometry electrodes. A two-wire line is connected to an ohmmeter and is placed on the sample to be measured as shown in Fig.(4.9). The relation of sheet resistivity R_s (ohms/sq.) to the measured resistance R_m (ohms) is obtained next.

The geometry of the problem is a planar one (all fields lie in the sheet) and the pertinent variables are the current density and the electric field within the sample. One can visualize this as a section of a coaxial line filled with conductive dielectric whose length approaches to zero in the limit. Thus, we start with Laplace's equation in cylindrical coordinates

$$\nabla^2\Phi = 0 \tag{4.3}$$

where Φ is the electric potential.

Since there is no variation in the z or ϕ directions Eq.(4.3) becomes

$$\frac{1}{r}\frac{d}{dr}\left(r\frac{d\Phi}{dr}\right) = 0 \tag{4.4}$$

and its solution is

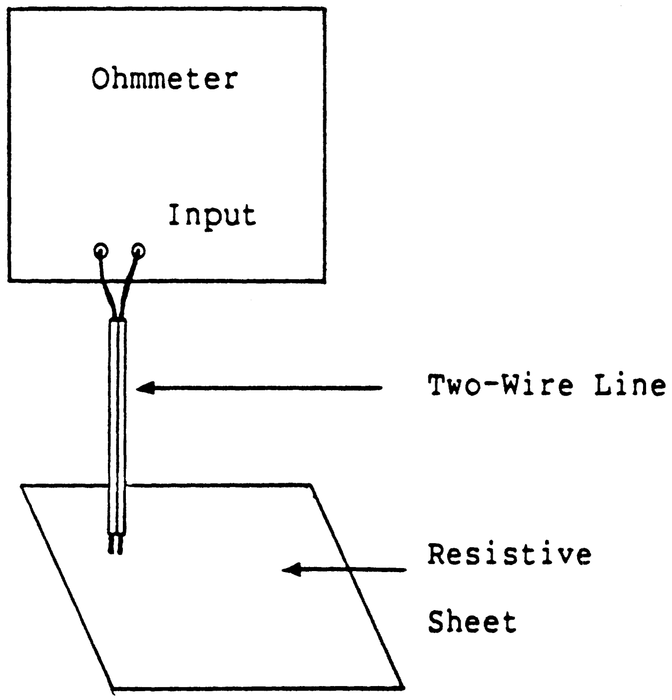

Fig. 4.9 DC Measurement of Sample Using Two-Wire Line.

$$\Phi = \left(\frac{\ln r - \ln a}{\ln \frac{b}{a}} \right) V \tag{4.5}$$

where a and b are the inner and outer radii respectively, and V is the voltage applied, (see Fig.(4.10a)). The electric field intensity is

$$E = -\frac{\partial \Phi}{\partial r} = \frac{V}{r \ln(\frac{b}{a})} \tag{4.6}$$

Next define sheet resistivity R_s

$$R_s = \lim_{\substack{\Delta \to 0 \\ \sigma \to \infty}} \frac{1}{\sigma \Delta}$$

where

σ is the conductivity

Δ is the thickness.

and, $R_m = \dfrac{V}{I}$ = Resistance measured in DC.

Starting with resistive sheet boundary condition from Eq.(1.7), we have

$$E = R_s J \tag{4.7}$$

$$I = 2\pi r J \tag{4.8}$$

$$I = \frac{2\pi r E}{R_s} \tag{4.9}$$

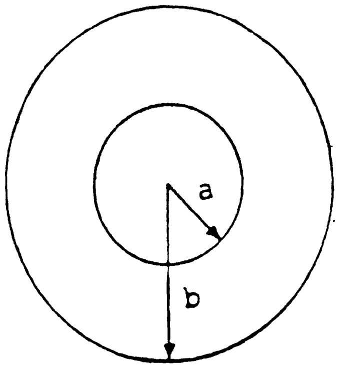

(a) Coaxial Line

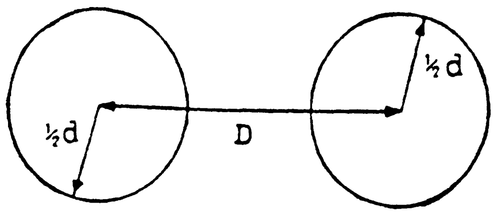

(b) Two-Wire Line

Fig. 4.10 Dimensions of Probe Geometries;
(a) Coaxial Line, (b) Two-Wire Line.

Using Eqs.(4.6), (4.7) and (4.9), one then obtains

$$\frac{V}{r\ln(\frac{b}{a})} = \frac{IR_s}{2\pi r} \tag{4.10}$$

$$R_s = \frac{V}{I}\frac{2\pi}{\ln(\frac{b}{a})} \tag{4.11}$$

$$R_s = R_m\frac{2\pi}{\ln(\frac{b}{a})} \tag{4.12}$$

Similarly, for the two-wire line, from Ramo, Whinnery and Van Duzer [33], we have

$$\Phi = \frac{V\ \beta}{2\ \alpha} \tag{4.13}$$

$$E_x = -\frac{\partial\Phi}{\partial x} = \frac{V\xi}{2\alpha} \tag{4.14}$$

$$I = \frac{2\ \pi\ E_x}{R_s\ \xi} \tag{4.15}$$

where

$$\alpha = \ln[\frac{D}{d} + \{(\frac{D}{d})^2 - 1\}^{\frac{1}{2}}]$$

$$\beta = \ln[\frac{(x - a)^2 + y^2}{(x + a)^2 + y^2}]$$

$$\xi = \ln[\frac{x - a}{(x - a)^2 + y^2} - \frac{x + a}{(x + a)^2 + y^2}]$$

Equating Eq.(4.14) and Eq.(4.15), one obtains

$$R_s = \frac{V}{I}\,\frac{\pi}{\alpha} \tag{4.16}$$

thus,

$$R_s = R_m \frac{\pi}{\ln[\frac{D}{d} + \{(\frac{D}{d})^2 - 1\}^{\frac{1}{2}}]} \tag{4.17}$$

D = Distance between the center of the two-wire line.

d = Diameter of the two-wire line, (see Fig.(4.10b)).

The sheet resistivity R_s can be measured using two-wire and coaxial geometry probes. When these probes are brought in contact with the resistive sheet, the resistance measurments are related to the sheet resistivities via Eq.(4.17) and Eq.(4.12), respectively. For both probe designs, the resistance measurements were found to vary significantly from one measurement to another, even when measured at the same point. This is a result of non-total contact of the sheet with the probe, and, indeed, Eq.(4.17) and Eq.(4.12) show that the resistivity measured is a contact geometry sensitive. Various approaches such as carefully polishing the probe tips to make them flat or varying the pressure applied did not alleviate the problem. The only alternative was to make a lot of measurements, and to average them.

Two sizes of two-wire probes were used and with each probe twenty measurements were taken for each of the five samples studied. Table (4.2) shows the averaged results which are compared to the values obtained by the direct measurement. Note, the deviations are from -12.59 to 32.75 percent from the direct measurement values.

Measurements were also tried using the coaxial line probe, but here, the measurement variations were even greater, attributed to the fact that a uniform contact is difficult to achieve with the circular electrodes. Hence, no further measurements were made with this probe, nor are they reported herein.

4.3.2 AC Measurements

Even though the coaxial probe method does not work well at DC, a similar technique works well at microwave frequencies (AC). This can be explained by the fact that the small non-contact spacing that gave errors at DC, has capacitance that at AC for all practical purposes provides a short. An important fact is that this is a non-destructive measurement technique, and can provide resistivities in the frequency range of interest.

The concept is relatively simple. An open-ended coaxial transmission line provides an almost perfect open circuit, except for a small stray capacitance. If a resistive sheet is placed against the end, the impedance

Resistivity (ohms/square)				
Direct Method	Two-Wire Line Avg. of 20 Measurements		Percentage Error	
	D= 0.088 cm d= 0.032 cm	D= 0.049 cm d= 0.036 cm	D= 0.088 cm d= 0.032 cm	D= 0.049 cm d= 0.036 cm
3123	3384	2790	8.36	-10.6
2126	2444	2200	14.68	3.48
1215	1600	1062	31.68	-12.59
504	564	480	11.90	-4.76
58	77	66	32.75	13.70

Table 4.2 Comparison of Resistivity Values Obtained Using DC Measurements.

seen would then be due to the resistance plus the stray capacitance in parallel as shown in Fig.(4.11).

The Hewlett Packard 8745A S-parameter test set with a model HP 8410A network analyzer was used. A 5 cm long, 7 mm air-line was attached to the test port and served as the probe. To make the reflection measurements - switch S_{11} was on. For calibration, a shunt was connected and the test channel gain and phase offset adjusted for zero dB amplitude and 180 degrees phase readings, respectively. With the short removed, the resistive sheet to be measured was then placed against the open-ended coaxial line, and pushed firmly with a styrofoam block. The amplitude and phase of parameter S_{11} which is also known as (voltage) reflection coefficient was then recorded.

The parameter S_{11} is directly related to the complex impedance of the load by

$$\frac{Z_\ell}{Z_o} = \frac{1 + S_{11}}{1 - S_{11}} \tag{4.18}$$

where

Z_o is the characteristic impedance of the coaxial line probe and for this setup Z_o = 50 ohms.

The expression relating measured resistance R_m at DC and sheet resistivity R_s for a coaxial line geometry still applies, and Eq.(4.12) becomes

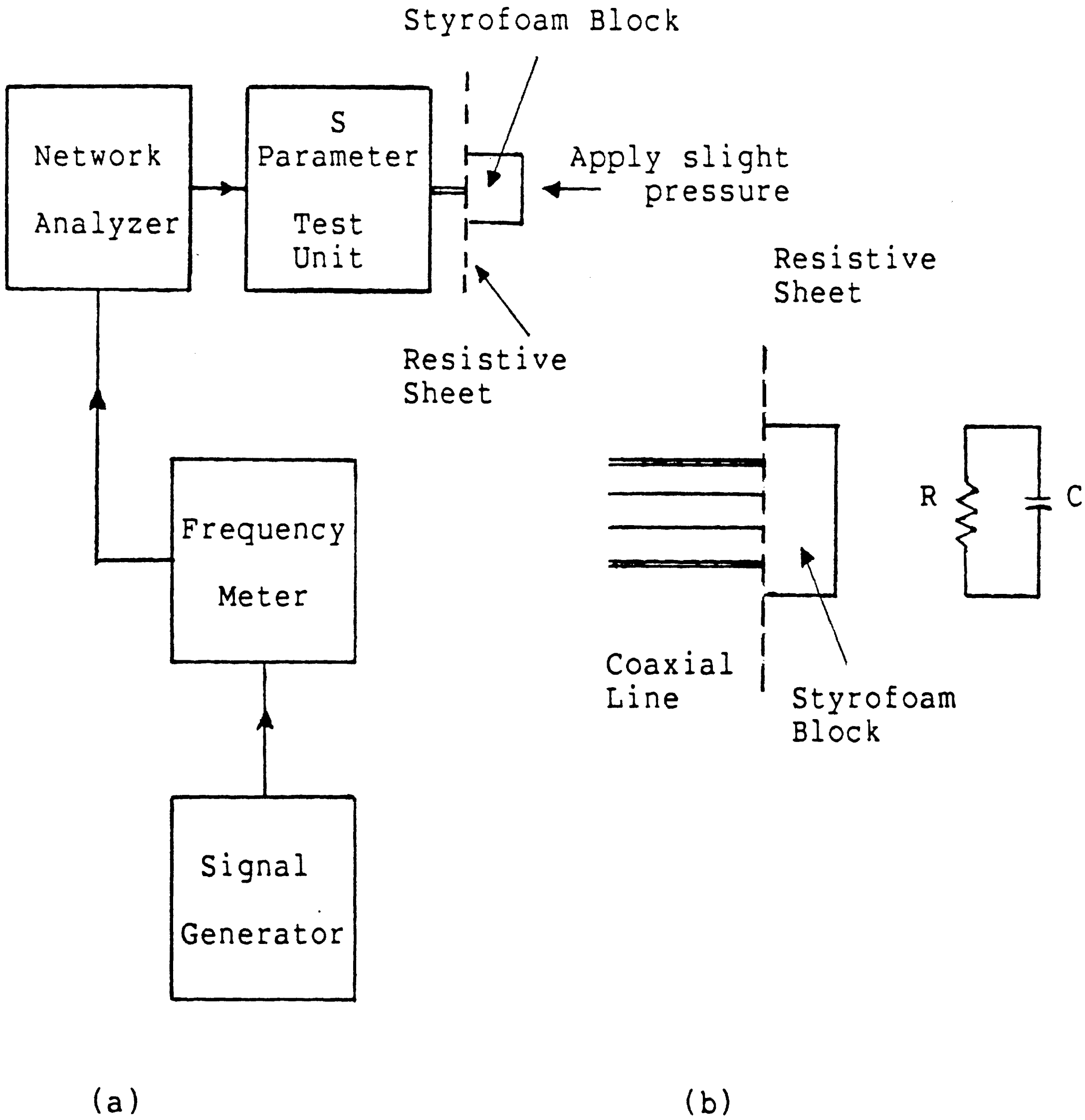

Fig. 4.11 Equipment Block Diagram; (a) AC Measurement of Sample Using a Network Analyzer, (b) Equivalent Circuit.

$$R_s = Z_\ell \frac{2\pi}{\ln(\frac{b}{a})} \tag{4.19}$$

where the radii a and b for the 7 mm line are 7.01 mm and 3.05 mm, respectively.

Table (4.3) shows the comparison between the DC and AC measurements for the eight samples at three different frequencies (1000 MHz, 1500 MHz and 2000 MHz). As observed, the resistivity (ohms/sq.) of the sample does not change significantly with frequency (or measurement). A variation of 5 to 10 percent is an acceptable result. A small capacitive component is also measured and varies from 0.02 pF to 0.08 pF for the frequencies measured (see Table (4.4)). This capacitance in part, is attributed to the outside fringing fields of the coaxial line and, in part, to the resistive paint and the base material used. However, the capacitance does not significantly influence the resistivity measurement of the sheets. As shown, the resistivity of the resistive sheet remains relatively constant from DC to 2 GHz.

Resistivity DC (ohms/sq.)	Resistivity for various Frequencies (MHz)			AC AVG	Percent Diff.
	1000	1500	2000		
3123	3078	3038	3188	3101	-0.73
2627	2579	2651	2500	2577	-1.90
2126	2166	2036	2220	2140	0.65
1215	1299	1286	1280	1288	6.00
504	539	493	507	513	1.78
137	153	135	140	143	4.37
58	64.4	64	58	62	6.89
12	11.9	11.5	10.86	11.4	-5.00

Table 4.3 Comparison of AC and DC Measurements.

Resistivity DC (ohms/sq.)	Capacitance (pF) for various Frequencies (MHz)			Average capacitance value (pF)
	1000	1500	2000	
3100	0.0448	0.0389	0.0249	0.0361
2600	0.0851	0.0779	0.0451	0.0693
2100	0.0445	0.0296	0.0496	0.0412
1200	0.0645	0.0512	0.0428	0.0528
500	0.0489	0.0452	0.0331	0.0424
140	0.0615	0.0509	0.0573	0.0565
60	0.0226	0.0319	0.0133	0.0226
12	0.0671	0.0842	0.0735	0.0749

Table 4.4 Comparison of Shunt Capacitance at Different Frequencies.

CHAPTER V. EXPERIMENTAL ANTENNA MODEL

5.1 Introduction

The design and construction of resistive ground planes, monopole and the measurements are presented in this section.

It has been shown by Senior and Liepa [16] that a tapered resistivity extension applied to a metal edge can drastically reduce its backscattering. The resistivity should vary from a low value (≃ 0 ohm/sq.) adjoining the metal edge to a large value (≃ 1000 ohms/sq.) at the outer edge. A quadratic resistivity taper that follows t^2 form, where t is the distance measured from the edge adjoining the metal, is near optimum and was selected for use here. As shown in [16] the width of this taper should be 0.75 wavelength or wider to be effective.

Using these design criteria, an edge treatment was chosen and the model constructed. Besides the resistive ground plane model, a similar metal ground plane of the same size and another large metal ground plane which was used to simulate an "infinite" ground plane were constructed.

Measurements of antenna impedance and radiation patterns were made on these three models. The results are consistent with a simple reflection model concept. The outward travelling wave on the ground plane is reflected by the edge of the ground plane to produce an inward wave of lower amplitude. Resistive material near the edge attenuates the outward travelling wave as well as the reflected wave. The antenna impedance curve of a finite ground plane with resistive edge appears to be very close to that of a large ground plane of five wavelengths in radius which can be considered, for all practical purposes, as an infinite ground plane, because the error in antenna impedance is only three percent (see Storer [4]).

5.2 Construction of the Circular Ground Plane with Resistive Edge Loading

The resistive coatings can be made in the laboratory by appropriately blending conductive paints and spraying on a nonconductive base. This was presented in Chapter IV. A plastic sheet of 0.127 cm thick was chosen for the base material and a disc of twelve centimeters in radius was cut.

Table (5.1) shows the proposed resistivity variation for the ground plane. Right at the base, from zero to three centimeters radius, the resistivity is zero which then proceeds to 1350 ohms/square in eleven steps. One can visualize this resistivity as being applied in bands using different paint mixtures and number of coatings as determined in Chapter IV. In practice this was accomplished by using a series of masks with circular holes cut from three to nine

Resistivity (ohms/sq.)	Distance from center (cm)	Number of Coatings	Paints used
5	3 - 3.5	8	Electrodag 109
9	3.5 - 4	6	Electrodag 109
12	4 - 4.5	4	Electrodag 109
20	4.5 - 5	2	Electrodag 109
100	5 - 6	7	Electrodag* 109&502 = 1:4
150	6 - 7	6	Electrodag 109&502 = 1:4
175	7 - 8	5	Electrodag 109&502 = 1:4
250	8 - 9	4	Electrodag 109&502 = 1:4
380	9 - 10	3	Electrodag 109&502 = 1:4
700	10 - 11	2	Electrodag 109&502 = 1:4
1350	11 - 12	1	Electrodag 109&502 = 1:4

* By weight

Table 5.1 Number of Coatings and Mixtures Used in Preparing the Actual Model.

centimeters in radius. The resistivity within the unmasked region is controlled by the number of coatings applied. The portion of the band that is coated most, i.e., the central region, has the lowest resistivity. Figure (5.1) shows the actual painting of the material.

The paint was sprayed with an air-brush onto the model which was placed on a phonograph turntable rotated at 16 rpm, Fig.(5.1). To get a consistent deposition or spray, it is sprayed slower at the outer edge and faster at the center. After the first band was sprayed, a new mask of larger radius was laid on the model to cover the portion that was not yet coated. Thus, by repeating the same process with nine different radii masks, a tapered resistivity variation on the circular model was obtained.

After painting and letting it dry for two to three days, the resistivity of the resistive disc was measured using the AC method, where the sheet was brought against an open end of the coaxial line and its reflectivity was measured, as discussed in Chapter IV. The measurements were made at 2500 MHz and the results are shown in Fig.(5.2). Note, the resistivity variation is parabolic and follows closely to the proposed design given in Table (5.1).

5.3 Antenna Impedance Measurements

To provide a means of mounting the monopole on the resistive ground plane, a 3 cm metal disc was mounted on top

Fig. 5.1 Making of Circular Resistive Sheet Using an Air-Brush and a Phonograph Turntable.

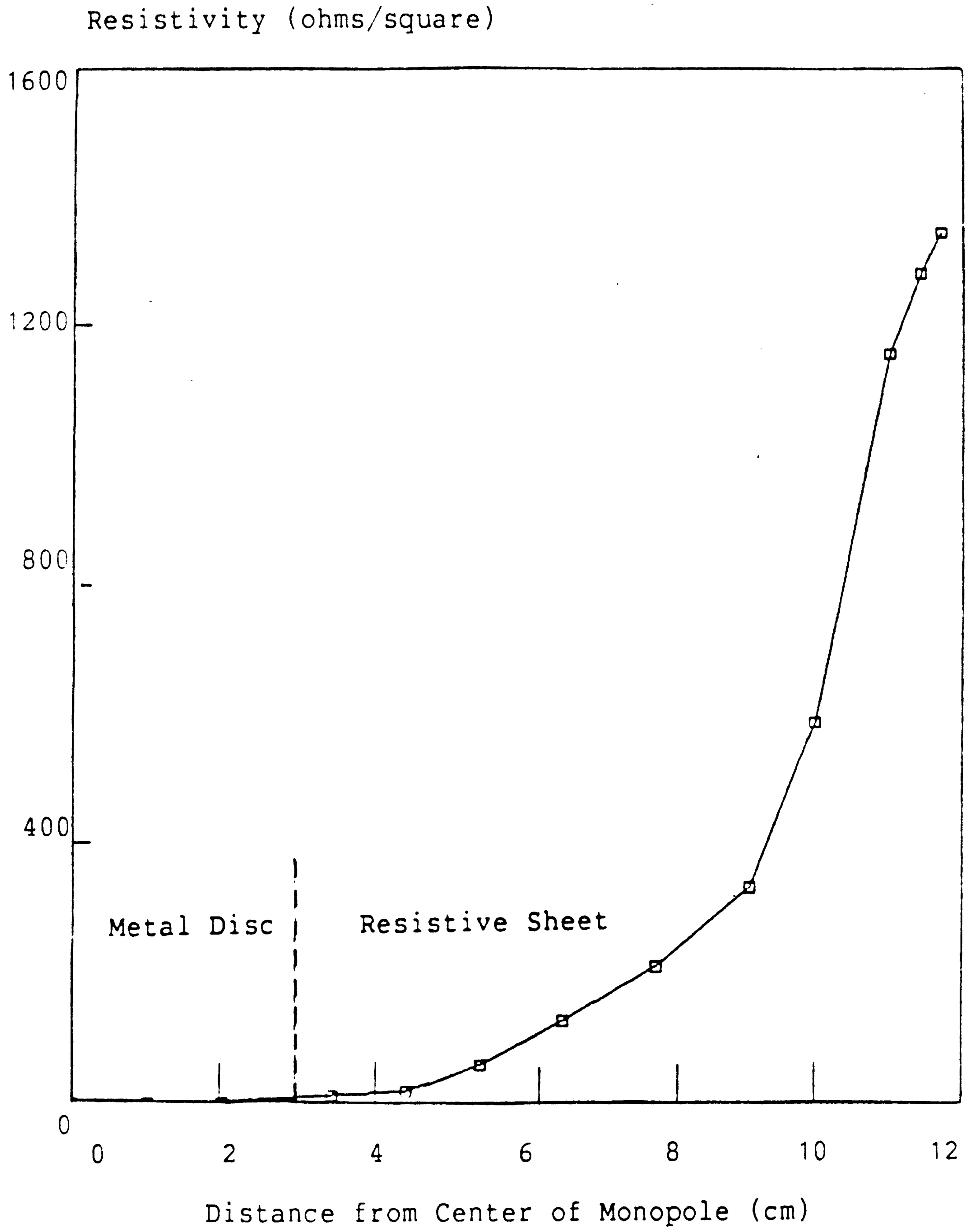

Fig. 5.2 Resistivity vs. Distance from Center of Monopole Measured Using AC Method.

of the painted surface at the center to which a rectangular flange mount SMA connector was attached. To assure a good electrical as well as mechanical continuity between the metal edge and the resistive material, a lacquer-based silver paint was used (c.f. Fig.(5.3)). The dimensions of the resistive ground plane and the monopole are given in Fig.(5.4). The monopole was made of silver-plated copper wire, 2.68 cm high and 0.048 cm in radius.

A network analyzer was used to measure the antenna impedance and was set up as shown in Fig.(5.5). A 20 cm air-line extension plus a 7mm-to-SMA adaptor were used to connect the antenna to the S-parameter test set. Figure (5.6) to Fig.(5.8) show photographs of the setup with the resistive (12 cm radius), metallic (12 cm radius), and metallic large ground plane (60 cm radius), respectively. Where needed, styrofoam blocks were used to support the antenna. For calibration of the network analyzer, a small circular copper tape disc was placed over the monopole, thus shorting it at its base to the ground. After each calibration, the copper tape was removed and the reflection coefficient S_{11} was measured. The impedance of the monopole was then evaluated using Eq.(4.18). Identical procedures were repeated for different frequencies and different models.

Figure (5.9) shows the impedance measurements for the monopole antenna with three different ground planes at five different frequencies. In general, the impedance has

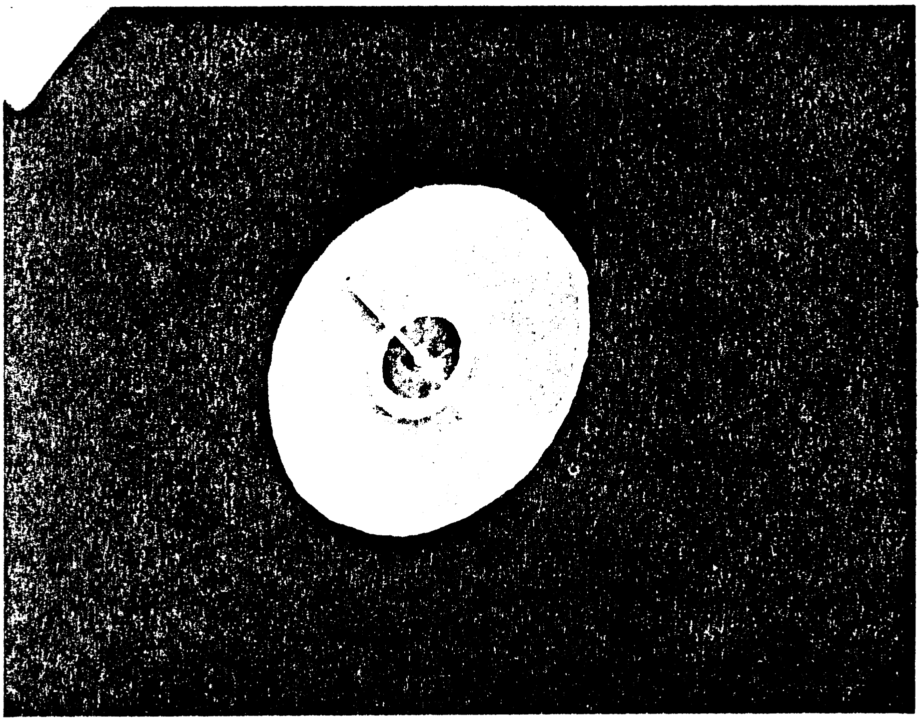

Fig. 5.3 Photograph Showing the Contacts between the Ground Plane and the Resistive Sheet, the Ground Plane and the Monopole Antenna.

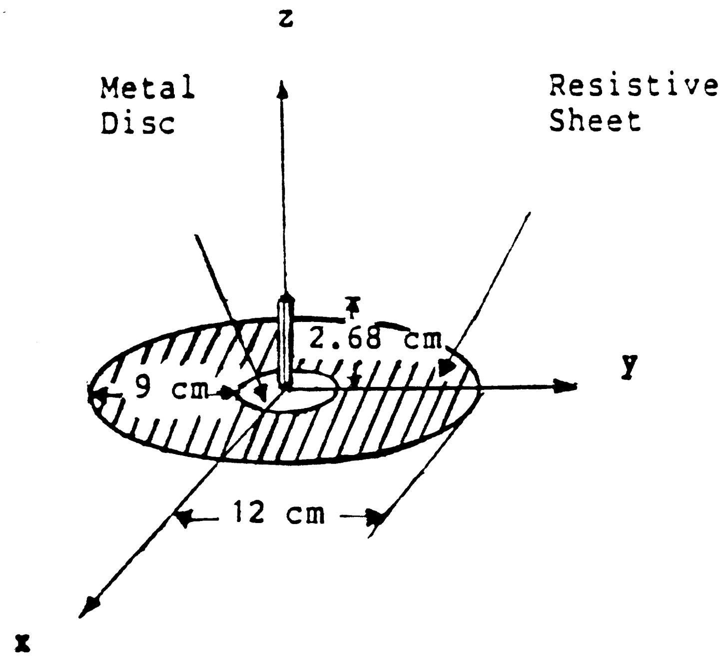

Fig. 5.4 Dimensions of the Actual Model.

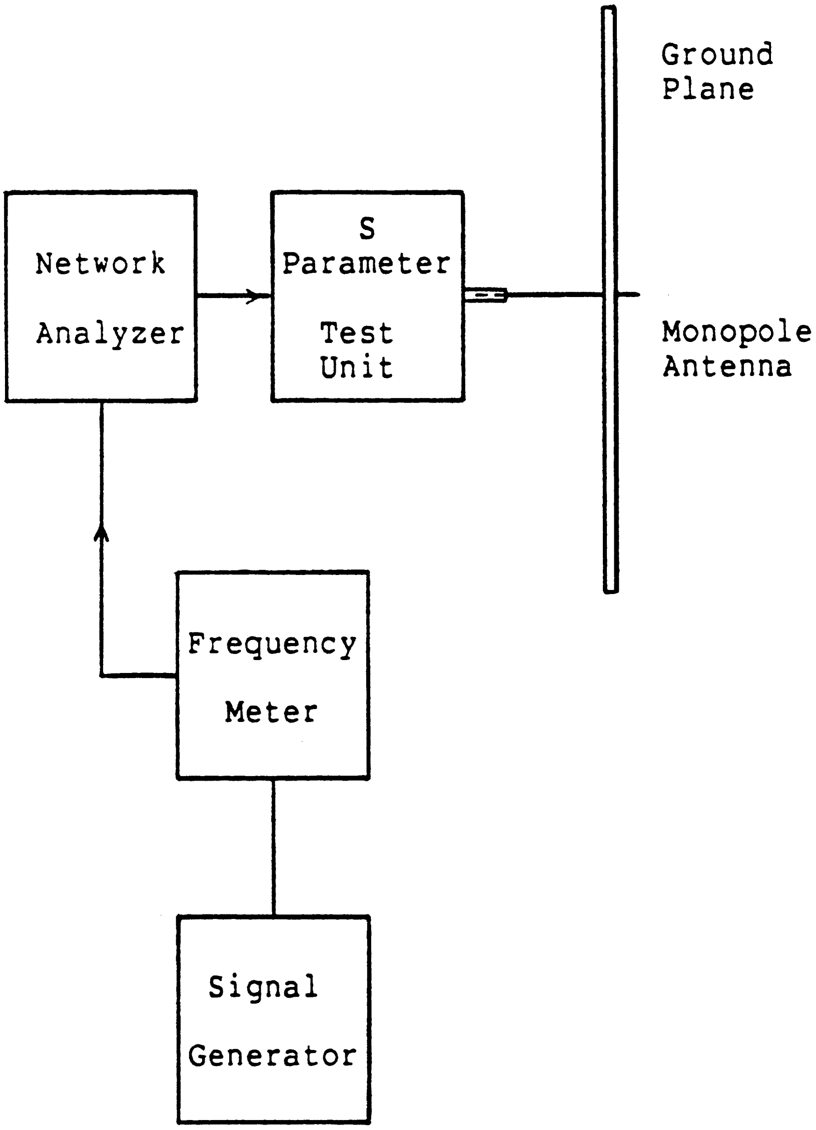

Fig. 5.5 Antenna Impedance Measurement Setup.

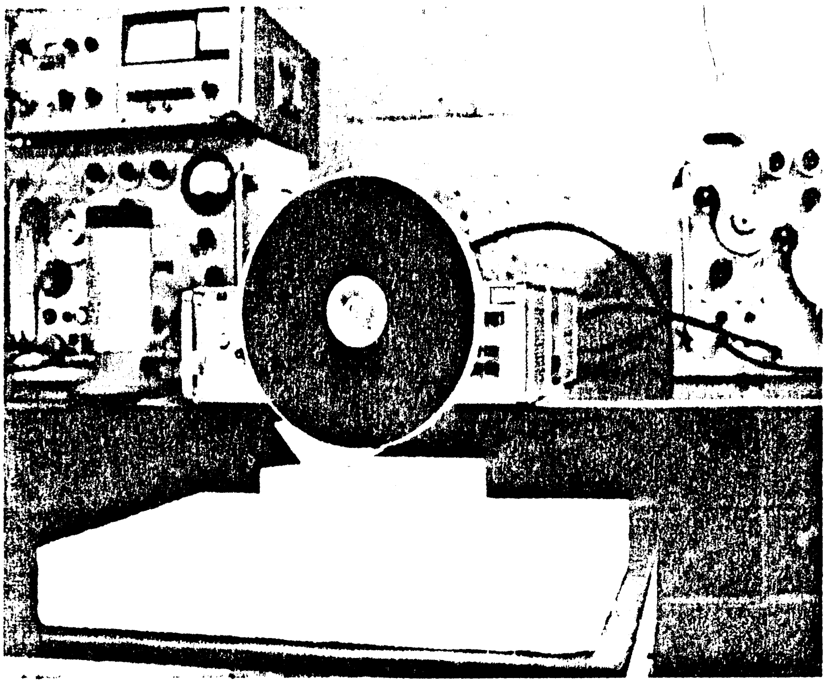

Fig. 5.6 Measurement of Impedance of the Monopole Mounted on a Finite Size Ground Plane With Resistive Sheet of Radius 12 cm.

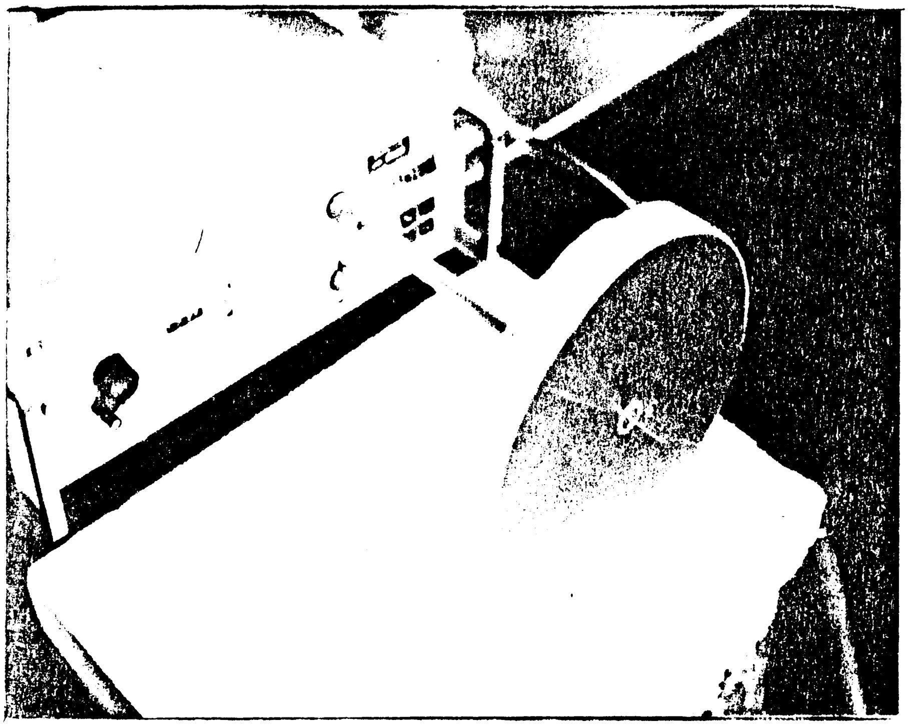

Fig. 5.7 Measurement of Impedance of the Monopole Mounted on a Finite Size Ground Plane of Radius 12 cm.

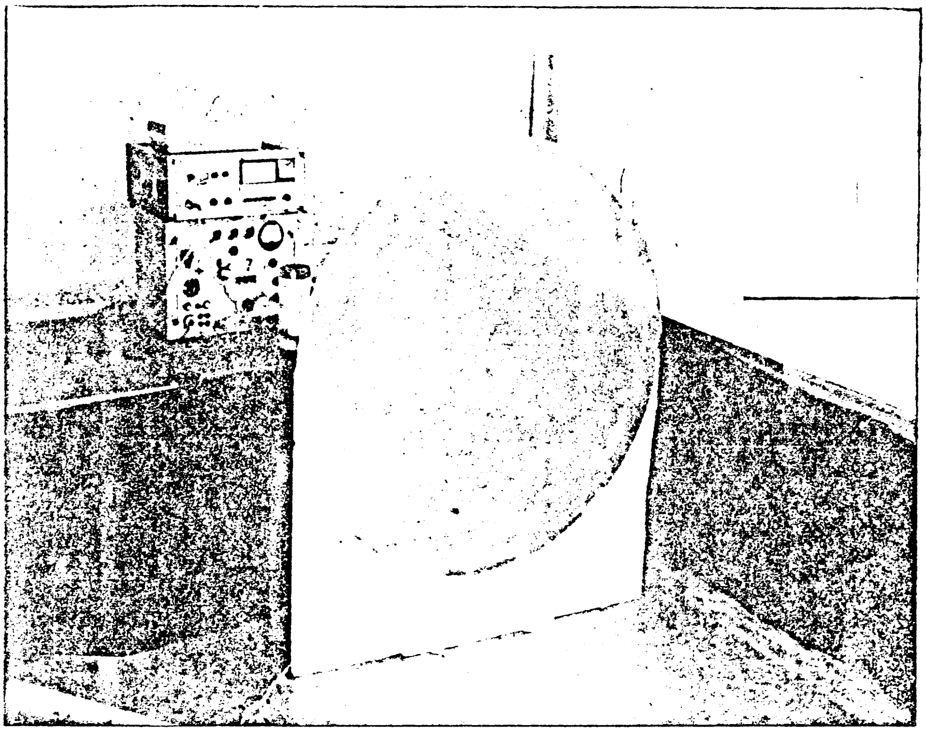

Fig. 5.8 Measurement of Impedance of the Monopole Mounted on a Large Ground Plane of Radius 60 cm.

similar behavior for all three ground planes, mainly because the antenna impedance is dictated more by the monopole height than by the ground plane. The monopole height is 2.68 cm and at 2606 MHz where the reactive component is zero (resonant condition), the equivalent antenna height is 0.233 wavelength. At 2500 MHz, the real part of the antenna impedance is 37.8 ohms with the (finite) metal ground plane, 33.1 ohms with the large metal ground plane, and 32.5 ohms with the resistive ground plane. Note, the antenna on the resistive ground plane has an impedance very close to that of the large ground plane model not only at 2500 MHz but throughout the frequency range measured. Table (5.2) gives the numerical values of the measured impedance so that more accurate assessments can be made if needed.

5.4 Far Field Measurements

For the far field pattern measurements, both the E and H-plane field patterns were measured. The measurements were made in a relatively small antenna pattern range. There, a turntable provided a means of rotating the tested antenna about its center of radiation. The antenna under test was used as the receiving antenna. Attached to the antenna was a crystal detector, the output of which was fed into the pen amplifier of the antenna pattern recorder. The received signals as a function of test antenna rotation were recorded. For the H-plane pattern measurements, the monopole

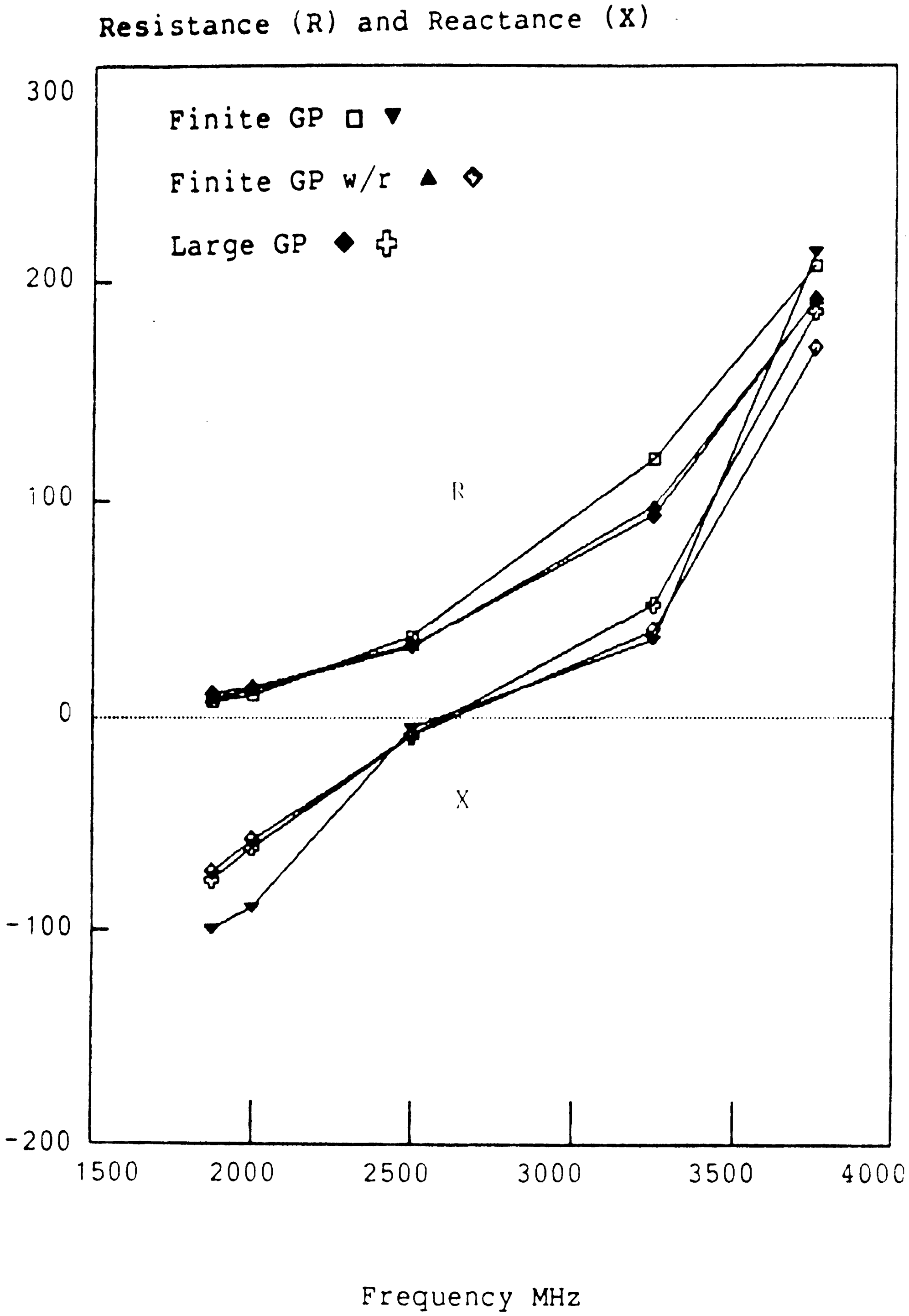

Fig. 5.9 Measured Monopole Impedance for Various Ground Planes.

Frequency (MHz)	Finite GP	Finite GP with resistive sheet	Large GP
1875	7.2 - j 100	8.4 - j 73	10.8 - j 77
2000	10.1 - j 90	12.8 - j 58	14 - j 62
2500	37.8 - j 5	32.5 - j 8.8	33.1 - j 8.5
3250	119 + j 36	97.5 + j 40	93.1 + j 52
3750	208 + j 214	192 + j 170	194 + j 187

Monopole Height : 2.68 cm

Radius - Finite Ground Plane : 12 cm

Radius - Finite Ground Plane with Resistive Sheet : 12 cm

Radius - Large Ground Plane : 60 cm

Table 5.2 Comparison of Impedance for a Monopole with Different Ground Planes.

was mounted vertically so that when it was rotated in the horizontal plane, and the H-plane pattern was recorded. Conversely, the antenna was mounted on a side so that the monopole was horizontal and when rotated in the horizontal plane the E-plane pattern was obtained.

A waveguide horn antenna was used at the transmitter. The separation distance between the transmitting antenna and the receiving antenna should be large enough to insure that the far field patterns are being measured. For this, the separation distance should be equal to or greater than $2\ D^2/\lambda$, where D is the maximum aperture dimension involved in either transmitting or receiving antenna. In this study for the test antenna, the ground plane was treated as part of the antenna, and the far field requirements were met in the measurements.

To avoid errors due to reflections, radar absorbing material whenever appropriate was placed around the tested antenna. A block diagram of equipment used is shown in Fig.(5.10).

The measurement frequencies used are 2.25 GHz, 2.5 GHz and 2.75 GHz. The measurements were made first with the monopole antenna section (consisting of the 2.68 cm monopole, SMA connector and the 3 cm radius metal disc) mounted on the resistive ground plane. Then the section was transferred and mounted on the same size metal ground plane and the far field patterns were measured. No measurements

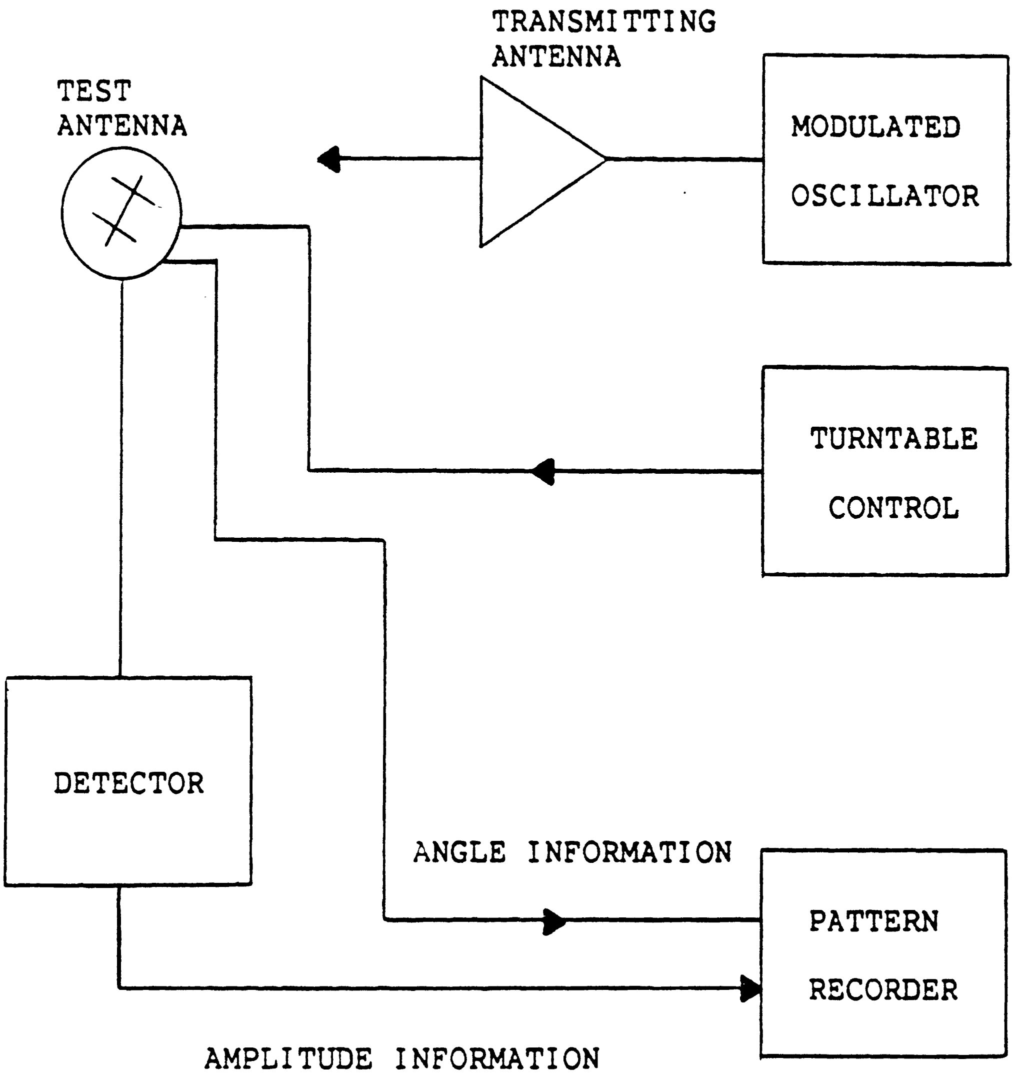

Fig. 5.10 Block Diagram for Measuring the Far Field Patterns

were made with the large 60 cm radius ground plane since such size could not be accommodated in the small chamber. Figure (5.11) and Fig.(5.12) show the mounting arrangement of the resistive antenna for the H-plane and the E-plane measurements, respectively. Styrofoam blocks and masking tape were used to support the antenna on the turntable.

The recorded patterns are shown in Fig.(5.13) through Fig.(5.15) for 2.25 GHz, 2.5 GHz and 2.75 GHz, respectively. The H-field patterns are concentric circles, the larger circle is for the monopole on the finite ground plane (12 cm in radius), and the smaller circle is for the monopole on the resistive finite ground plane.

The E-field patterns are similar to those of a monopole on an infinite ground plane but below (or spilling over) the horizontal axis. The side lobes are very dominant for the monopole antenna on the metal ground plane. The lobes do not exist for the monopole antenna with the resistive ground plane because the effects of edge diffraction have been minimized by the resistive treatment.

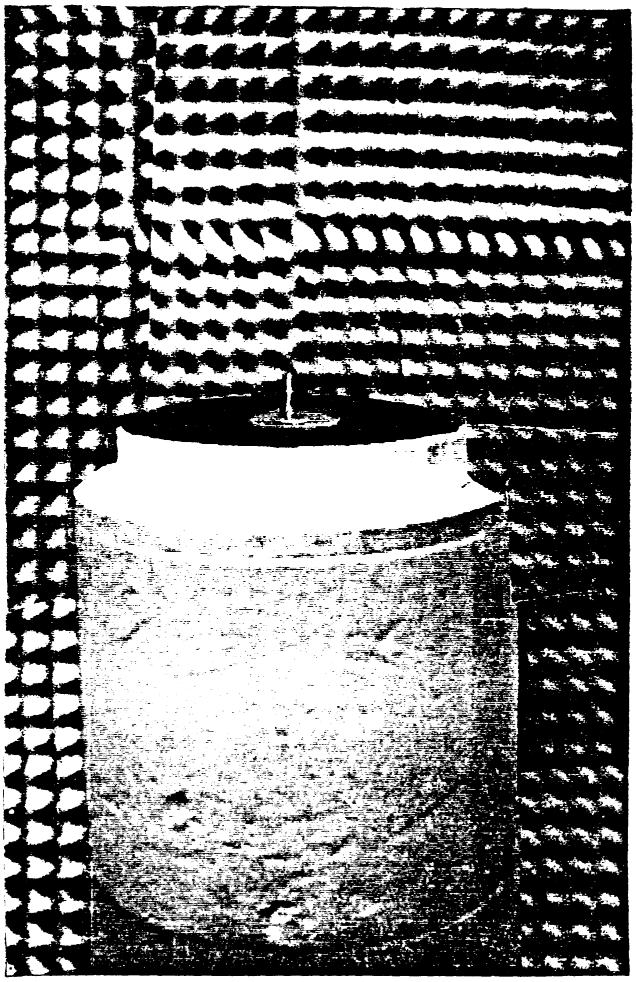

Fig. 5.11 Test Antenna Placement for Measuring the H-Field Pattern.

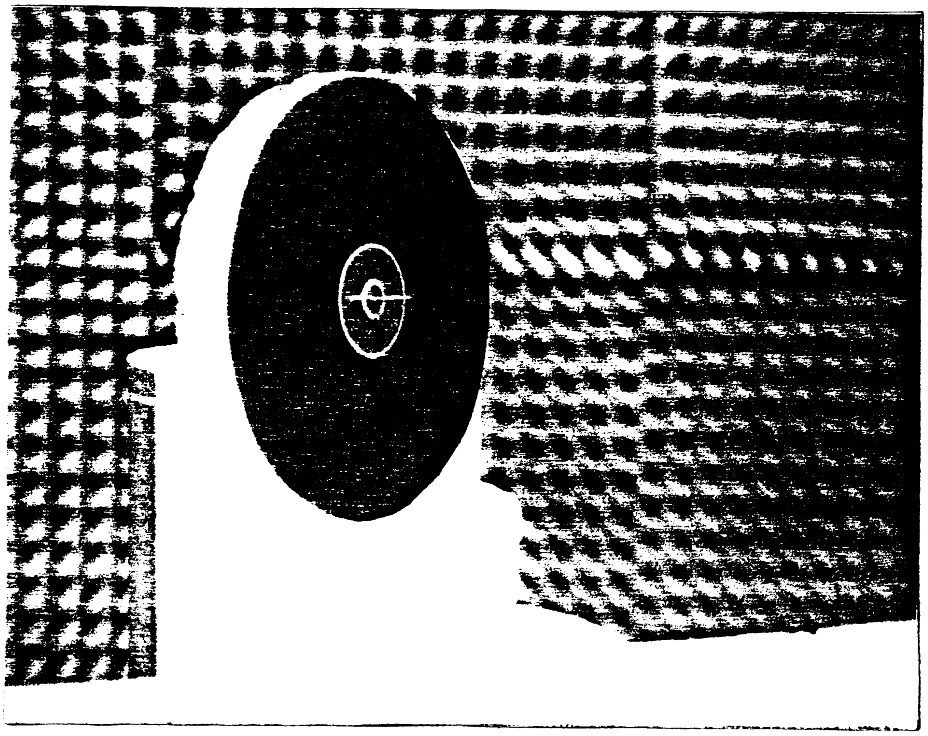

Fig. 5.12 Test Antenna Placement for Measuring the E-Field Pattern.

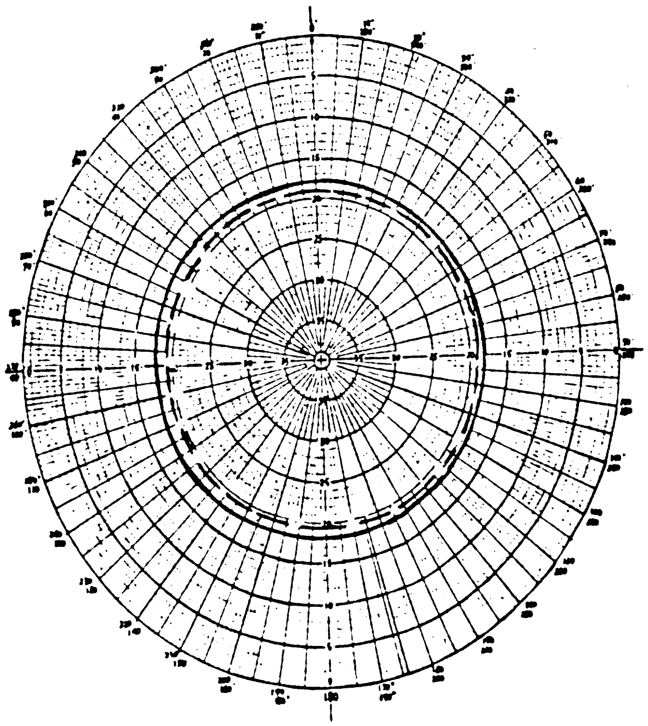

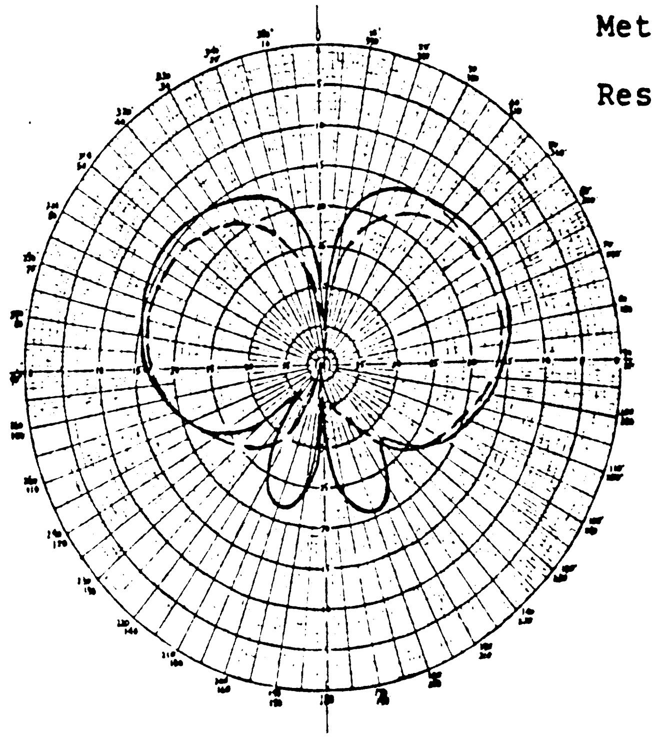

Fig. 5.13 Measured Far Field Patterns at 2.25 GHz.

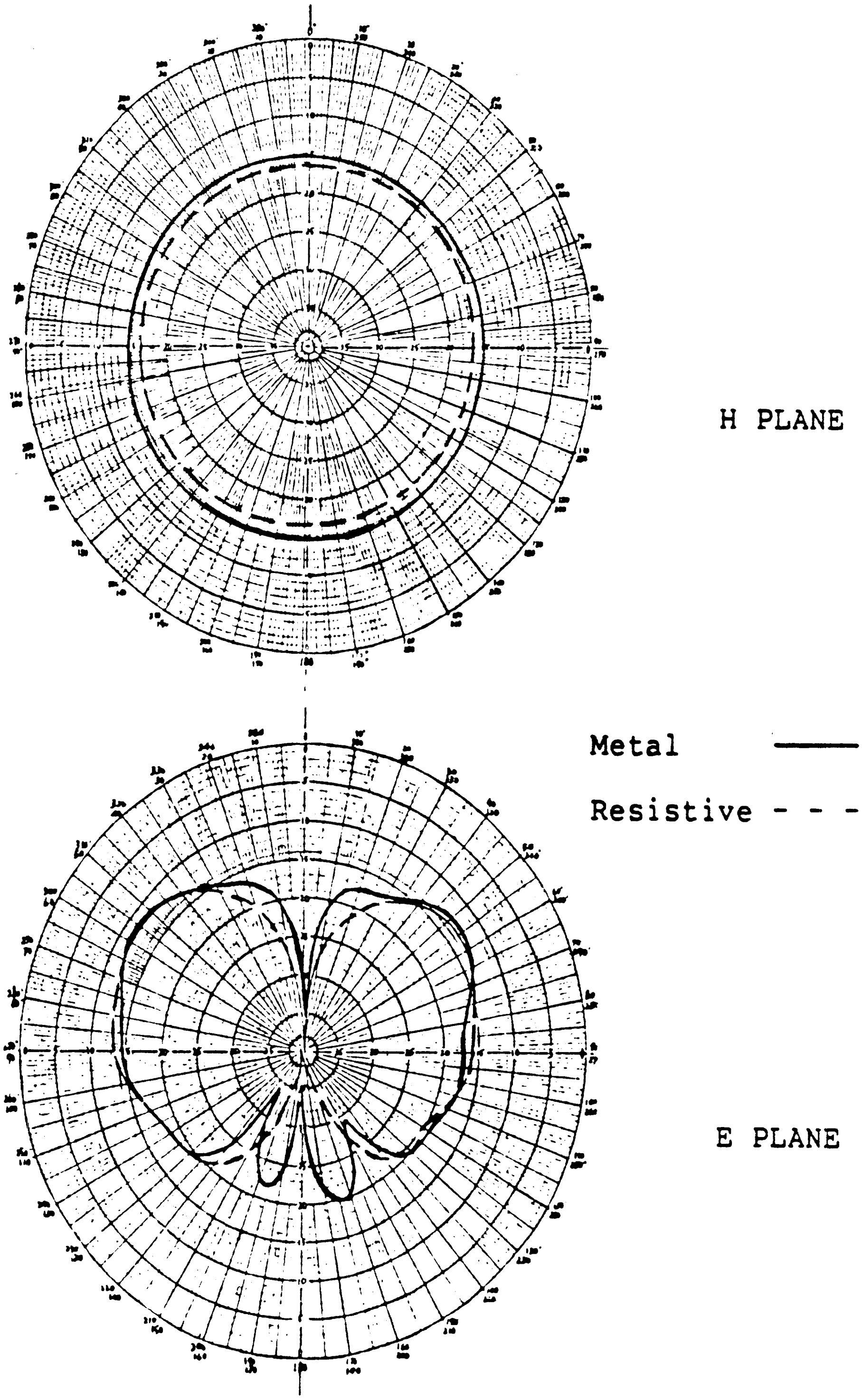

Fig. 5.14 Measured Far Field Patterns at 2.50 GHz.

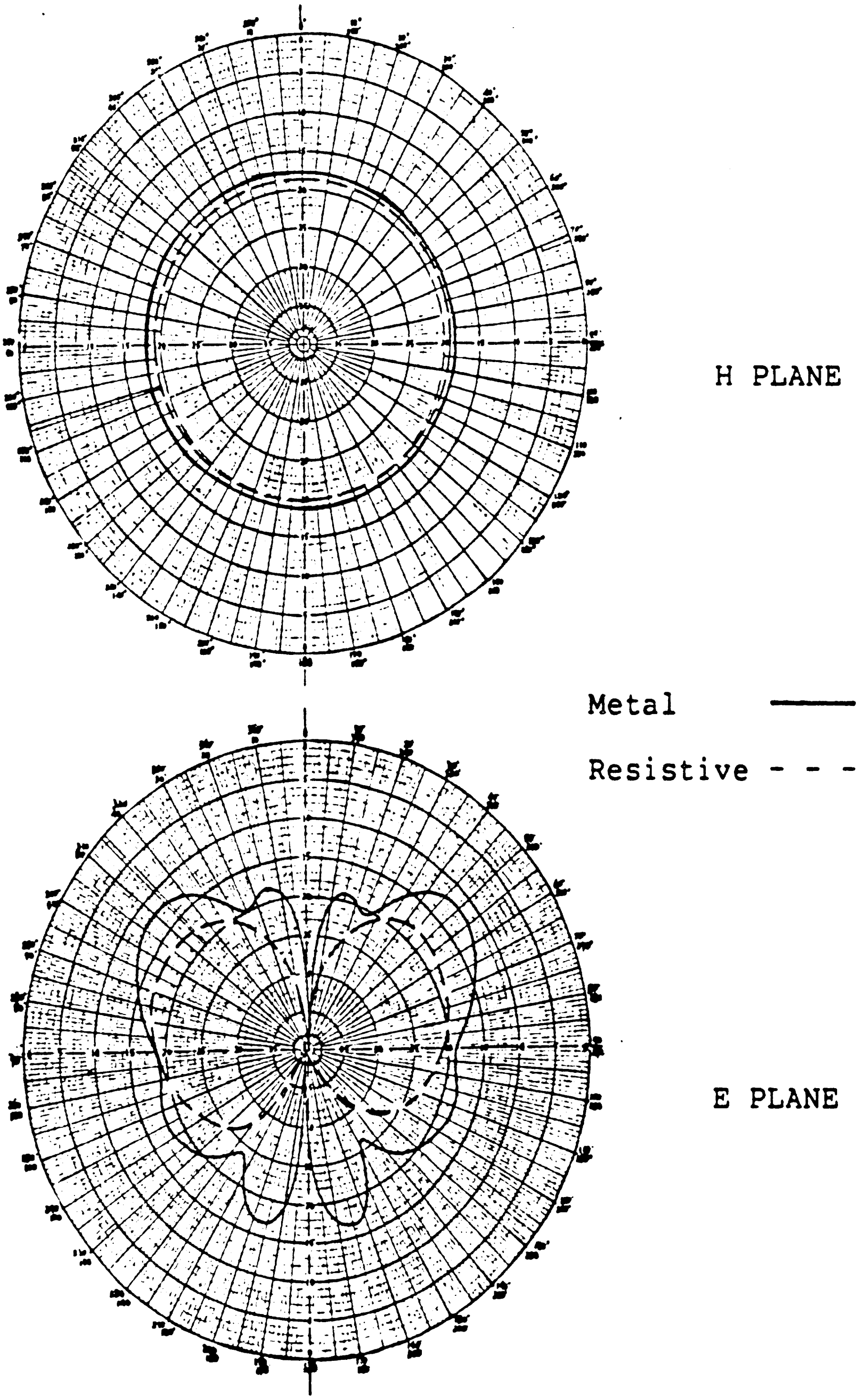

Fig. 5.15 Measured Far Field Patterns at 2.75 GHz.

CHAPTER VI. NUMERICAL STUDIES

6.1 Introduction

The best test of a computer program is to compare the (computed) numerical results with the experimental data. In this chapter a computer program is discussed that was developed to solve the electromagnetic problem of a monopole located at the center of a circular ground plane that can be metallic and/or resistive. The program computes the antenna currents on the monopole as well as on the ground plane, the far field patterns and the antenna impedance. The description of the program is discussed and numerical results relative to experimental data are presented.

6.2 Program Description

The program is called RW.PROJECT which is based on Eqs.(3.28) through (3.47) to solve the current distribution on the monopole and on the ground plane, as well as the far field. The method of integration used in evaluating the integrals of Green's function in the ϕ direction is the four-point Simpson integration. Special attention is given when the observation point falls within the source segment. Detailed analytical evaluation of such a segment is given in Appendix B.

The FORTRAN source program consists of 1454 lines of statements which include the main program and eleven subroutines.

The structure of the program is shown in Fig.(6.1). The entire simulation process is controlled by the routine "PROCES". It governs four important steps, which are : 1) Initialization, 2) Partition, 3) Computation, and 4) Post-processing.

6.2.1 Initialization

Subroutine INITAL

This subroutine is used to initialize all the variables and the constants used in the computation process. Constants such as pi (π), imaginary number (j), mu (μ), the conversion of degrees to radian (DTR), are defined. The variables SOUMAX, OBSMAX, corresponding to the maximum numbers of source points and observation points respectively, are known as programming parameters and are used to control the programming arrays. Variables such as wavelength, the beginning angle (THETA1) and ending angle (THETA2) and its increments (INC) for the far field computation are read. Other variables are used for logic control function, for example, the far field index (FARIDX) which controls if the the measurement of far field is necessary. The resistive segments are also determined in this subroutine.

Flow chart with the top-down approach :

```
                          MAIN
                           ||
    --------------------------------------------------
    ||                     ||                      ||
  ------              ----------                 ------
  INITAL                 PROCES                  OUTPUT

                           ||
    --------------------------------------------------
    ||                     ||                       ||
  ------                 ------                   ------
  READER                 COMPUT                   FARFLD
    ||                     ||
  -------      --------------------------
  SEGMENT      ||          ||          ||
  (LINE)     ------      ------      ------
             DISTAN      GREENS      MULTPY
                           ||
                         ------
                         APPRMX
```

Fig. 6.1 Structure of the Simulation Program.

6.2.2 Partition

(a) Subroutine READER

As the name implies, this subroutine reads all the input data, such as the beginning and the ending segments, voltage and impedance associated with each segment and the curve type (a line or a curve) and the index to calculate the variation of resistivity in each region in a parabolic manner. Since every segment must be defined continuously, it is also used to check for the discontinuous segments by giving an error message if such occur.

(b) Subroutine SLINE

This subroutine places the observation points, the source points and impedance associated with each segment in an array. The segments are partitioned in the way shown in Fig.(6.2), and are divided in such a manner that there are at least twelve points per wavelength. For example, if there are three segments, each has to be divided into ℓ,m,n number of cells, according to a new way of partition. The beginning segment is divided in (ℓ + 1/2) equal divisions. The middle segment is divided into m divisions with the distance between the cells at the end being one half the length of that on the middle. The end segment is also divided into (n + 1/2) equal divisions. This kind of partition has the advantage since the spacing between the two transition

```
        . . . . . .  d      d'...        d" . . . . . .
---X---X---X---X---|--X--X--X--|-----X-----X-----X-----
               A      B     C        D

    Segment 1        Segment 2           Segment 3
```

(a)

```
                 e    e   e'     e'         e"    e"
     . . . .          -   -                 -              . . . . .
                      2   2                 2
----X----X----X--|--X----X----X--|--X------X------X-----
              A'    B'        C'    D'
```

(b)

Where $\overline{AB} > \overline{A'B'}$

$\overline{CD} > \overline{C'D'}$

Fig. 6.2 Diagram Showing how the Segments are Partitioned; (a) Old Method, (b) New Method.

regions $\overline{A'B'}$ or $\overline{C'D'}$ is smaller than $\overline{AB}$ or $\overline{CD}$ as shown in Fig.(6.2). Also in the transition region (e+e')/2 is smaller than (d+d'). Though e and e' is a little larger than d and d' since

$$d = \frac{\text{Distance of each segment}}{n} \tag{6.1}$$

$$e = \frac{\text{Distance of each segment}}{n + 1/2} \tag{6.2}$$

and, for large n, $d \simeq e$.

With this kind of partition, a more accurate result is obtained as compared to the partition by the old method, as there is no discontinuity in the transition region between two adjacent segments.

6.2.3 Computation

(a) Subroutine DISTAN

The subroutine is used to compute the distance between the source point and the observation point. These distances are denoted as DS and DSS, which are defined as R_1 and R_2 in Eqs.(B.7) and (B.11).

Thus,

$$DS = [(r_i - r_j)^2 + (z_i - z_j)^2]^{1/2} \tag{6.3}$$

$$DSS = [(r_i + r_j)^2 + (z_i - z_j)^2]^{1/2} \qquad (6.4)$$

There are eight integrals to be evaluated in Eq.(3.28). Using a three-point Simpson's integration, there should be at least twenty-four DSs and DSSs, since some distances are repeated, only fifteen of such values are required for each value of i and j.

(b) Subroutine COMPUT

This subroutine is the center of computation process which evaluates the MOM impedance matrix in Eq.(3.28). To compute the Green's function integrals, routine "GREENS" is called. After computation, the MOM [Z] matrix is solved by using routine "MULTPY".

(c) Subroutine GREENS

The integrals involving Green's function in Eq.(3.28) are evaluated in this subroutine. Since there are eight integrals to be integrated, they are denoted as G1 through G8 in the computation. Three point Simpson integration is used for the t integration whereas four-point Simpson's integration is used in the ϕ integration, which enhance the accuracy of the results. Special attention is given when the observation point lies within the source segment. If special treatment is needed, routine "APPRMX" is called.

(d) Subroutine APPRMX

As |R - R'| approaches to zero which makes the integrals of the Green's function in Eq.(3.28) to become singular, subroutine APPRMX is called upon, which is based on Eq.(B.1) through Eq.(B.16) in Appendix B. This routine also calls subroutine ELTKP if the elliptical function of the first kind is necessary in the computation.

(e) Subroutine ELTKP

Subroutine ELTKP is used to compute the elliptical function of the first kind K(m)

where

$$K(m) \simeq a_o+a_1m_1+a_2m_1^2+a_3m_1^3+a_4m_1^4-\ln(m_1)(b_o+b_1m_1+b_2m_1^2+b_3m_1^3+b_4m_1^4) \tag{6.5}$$

$$m_1 = 1 - m \tag{6.6}$$

where

$a_o \ldots\ldots a_4$, $b_o \ldots\ldots b_4$ are given in the Handbook of Mathematical Functions by Abramowitz and Stegan [34].

(f) Subroutine MULTPY

The final phase of computation is to solve the [N by N] matrix . This routine is used for solving the matrix [Z] using Gaussian's elimination method to determine the current distribution [I] on the monopole and on the ground plane. Once $[Z]^{-1}$ is known, the current is obtained by

$$[I] = [V]\,[Z]^{-1} \tag{6.7}$$

The elements in the excitation matrix [V] given in Eq.(6.7) are usually zero except at the source point (which is the voltage across the gap) for the radiation problem discussed here.

6.2.4 Post-processing

Subroutine FARFLD

The computed current distribution obtained from the matrix inversion of $[Z]_{ij}$, the MOM impedance matrix, can be used for calculating the far field. This is done by evaluating Eq.(3.47) in which the Bessel functions of the first kind (J_o and J_1) are computed. The scattered far field are then obtained by multiplication of the current distribution [I] and the MOM matrix $[Z]_n$, Eq.(3.45). Subroutine "FARFLD" is the final phase of the simulation process, it is an optional feature. Its operation is controlled by the index "FARIDX", which is initialized in the subroutine "INITAL".

6.3 Numerical Results

In this section, numerical results are presented for the current distribution on the ground plane with the monopole located at the center of the ground plane. A gap voltage of one volt (rms) is applied between the ground plane of size 12 cm and the monopole whose height is 2.68 cm with a radius of 0.048 cm. The gap width used in the computation is 0.048 cm, the same as the monopole radius. Comparisons are made between : i) the finite size ground plane (12 cm in radius), ii) our model, a ground plane (12 cm in radius) with tapered resistive sheet, and iii) a large size ground plane (60 cm in radius).

Figure (6.3) shows the effect of gap distance on the input impedance of a half-wave dipole (height 0.461 wavelength, radius = 0.0053 wavelength). As noted, the input resistance is relatively independent of gap width which varies from 0.001 wavelength to 0.04 wavelength, but the input reactance changes significantly when the gap is shortened. A large negative reactance shows that the capacitive component is very dominant when the gap is small. For this study it was concluded that the gap width for the practical antenna should be about the same as the diameter of the antenna in order to escape the drastic capacitive effect.

The impedance of the monopole (height 2.68 cm, radius 0.048 cm) on different ground planes, i) a finite size ground plane (12 cm in radius) with resistive edge, and ii) without resistive edge, and iii) a large ground plane (60 cm in radius) were computed for different frequencies from 1875 MHz to 3750 MHz and are shown in Fig.(6.4). Although improvement is not very pronounced, the finite size

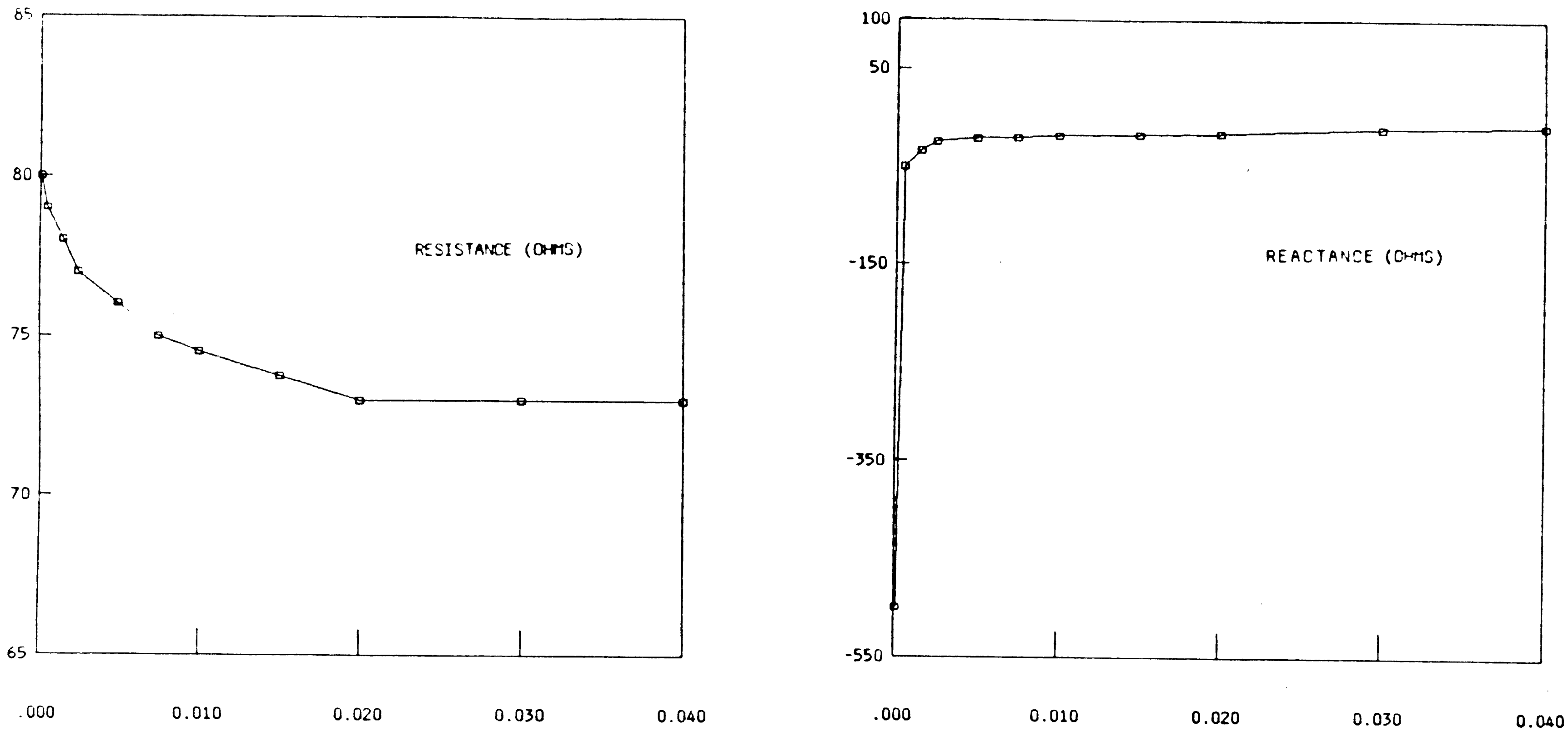

Length of Dipole : 0.461 Wavelength

Radius of Dipole : 0.005 Wavelength

Gap Width in Wavelength

Fig. 6.3 Effect of Gap Width on Impedance of a Half-Wave Dipole.

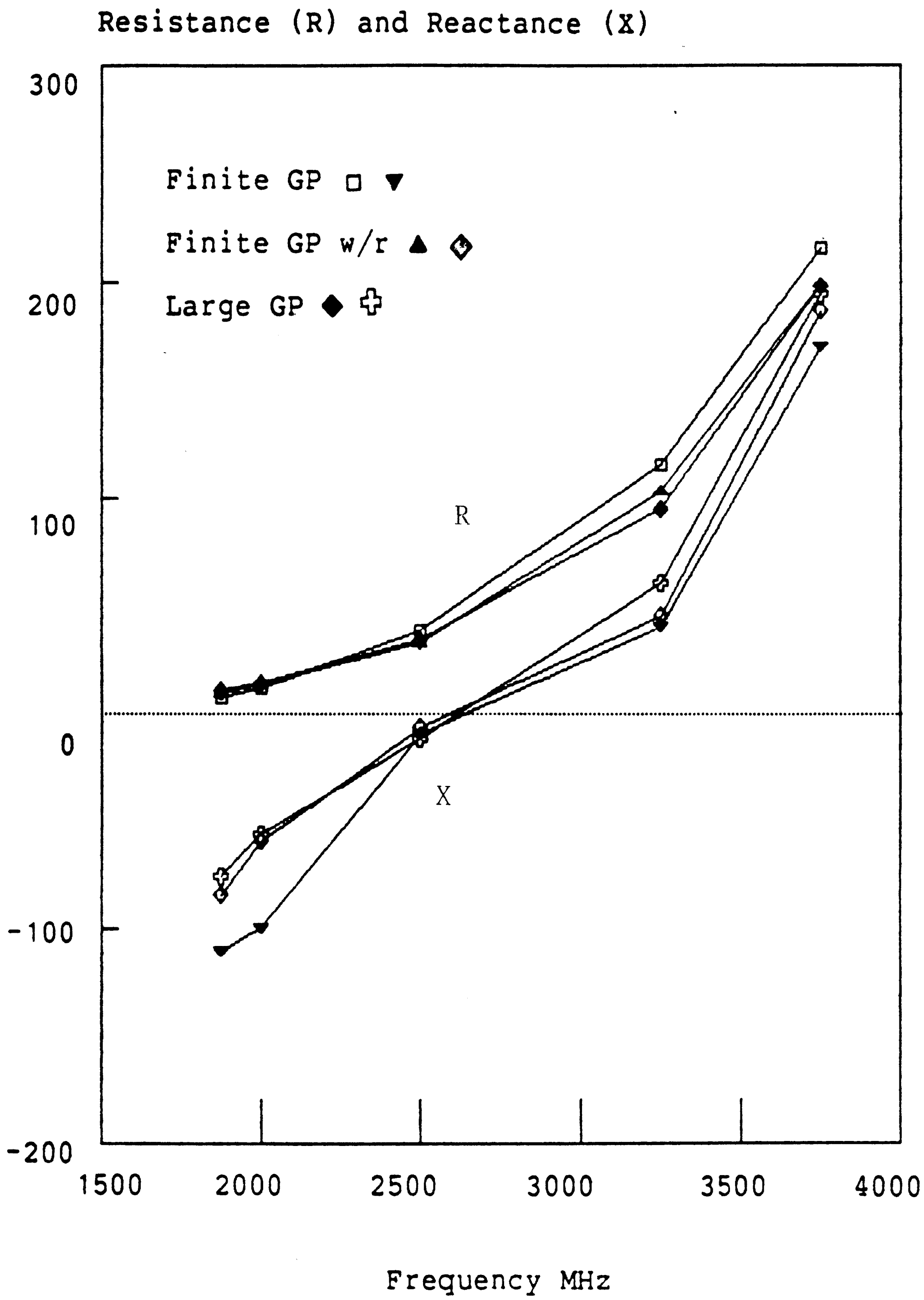

Fig. 6.4 Compute. Monopole Impedance for Various Ground Planes (Height 2.68 cm) vs. Frequency.

ground plane with resistive edge shows a good approximation to the large size ground plane. It is noted that, since the monopole is of height 2.68 cm (0.223 wavelength), it is shorter than 0.235 wavelength that typically would resonate at 2500 MHz. This explains why slight capacitive components are present at 2500 MHz.

Figure (6.5) shows the monopole impedance as a function of the ground plane size. Computed results are for metal and resistively treated ground planes. For the metallic ground plane case, the results are compared with Meier & Summers' [1] experimental data. The metallic ground plane varies from 0.25 wavelength to 2.0 wavelength in radius in both Meier and Summer's experiments and our numerical computations. The resistive ground plane was made of metal of 0.25 wavelength radius, plus an added tapered resistive sheet (0-1000 ohms/sq.) whose width ranges from zero to 1.75 wavelength. The monopole is of height 0.223 wavelength and radius 0.003 wavelength. With the resistive ground plane at small radii, the resistive strip is narrow and hence the curve begins the same as for the metallic one. For ground plane radius one wavelength and larger, the impedance is almost constant as one would expect for the infinite size ground plane. This shows that tapered resistance can match the surface field.

Figure (6.6) shows the comparison of the current on a metallic ground plane for different radii of the monopoles

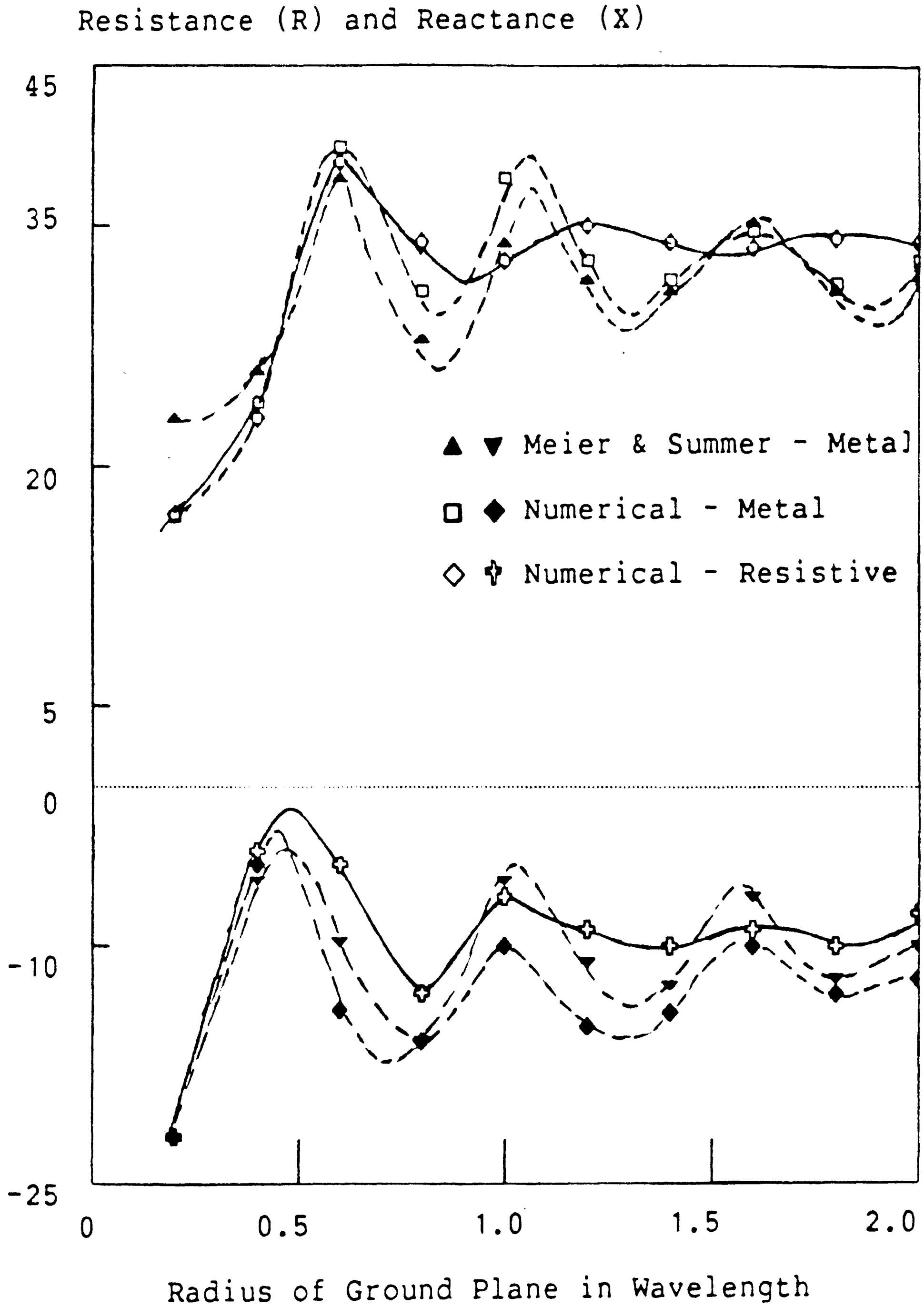

Fig. 6.5 Impedance of Monopole (Height 0.223 Wavelength, Radius 0.004 Wavelength) vs. Ground Plane Size at 2500 MHz.

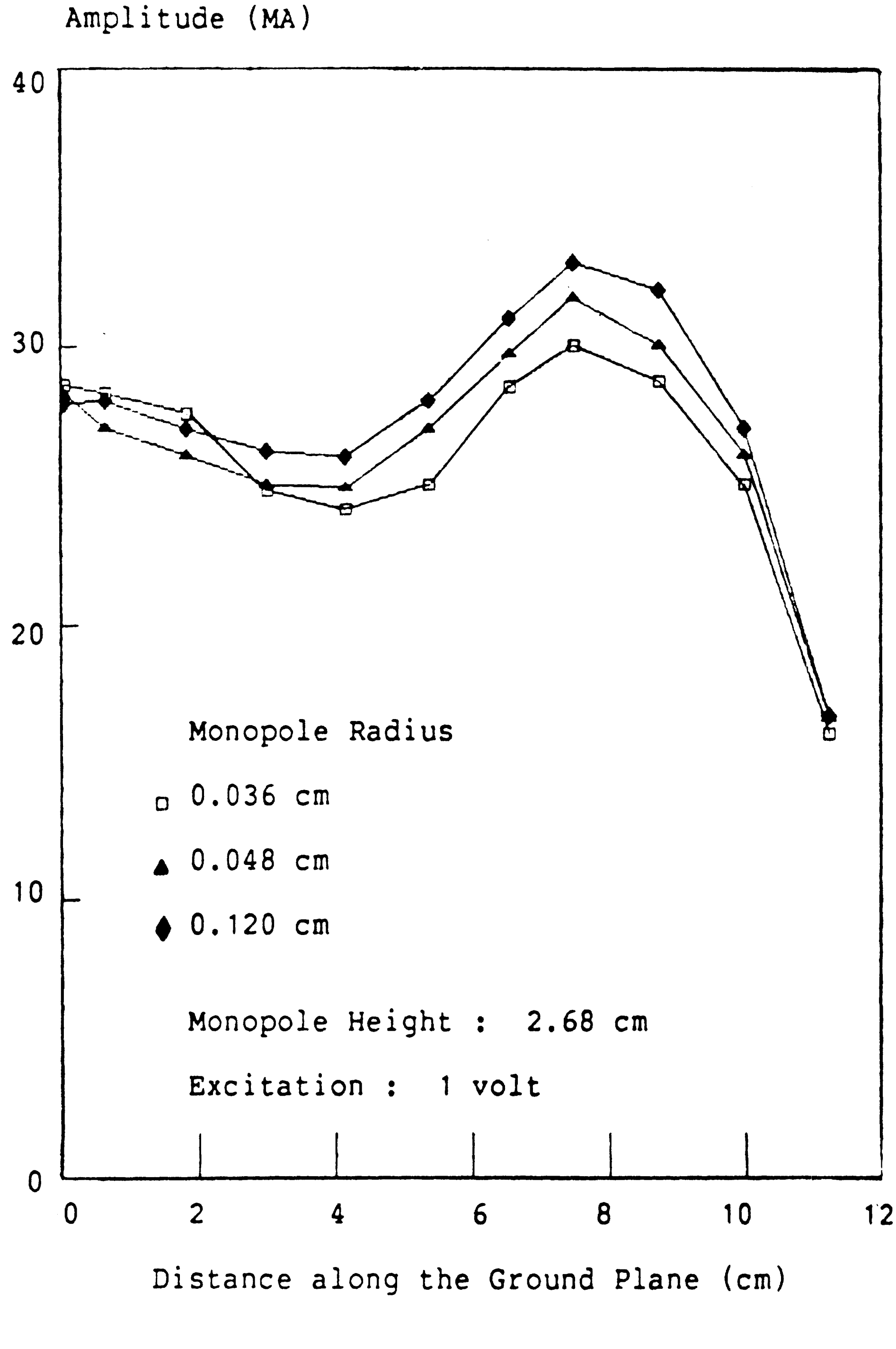

Fig. 6.6 Current Distribution on Ground Plane with Different Monopole Radii at 2500 MHz.

(0.003, 0.004, 0.01 wavelength; height 0.223 wavelength) at 2500 MHz. As can be seen, the current distribution on the ground plane does not change significantly for these different radii of the monopole.

With the monopole (height 2.68 cm, radius 0.048 cm), at the center of a circular ground plane (radius 12 cm), the current distributions on the ground plane are compared in Fig.(6.7) through Fig.(6.10) for metallic and resistive ground planes. Consider first the metallic ground plane, at 1875 MHz and 2500 MHz the ground plane radii are less or equal to one wavelength, hence one current minimum is observed in Fig.(6.7) and Fig.(6.8). At 3000 MHz and 3750 MHz, the radii of the metallic ground planes are 1.2 wavelength and 1.5 wavelength respectively, and consequently two minima are observed in Fig.(6.9) and Fig.(6.10). With the resistive ground plane there are no minimum other than at the feed point (monopole) and the outer edge. Therefore, one can conclude that with resistive treatment the effects of travelling waves are minimized.

Figure (6.11) shows the comparison of the current distribution on the monopole (height 2.68 cm, radius 0.048 cm), i) for a ground plane with resistive edge and ii) a ground plane without resistive edge (each has 12 cm in radius). The magnitude of current does not vary significantly. The phase of the currents on the monopole on the metallic ground plane and the resistive one have

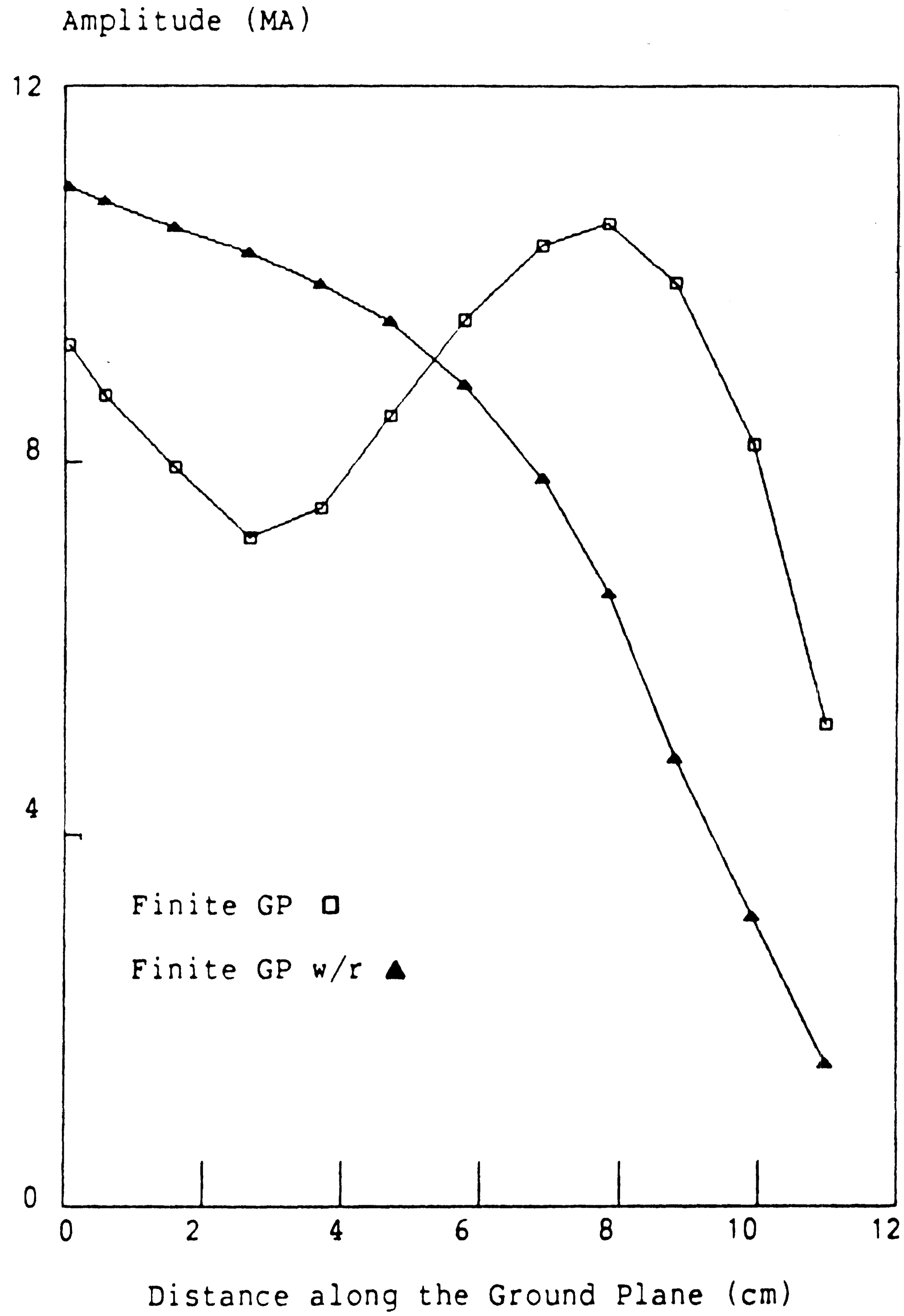

Fig. 6.7 Current Distribution on Ground Plane at 1875 MHz (Monopole Height 2.68 cm, Radius 0.048 cm, Excitation 1 volt).

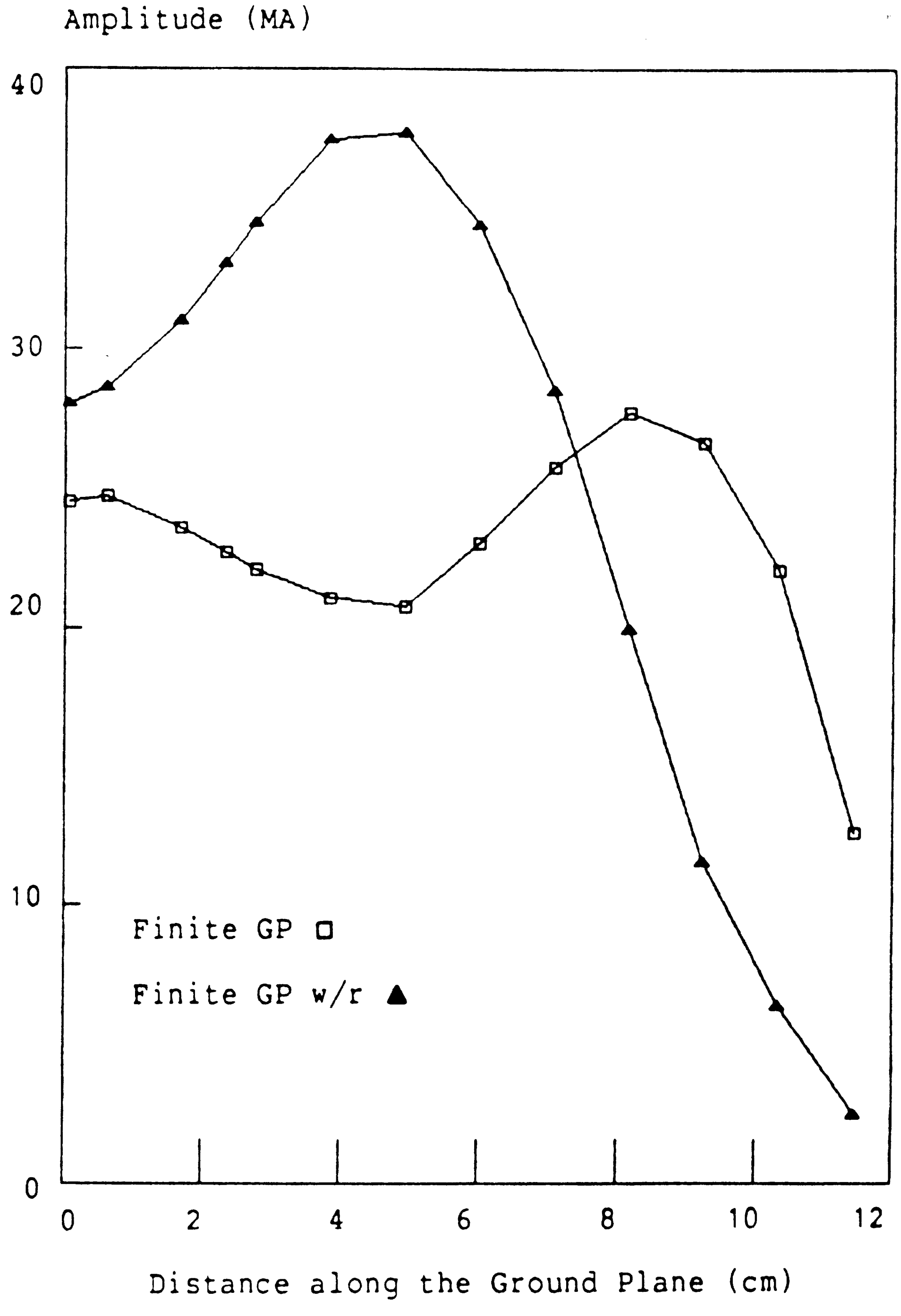

Fig. 6.8 Current Distribution on Ground Plane at 2500 MHz (Monopole Height 2.68 cm, Radius 0.048 cm, Excitation 1 volt).

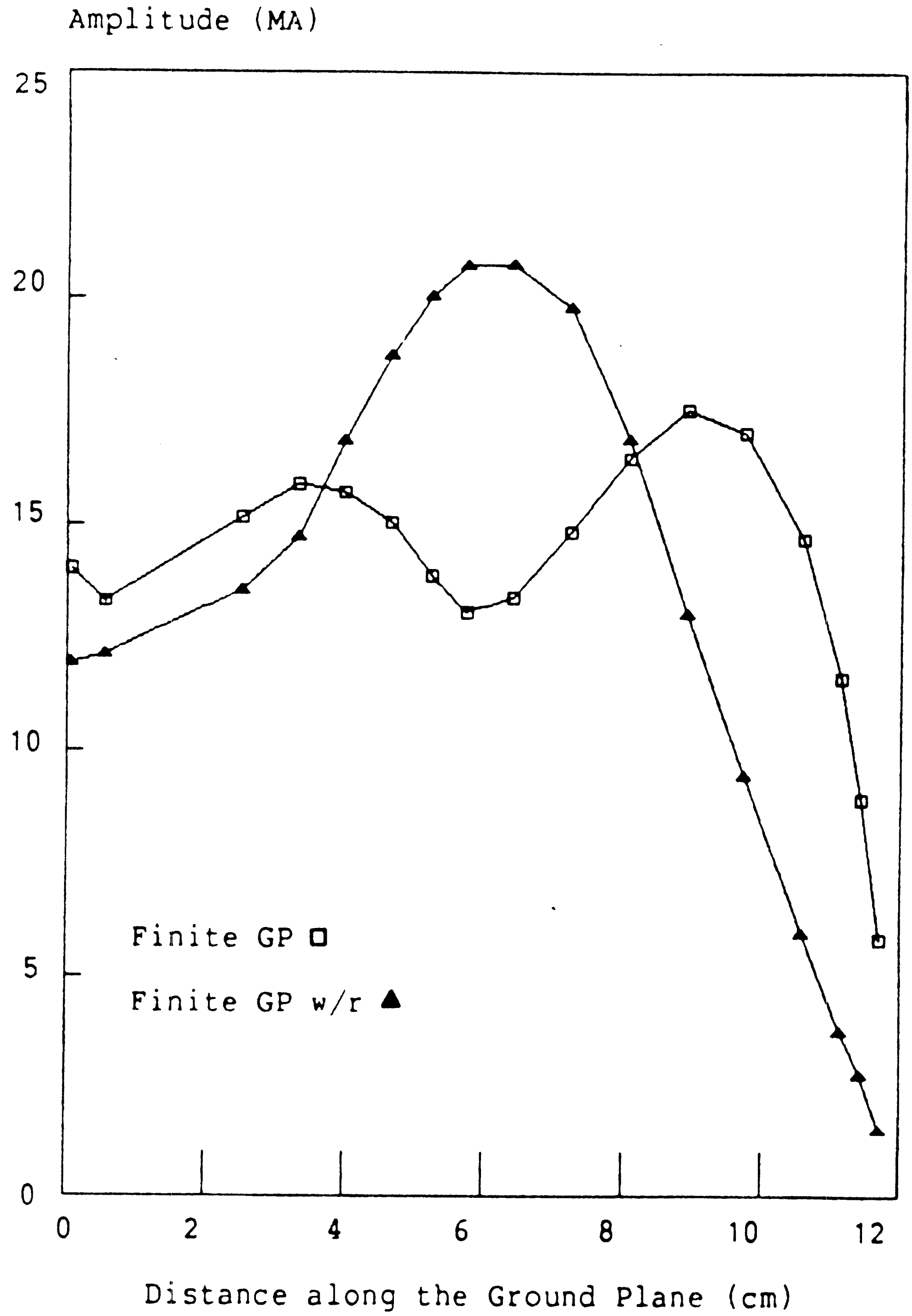

Fig. 6.9 Current Distribution on Ground Plane at 3000 MHz (Monopole Height 2.68 cm, Radius 0.048 cm, Excitation 1 volt).

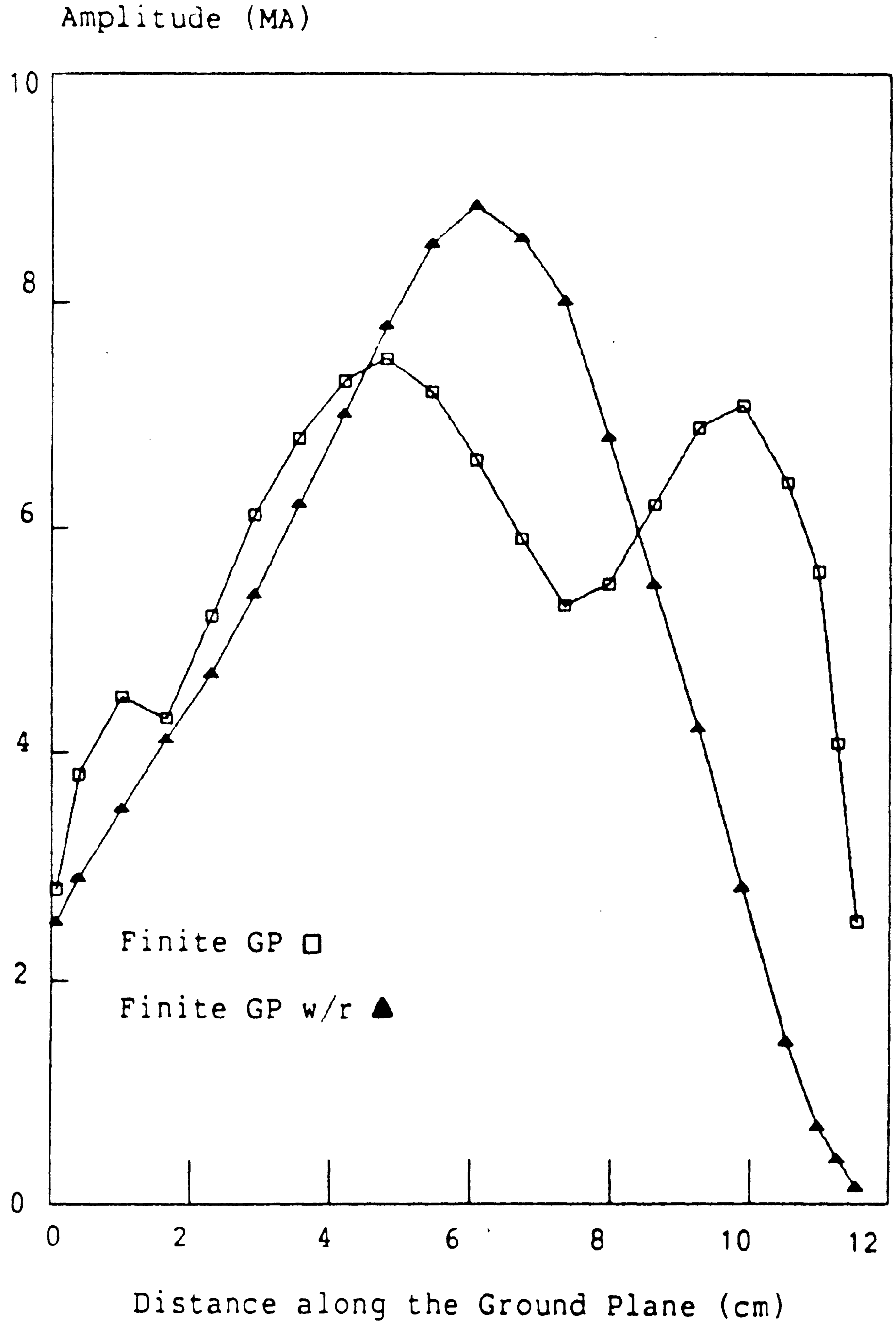

Fig. 6.10 Current Distribution on Ground Plane at 3750 MHz (Monopole Height 2.68 cm, Radius 0.048 cm, Excitation 1 volt).

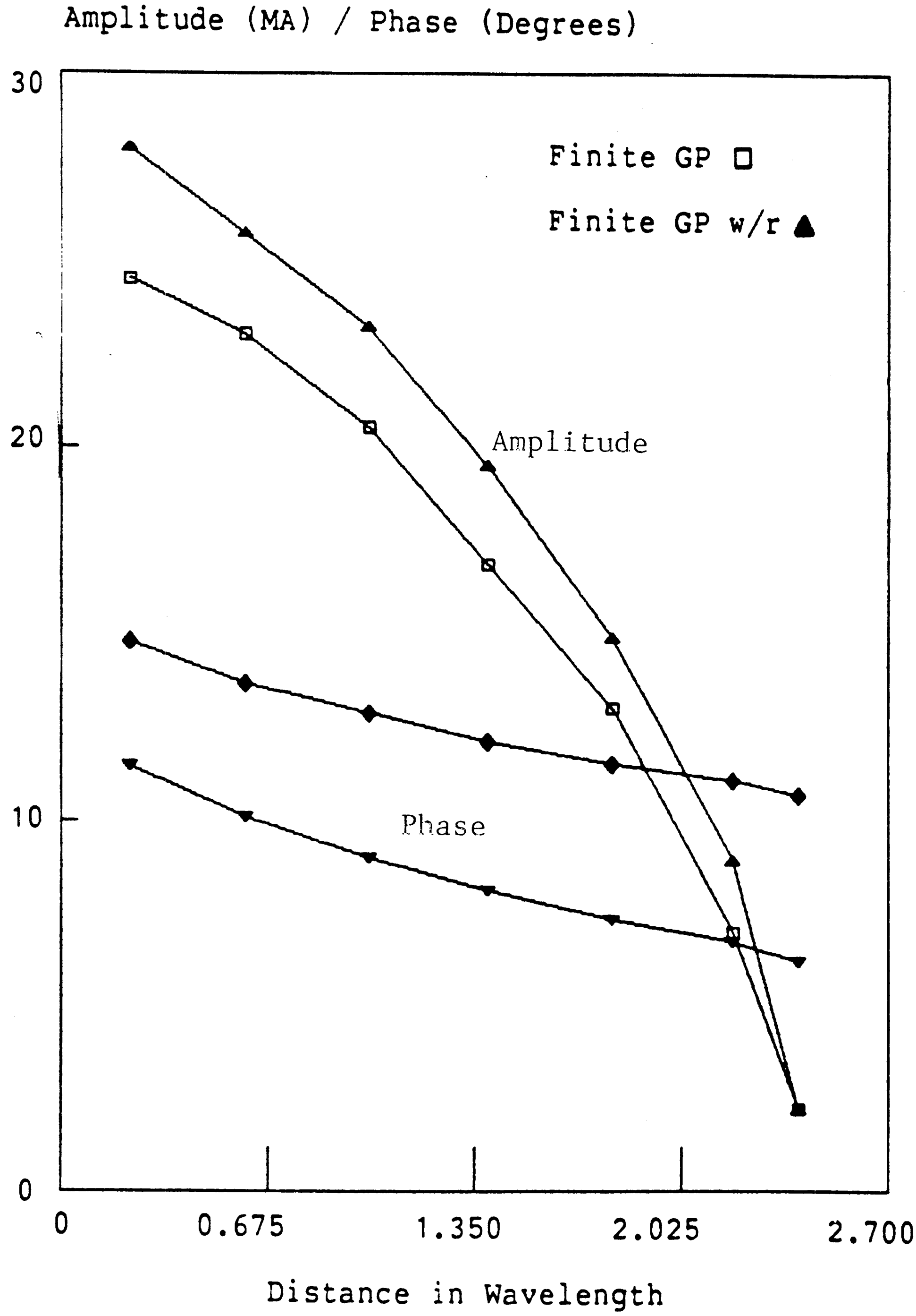

Fig. 6.11 Current Distribution on Monopole (Height 2.68 cm, Radius 0.048 cm, Excitation 1 volt) at 2500 MHz.

positive phase which indicate that the impedance of the monopole is capacitive because the height of the monopole which is 0.223 wavelength at 2500 MHz is shorter than the resonance length.

The computed far field patterns are shown in Fig.(6.12) through Fig.(6.14). As in the experimental cases, the side lobes are eliminated when a resistive ground plane is used. In the computation, the ground plane radius is 12 cm, monopole height is 2.68 cm and radius is 0.048 cm, the frequencies used for far field computations are 2.25 GHz, 2.50 GHz and 2.75 GHz.

6.4 Comparison Between Experimental and Numerical Results

It is a good practice to use experimental data to verify numerical simulations, especially when computations are approximated to make them feasible. Here, comparisons are made between the experimental and numerical cases. The monopole impedance as a function of frequency as well as the far field patterns (E field patterns) are plotted and tabulated.

Table (6.1) shows the comparison between the numerical and experimental results for the impedance of the monopole (height 2.68 cm, radius 0.048 cm) at 1.875 GHz, 2.5 GHz, and 3.75 GHz. Various ground planes are used, i) the finite size ground plane (12 cm radius), ii) the finite size ground plane with resistive sheet (also 12 cm in radius) and, iii) the large ground plane (60 cm in

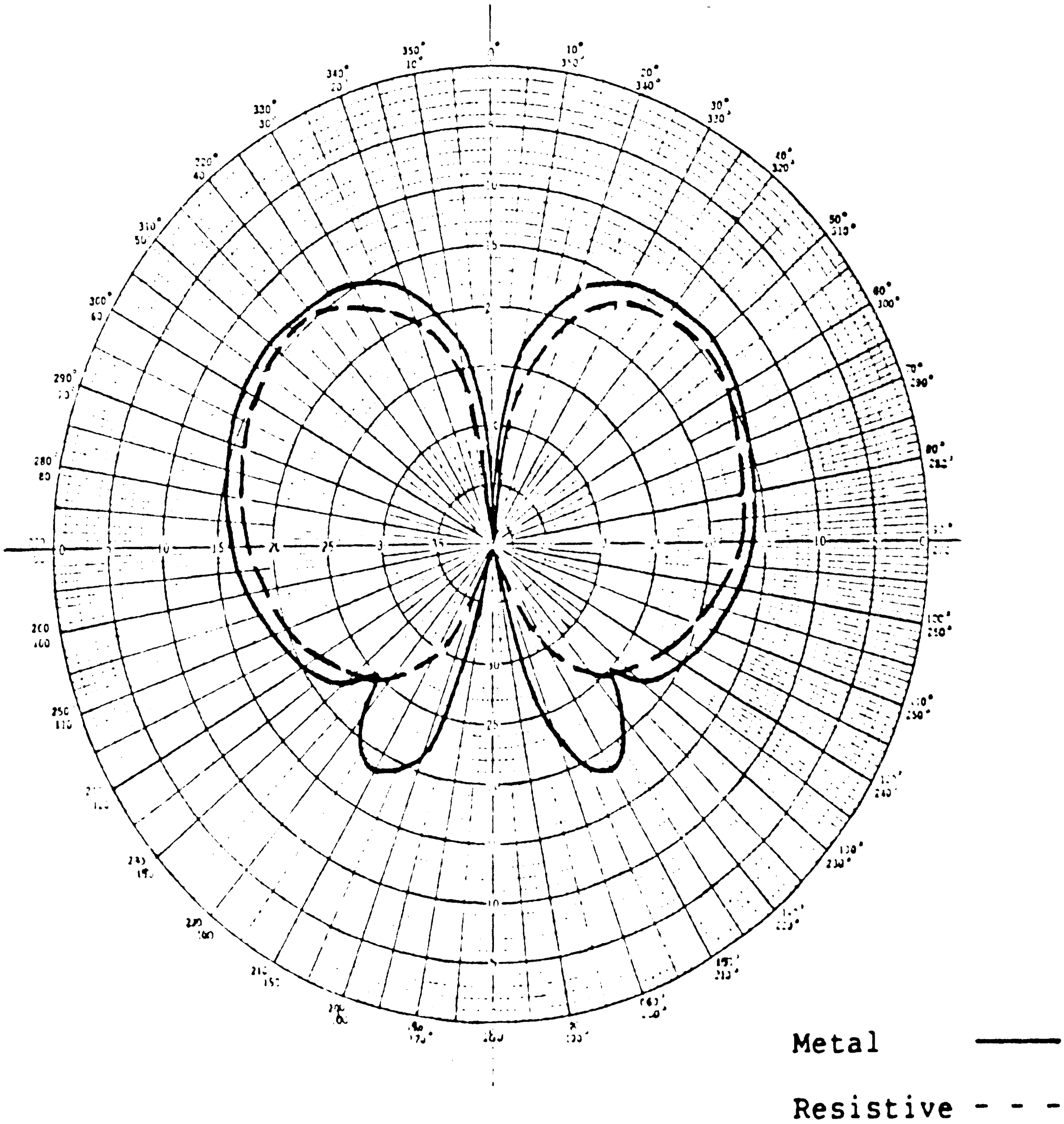

E PLANE

Fig. 6.12 Computed Far Field Patterns at 2.25 GHz.

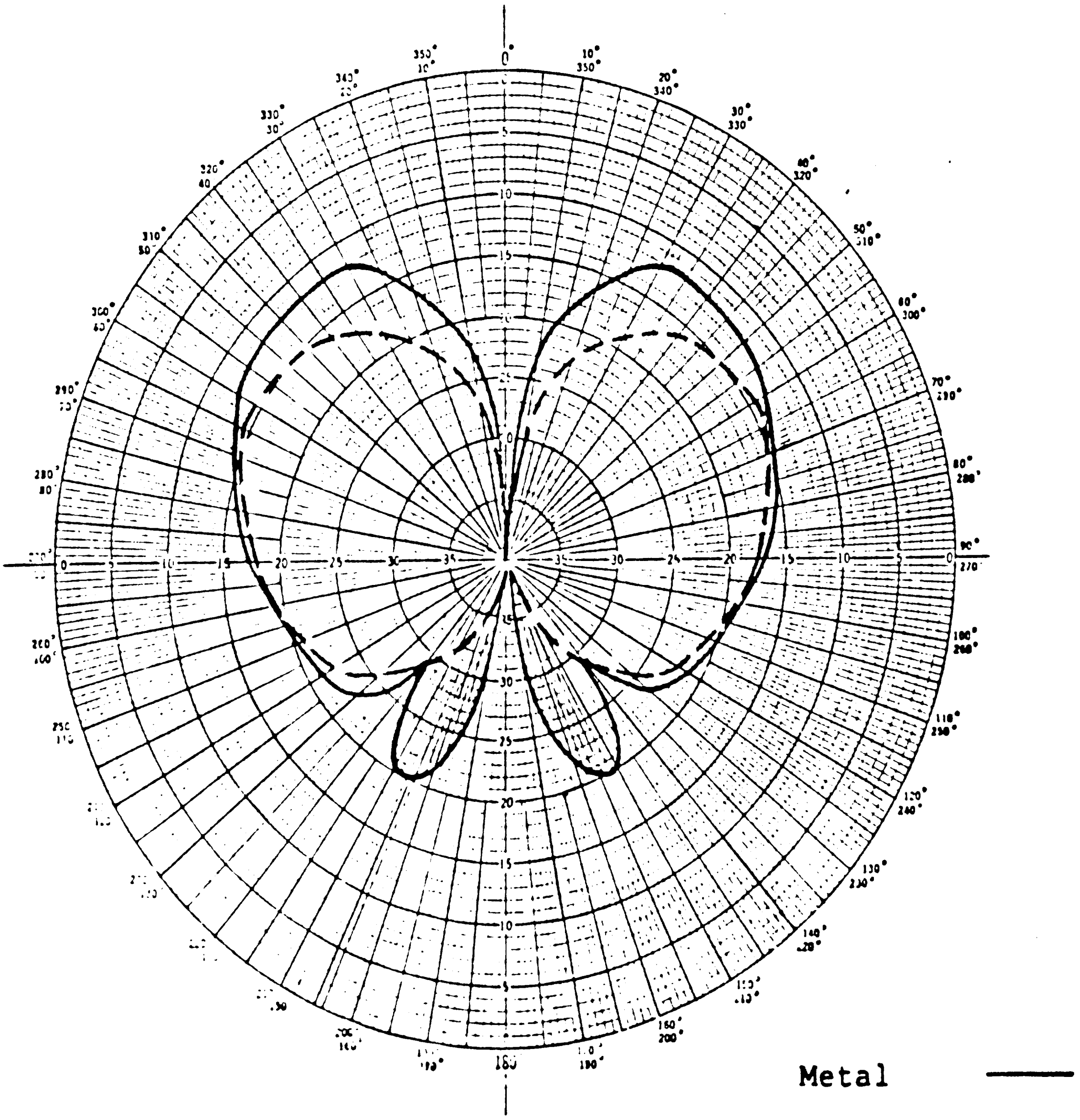

E PLANE

Fig. 6.13 Computed Far Field Patterns at 2.50 GHz.

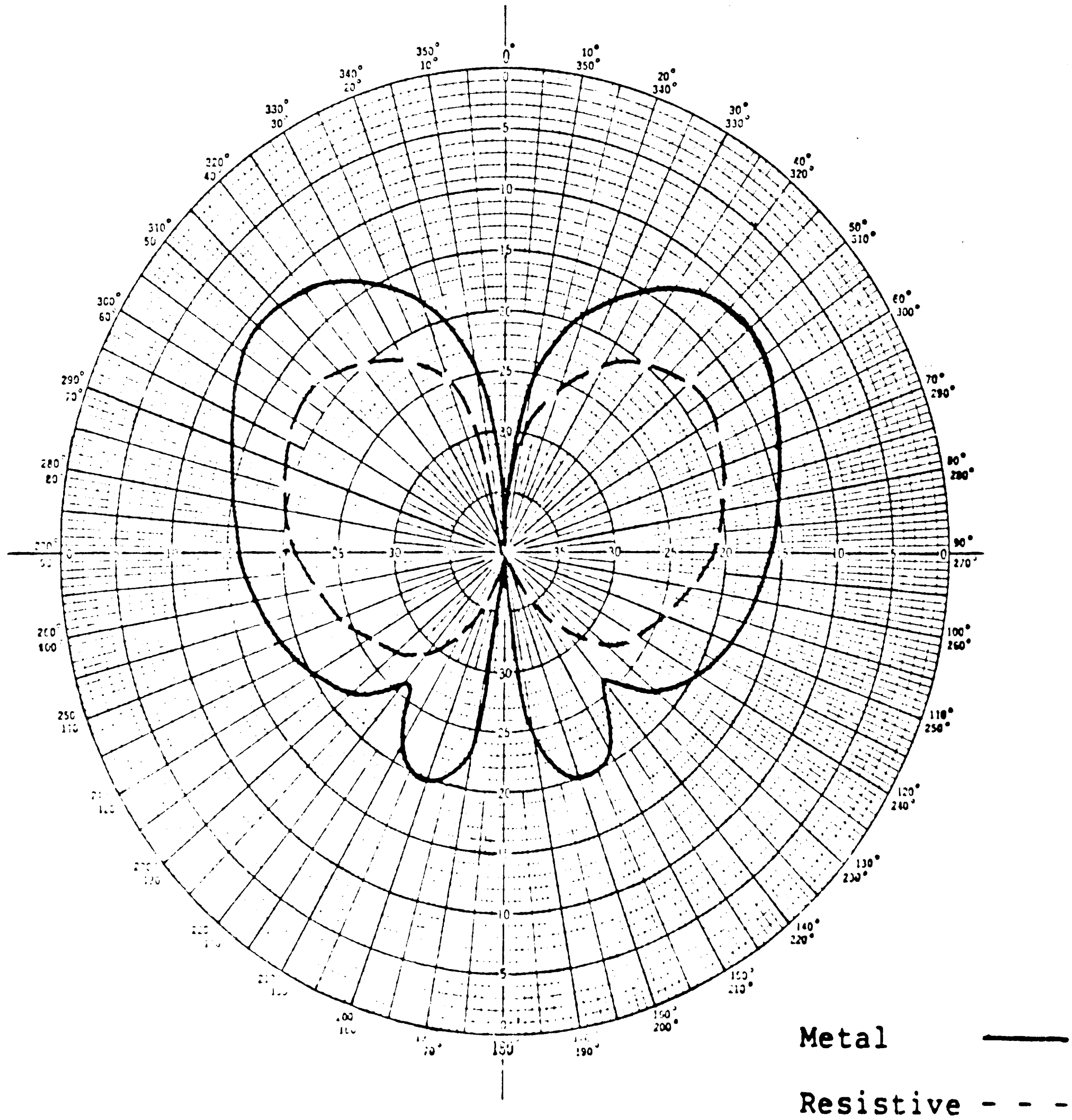

E PLANE

Fig. 6.14 Computed Far Field Patterns at 2.75 GHz.

Frequency (MHz)	Finite Ground Plane (Radius : 12cm)		Finite Ground Plane with resistive sheet (Radius : 12cm)		Large Ground Plane (Radius : 60cm)	
	Theory	Experiment	Theory	Experiment	Theory	Experiment
1875	$7.4 - j111$	$7.2 - j100$	$8.9 - j85$	$8.4 - j73$	$10 - j76$	$10.8 - j77$
2000	$11 - j102$	$10.1 - j90$	$13 - j60$	$12.8 - j58$	$14.3 - j56$	$14 - j62$
2500	$38 - j10$	$37.8 - j5$	$32.8 - j6.8$	$32.5 - j8.8$	$33.8 - j12$	$33.1 - j8.5$
3250	$115 + j40$	$119 + j36$	$103 + j45$	$97.5 + j40$	$95 + j60$	$93.1 + j52$
3750	$216 + j170$	$208 + j214$	$199 + j186$	$192 + j170$	$198.2 + j195$	$194 + j187$

Height of Monopole : 2.68 cm

Radius of Monopole : 0.048 cm

Table 6.1 Comparison of Monopole Impedance - Theory and Experiment.

radius) which is used for comparison. Close agreement exists between the experimental model and the numerical cases. The monopole impedance on the finite size ground plane with resistive edge is a close approximation to that of a large ground plane.

Figures (6.15) through (6.17) show the far field pattern of the same monopole on the finite size metallic ground plane and the resistive one at three different frequencies, 2.25, 2.5 and 2.75 GHz. Close agreement again exists between numerical and experimental data. The large size ground plane (60 cm in radius) was not used in the comparison because it was impossible to mount it and rotate it for the antenna measurements. Another factor was the size of the anechoic room, in which it was not feasible to obtain the far field criterion $2D^2/\lambda$ using the large ground plane diameter for D.

It has been shown that good agreement exists between the numerical simulation and experimental data. Since the difference between the numerical and the experimental data of the antenna impedance and the far field patterns is typically only five percent or less, this provides a good verification that numerical computations or simulation codes are valid.

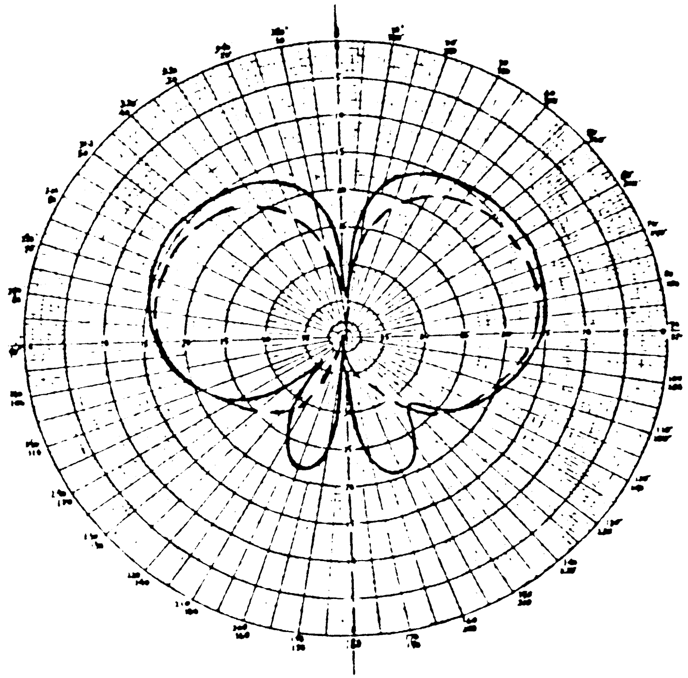

Measured

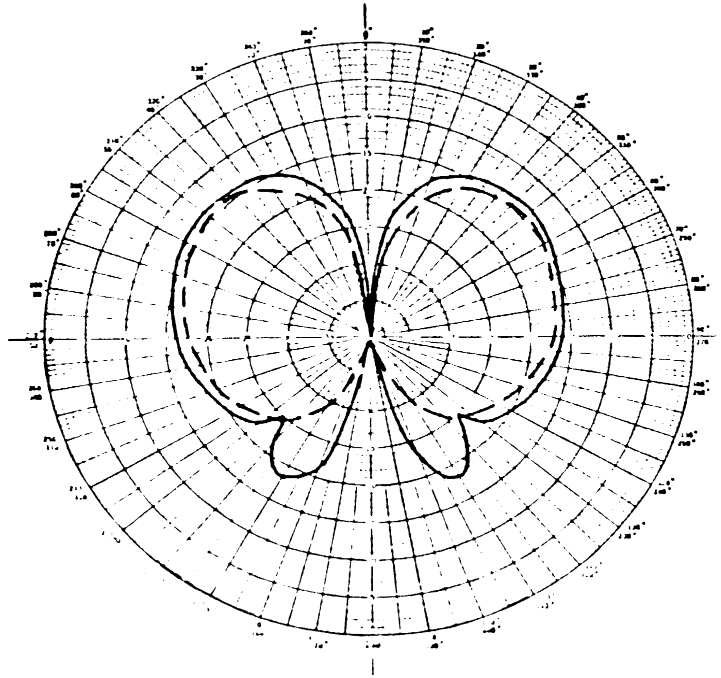

Computed

Metal ———

Resistive - - -

Fig. 6.15 Comparison of Measured and Computed Far Field Patterns at 2.25 GHz.

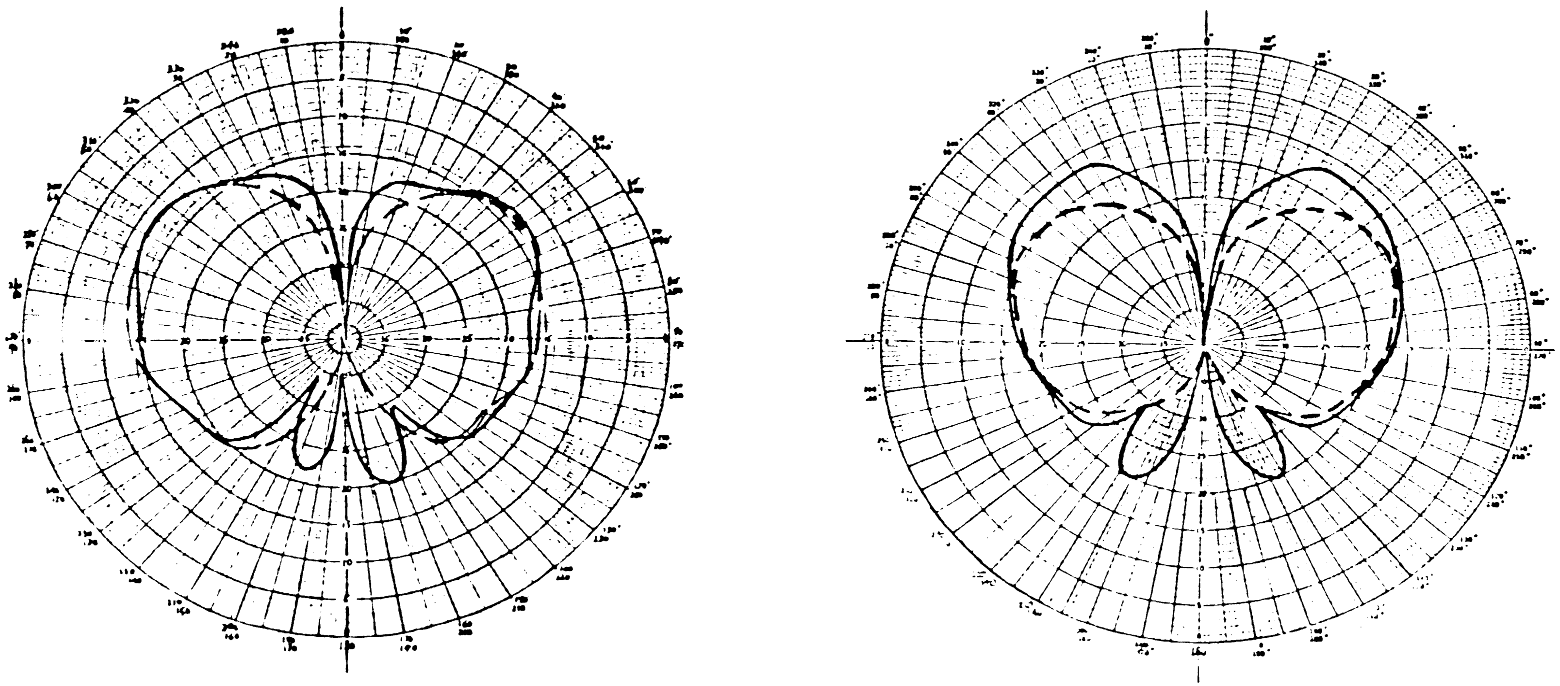

Measured

Computed

Metal ———

Resistive - - -

Fig. 6.16 Comparison of Measured and Computed Far Field Patterns at 2.50 GHz.

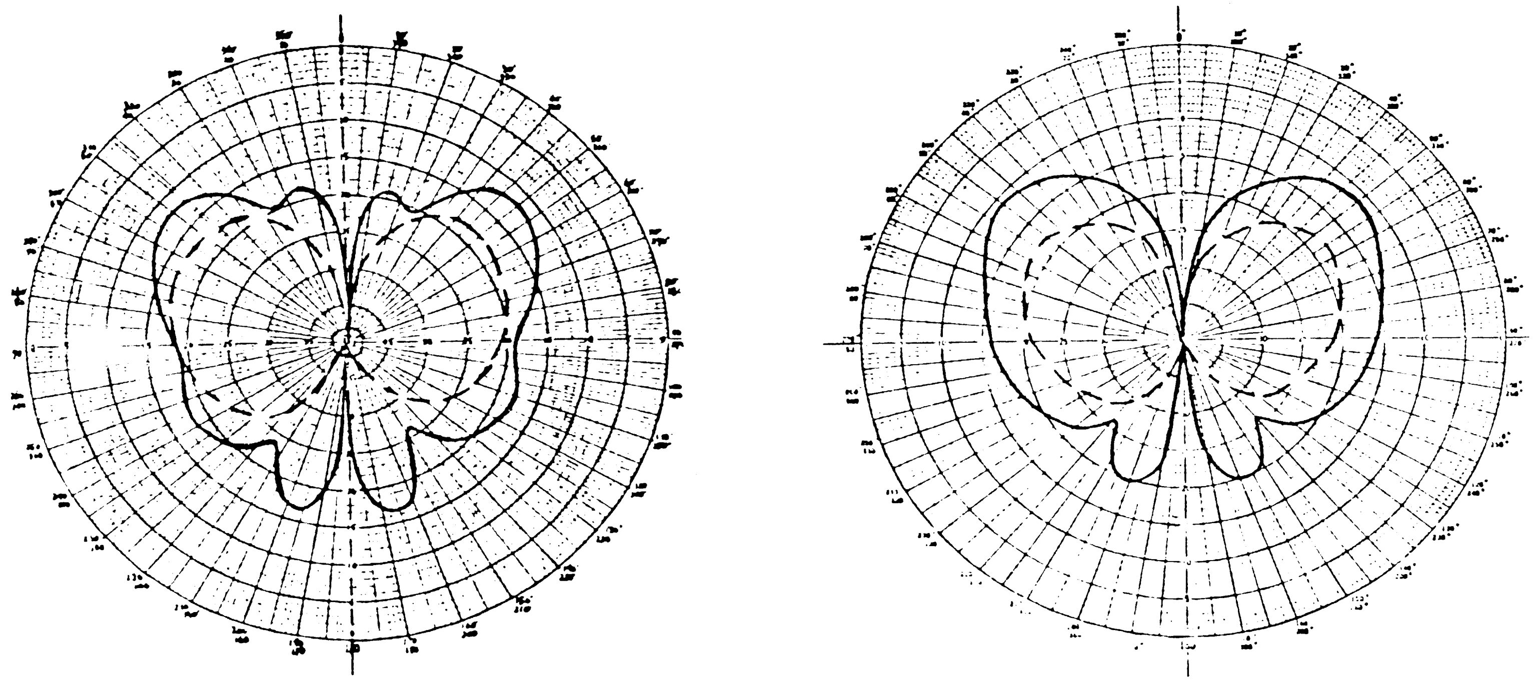

Measured

Metal -----

Resistive - - -

Computed

Fig. 6.17 Comparison of Measured and Computed Far Field Patterns at 2.75 GHz.

CHAPTER VII. CONCLUSIONS

The problem of a monopole located on a finite size circular ground plane is solved using the surface of revolution technique and the method of moments. The resistive boundary condition is also included in the formulation. The numerical procedure was tested by comparison with the experimental measurements for impedance of the monopole and the far field patterns for both the metallic and resistive ground plane.

Naor [17] studied the scattering of resistive plates, but his program has limitations as it handles only rectangular plate and the maximum area of this plate is restricted in practice to about a square wavelength. Since the body of revolution geometry is the characteristic of many physical structures, this method has the advantage of utilizing three-dimensional structures which can be much larger in wavelength. In the modelling of an infinite ground plane, a ground plane of five wavelengths in radius is used. It has been shown that such a size would give at most three percent error in antenna impedance measurements.

The impedance of the monopole on the metallic and the resistive ground planes are examined both experimentally and numerically. Close agreement exists between these results at the frequencies studied.

The current distributions of the monopole on different ground planes are also studied. It is observed that with the resistive edge, the standing wave pattern is eliminated. These standing waves which resulted from the edge diffraction, give rise to the side lobes in the far zone pattern.

A monopole antenna was built and evaluated for both the metallic and the resistive ground plane. The measured impedances of the antenna with different types of ground planes have been found to be in good agreements with corresponding numerical results. The measured far field patterns have also been found to be in good qualitative agreement with numerical results.

In some respect, the overall result may be regarded as a close approximation to the infinite ground plane case, but significant deviation may also exist. For example, even though the far field pattern of the edge treated monopole does not have any side lobe, it is still different from the pattern produced by a monopole above an infinite ground plane.

For further study, the effect of dielectric coating of the resistive material on antenna characteristics can be investigated.

APPENDICES

```
  *************************************************************

     This is Rose Wang's program for emulating a scattering
     result.

     To use this program, files should be attached to the
     corresponding I/O units as follows :

     Logical unit 1 : Input data file
                      (First record must be the parameter)
     Logical unit 5 : Terminal
     Logical unit 6 : Terminal

  *************************************************************
  *************************************************************


    XS ARRAY STORES THE X COORDINATES OF THE SOURCE POINTS.
    YS ARRAY STORES THE Y COORDINATES OF THE SOURCE POINTS.
    XB ARRAY STORES THE X COORDINATES OF THE OBSERVATION POINTS.
    YB ARRAY STORES THE Y COORDINATES OF THE OBSERVATION POINTS.

    DS ARRAY STORES THE DISTANCE BETWEEN AN OBSERVATION POINT
                               AND EACH OF THE SOURCE POINTS.

      REAL             XS     ,YS     ,DIS     ,DSQ
      COMMON /SOURCE/  XS(100),YS(100),DIS(100),DSQ(100)
      REAL             XB     ,YB
      COMMON /OBSERV/  XB(100),YB(100)
      REAL             DS        ,DSS        ,THETA1,THETA2,INC
      COMMON /DISTNS/  DS(100,15),DSS(100,15),THETA1,THETA2,INC
      INTEGER                                    DOTNUM,CURTYP
      REAL             XS1,YS1,XS2,YS2,XB1,YB1,XB2,YB2
      COMMON /VARIAB/  XS1,YS1,XS2,YS2,XB1,YB1,XB2,YB2,DOTNUM,CURTYP
      COMPLEX*8        GAA    ,GA    ,GAAP    ,GAP
      COMMON /FOUIIS/  GAA(15),GA(15),GAAP(15),GAP(15)
      COMPLEX*8        G1,G2,G3,G4,G5,G6,G7,G8,GB    ,GBB
      COMMON /FOUIES/  G1,G2,G3,G4,G5,G6,G7,G8,GB(15),GBB(15)
      INTEGER          FOUIIN
      REAL                    FK,FRQNCY,MEW,EPSILN,WAVE,DTR,BETA
      COMMON /VARIAC/  FOUIIN,FK,FRQNCY,MEW,EPSILN,WAVE,DTR,BETA(15)
      COMPLEX*8        VOLTGE     ,IMPEDC     ,CURENT
      COMMON /VARIAD/  VOLTGE(100),IMPEDC(100),CURENT(100)
      COMPLEX*8        IMAGI
      COMMON /CNSTAN/  IMAGI
      COMPLEX*8        VOLT,IMP
      COMMON /INPUT/   VOLT,IMP
      COMPLEX*8        Z
      COMMON /OUTPUT/  Z(99,99)

         THE VARIABLES IN THE "MAXIMN" CONTROL THE ARRAY SIZES
         FOR THE ARRAYS IN THE COMMON "SOURCE", "OBSERV".

      INTEGER          SOUMAX, OBSMAX
      COMMON /MAXIMN/  SOUMAX, OBSMAX

         THE VARIABLES IN THE "CONTAN" INDICATE THE CURRENT
         NUMBER OF VALID ENTRIES IN THE ARRAYS.
```

```

      INTEGER         SOUCTN, OBSCTN,RECCTN,PTR,IM,FARIDX,LASTSG
      COMMON /ARRCTN/ SOUCTN, OBSCTN,RECCTN,PTR,IM,FARIDX,LASTSG
      REAL            PI,RADIAN,ZO,XR1,YR1,XR2,YR2
      COMMON /CONSTN/ PI,RADIAN,ZO,XR1,YR1,XR2,YR2
      INTEGER         INPUTF, MESSGE, REPORT, TERMIN
      COMMON /IOUNIT/ INPUTF, MESSGE, REPORT, TERMIN

-----------------------------------------------------------------
        END OF COMMON
-----------------------------------------------------------------

      INTEGER KODE



      CALL INITAL(KODE)

      IF (KODE.NE.0) GO TO 999
      WRITE(MESSGE,10)
   10 FORMAT(1H ,/,1H ,10X,'***     Result from the simulation     ***')
       CALL PROCES

  999 STOP
      END
      SUBROUTINE INITAL(KODE)

*******************************************************

      This subroutine initializes variables in the
      "COMMON" section.

*******************************************************

      REAL            XS      ,YS      ,DIS      ,DSQ
      COMMON /SOURCE/ XS(100),YS(100),DIS(100),DSQ(100)
      REAL            XB      ,YB
      COMMON /OBSERV/ XB(100),YB(100)
      REAL            DS          ,DSS          ,THETA1,THETA2,INC
      COMMON /DISTNS/ DS(100,15),DSS(100,15),THETA1,THETA2,INC
      INTEGER                                     DOTNUM,CURTYP
      REAL            XS1,YS1,XS2,YS2,XB1,YB1,XB2,YB2
      COMMON /VARIAB/ XS1,YS1,XS2,YS2,XB1,YB1,XB2,YB2,DOTNUM,CURTYP
      COMPLEX*8       GAA     ,GA     ,GAAP     ,GAP
      COMMON /FOUIIS/ GAA(15),GA(15),GAAP(15),GAP(15)
      COMPLEX*8       G1,G2,G3,G4,G5,G6,G7,G8,GB     ,GBB
      COMMON /FOUIES/ G1,G2,G3,G4,G5,G6,G7,G8,GB(15),GBB(15)
      INTEGER         FOUIIN
      REAL                   FK,FRQNCY,MEW,EPSILN,WAVE,DTR,BETA
      COMMON /VARIAC/ FOUIIN,FK,FRQNCY,MEW,EPSILN,WAVE,DTR,BETA(15)
      COMPLEX*8       VOLTGE      ,IMPEDC      ,CURENT
      COMMON /VARIAD/ VOLTGE(100),IMPEDC(100),CURENT(100)
      COMPLEX*8       IMAGI
      COMMON /CNSTAN/ IMAGI
      COMPLEX*8       VOLT,IMP
      COMMON /INPUT/  VOLT,IMP
      COMPLEX*8       Z
      COMMON /OUTPUT/ Z(99,99)
      INTEGER         SOUMAX, OBSMAX
      COMMON /MAXIMN/ SOUMAX, OBSMAX
      INTEGER         SOUCTN, OBSCTN,RECCTN,PTR,IM,FARIDX,LASTSG
      COMMON /ARRCTN/ SOUCTN, OBSCTN,RECCTN,PTR,IM,FARIDX,LASTSG
      REAL            PI,RADIAN,ZO,XR1,YR1,XR2,YR2
      COMMON /CONSTN/ PI,RADIAN,ZO,XR1,YR1,XR2,YR2
      INTEGER         INPUTF, MESSGE, REPORT, TERMIN
      COMMON /IOUNIT/ INPUTF, MESSGE, REPORT, TERMIN

-----------------------------------------------------------------
```

```
          END OF COMMON
----------------------------------------------------------------------

        KODE=0
        SOUMAX=100
        OBSMAX=100
        FOUIIN controls the iteration in the FOURIER'S function
        PI=3.1415927
        EPSILN=8.85E-12
        MEW=(4.0E-7)*PI
        IMAGI=CMPLX(0.0,1.0)
        RADIAN=57.29578
        DTR=0.01745329
        ZO =SQRT(MEW/EPSILN)
        INPUTF=1
        MESSGE=6
        TERMIN=5
        REPORT=2


        FARIDX=1
        THETA1=0.0
        THETA2=0.0

      Read the parameters

        READ(INPUTF,10) WAVE,FOUIIN,THETA1,THETA2,INC,FARIDX,MCMFLG,
       *XR1,YR1,XR2,YR2
     10 FORMAT(F8.5,I3,3F7.2,I2,I1,4F6.2)
        IF (FOUIIN.GE.0.AND.FOUIIN.LE.10) GO TO 20
        WRITE(MESSGE,901)
    901 FORMAT(1H ,'*ERROR* : Fourier''s parameter out of ',
      *        'range.')
        KODE=-1
     20 IF (WAVE.GT.0) GO TO 30
        WRITE(MESSGE,902)
    902 FORMAT(1H ,'*ERROR* : Wrong wavelength.')
        KODE=-1
        GO TO 999
     30 FRQNCY=(3.0E8)/WAVE
        IF (MCMFLG.EQ.1) FRQNCY=(3.0E10)/WAVE
        FK=(2*PI)/WAVE
    999 RETURN
        END
        SUBROUTINE READER

***************************************************************

        This subroutine reads in input data record, then
        partition them into intervals before processing.

****************************************************************

        REAL             XS      ,YS      ,DIS      ,DSQ
        COMMON /SOURCE/  XS(100),YS(100),DIS(100),DSQ(100)
        REAL             XB      ,YB
        COMMON /OBSERV/  XB(100),YB(100)
        REAL             DS          ,DSS          ,THETA1,THETA2,INC
        COMMON /DISTNS/  DS(100,15),DSS(100,15),THETA1,THETA2,INC
        INTEGER                                          DOTNUM,CURTYP
        REAL             XS1,YS1,XS2,YS2,XB1,YB1,XB2,YB2
        COMMON /VARIAB/  XS1,YS1,XS2,YS2,XB1,YB1,XB2,YB2,DOTNUM,CURTYP
        COMPLEX*8        GAA     ,GA      ,GAAP     ,GAP
        COMMON /FOUIIS/  GAA(15),GA(15),GAAP(15),GAP(15)
        COMPLEX*8        G1,G2,G3,G4,G5,G6,G7,G8,GB      ,GBB
        COMMON /FOUIES/  G1,G2,G3,G4,G5,G6,G7,G8,GB(15),GBB(15)
        INTEGER          FOUIIN
        REAL                      FK,FRQNCY,MEW,EPSILN,WAVE,DTR,BETA
```

```
      COMMON /VARIAC/ FOUIIN,FK,FRQNCY,MEW,EPSILN,WAVE,DTR,BETA(15)
      COMPLEX*8       VOLTGE      ,IMPEDC      ,CURENT
      COMMON /VARIAD/ VOLTGE(100),IMPEDC(100),CURENT(100)
      COMPLEX*8       IMAGI
      COMMON /CNSTAN/ IMAGI
      COMPLEX*8       VOLT,IMP
      COMMON /INPUT/  VOLT,IMP
      COMPLEX*8       Z
      COMMON /OUTPUT/ Z(99,99)
      INTEGER         SOUMAX, OBSMAX
      COMMON /MAXIMN/ SOUMAX, OBSMAX
      INTEGER         SOUCTN, OBSCTN,RECCTN,PTR,IM,FARIDX,LASTSG
      COMMON /ARRCTN/ SOUCTN, OBSCTN,RECCTN,PTR,IM,FARIDX,LASTSG
      REAL            PI,RADIAN,ZO,XR1,YR1,XR2,YR2
      COMMON /CONSTN/ PI,RADIAN,ZO,XR1,YR1,XR2,YR2
      INTEGER         INPUTF, MESSGE, REPORT, TERMIN
      COMMON /IOUNIT/ INPUTF, MESSGE, REPORT, TERMIN

-------------------------------------------------------------------
        END OF COMMON
-------------------------------------------------------------------

      REAL      OLDX,OLDY
      INTEGER   LINE,CIRCLE,CURVE,FLAG,KODE
      DATA LINE/'LINE'/,CIRCLE/'CIRC'/,CURVE/'CURV'/
      PTR=1
      OLDX=-1E10
      OLDY=-1E10
      FLAG=1
      KODE=0
      RECCTN=0

    When "FLAG" is equal to one means that this is the first
    segment.

   10 READ (INPUTF,20,END=995) XB1,YB1,XB2,YB2,VOLT,IMP,DOTNUM,
     *                         CURTYP,IM,LASTSG
   20 FORMAT(4F9.5,2F6.2,2F8.2,I2,A4,I2,I1)
      RECCTN=RECCTN+1
      IF (PTR.NE.1.AND.(XB1.NE.OLDX.OR.YB1.NE.OLDY)) GO TO 120

    Find a proper subroutine to cut the line

      IF (CURTYP.NE.LINE) GO TO 50
      CALL SLINE(KODE,FLAG)
      IF (KODE.NE.0) GO TO 990
      FLAG=0
      OLDX=XB2
      OLDY=YB2
      GO TO 10
   50 WRITE(MESSGE,60) RECCTN
   60 FORMAT(1H ,'*ERROR* : Unrecognizable curve type at record',I8)
      GO TO 990
  120 WRITE(MESSGE,130) RECCTN
  130 FORMAT(1H ,'*ERROR* : Curve must be defined continuously',
     *     /,1H ,'          condition occurred at record',I8)
  990 SOUCTN=0
      GO TO 999
  995 SOUCTN=PTR-1
  999 RETURN
      END
      SUBROUTINE PROCES

*****************************************************

      This subroutine is the driver for the simulation
      process.

```

```
*******************************************************

      REAL            XS     ,YS     ,DIS     ,DSQ
      COMMON /SOURCE/ XS(100),YS(100),DIS(100),DSQ(100)
      REAL            XB     ,YB
      COMMON /OBSERV/ XB(100),YB(100)
      REAL            DS         ,DSS         ,THETA1,THETA2,INC
      COMMON /DISTNS/ DS(100,15),DSS(100,15),THETA1,THETA2,INC
      INTEGER                                         DOTNUM,CURTYP
      REAL            XS1,YS1,XS2,YS2,XB1,YB1,XB2,YB2
      COMMON /VARIAB/ XS1,YS1,XS2,YS2,XB1,YB1,XB2,YB2,DOTNUM,CURTYP
      COMPLEX*8       GAA     ,GA     ,GAAP     ,GAP
      COMMON /FOUIIS/ GAA(15),GA(15),GAAP(15),GAP(15)
      COMPLEX*8       G1,G2,G3,G4,G5,G6,G7,G8,GB     ,GBB
      COMMON /FOUIES/ G1,G2,G3,G4,G5,G6,G7,G8,GB(15),GBB(15)
      INTEGER         FOUIIN
      REAL                   FK,FRQNCY,MEW,EPSILN,WAVE,DTR,BETA
      COMMON /VARIAC/ FOUIIN,FK,FRQNCY,MEW,EPSILN,WAVE,DTR,BETA(15)
      COMPLEX*8       VOLTGE      ,IMPEDC      ,CURENT
      COMMON /VARIAD/ VOLTGE(100),IMPEDC(100),CURENT(100)
      COMPLEX*8       IMAGI
      COMMON /CNSTAN/ IMAGI
      COMPLEX*8       VOLT,IMP
      COMMON /INPUT/  VOLT,IMP
      COMPLEX*8       Z
      COMMON /OUTPUT/ Z(99,99)
      INTEGER         SOUMAX, OBSMAX
      COMMON /MAXIMN/ SOUMAX, OBSMAX
      INTEGER         SOUCTN, OBSCTN,RECCTN,PTR,IM,FARIDX,LASTSG
      COMMON /ARRCTN/ SOUCTN, OBSCTN,RECCTN,PTR,IM,FARIDX,LASTSG
      REAL            PI,RADIAN,ZO,XR1,YR1,XR2,YR2
      COMMON /CONSTN/ PI,RADIAN,ZO,XR1,YR1,XR2,YR2
      INTEGER         INPUTF, MESSGE, REPORT, TERMIN
      COMMON /IOUNIT/ INPUTF, MESSGE, REPORT, TERMIN

-----------------------------------------------------------------
        END OF COMMON
-----------------------------------------------------------------

      CALL READER
      IF (SOUCTN.LT.3) GO TO 999
      CALL COMPUT
      IF (FARIDX.EQ.O) GO TO 999
      CALL FARFLD
  999 RETURN
      END
      SUBROUTINE SLINE(KODE,FLAG)

************************************************************

       This subroutine puts the source points/observation
       points and the input voltage & impedance into
       proper position in the matrices.

       FLAG : is used to indicated if this is the first segment.

       Source segment and Non-source segment are processed
       in the same manner.

       However, the segments may have different partitioned
       length, depending on where they are on the curve.

       First segment  : 2 points

            ---------+---- ----.--+----------

       Middle segment : 2 points

```

```
             ---------+--.----.--+----------

         Last segment   : 2 points

             ---------+--.----.----+----------

        REAL            XS      ,YS      ,DIS      ,DSQ
        COMMON /SOURCE/ XS(100),YS(100),DIS(100),DSQ(100)
        REAL            XB      ,YB
        COMMON /OBSERV/ XB(100),YB(100)
        REAL            DS          ,DSS          ,THETA1,THETA2,INC
        COMMON /DISTNS/ DS(100,15),DSS(100,15),THETA1,THETA2,INC
        INTEGER                                          DOTNUM,CURTYP
        REAL            XS1,YS1,XS2,YS2,XB1,YB1,XB2,YB2
        COMMON /VARIAB/ XS1,YS1,XS2,YS2,XB1,YB1,XB2,YB2,DOTNUM,CURTYP
        COMPLEX*8       GAA     ,GA      ,GAAP     ,GAP
        COMMON /FOUIIS/ GAA(15),GA(15),GAAP(15),GAP(15)
        COMPLEX*8       G1,G2,G3,G4,G5,G6,G7,G8,GB     ,GBB
        COMMON /FOUIES/ G1,G2,G3,G4,G5,G6,G7,G8,GB(15),GBB(15)
        INTEGER         FOUIIN
        REAL                   FK,FRQNCY,MEW,EPSILN,WAVE,DTR,BETA
        COMMON /VARIAC/ FOUIIN,FK,FRQNCY,MEW,EPSILN,WAVE,DTR,BETA(15)
        COMPLEX*8       VOLTGE      ,IMPEDC      ,CURENT
        COMMON /VARIAD/ VOLTGE(100),IMPEDC(100),CURENT(100)
        COMPLEX*8       IMAGI
        COMMON /CNSTAN/ IMAGI
        COMPLEX*8       VOLT,IMP
        COMMON /INPUT/  VOLT,IMP
        COMPLEX*8       Z
        COMMON /OUTPUT/ Z(99,99)
        INTEGER         SOUMAX, OBSMAX
        COMMON /MAXIMN/ SOUMAX, OBSMAX
        INTEGER         SOUCTN, OBSCTN,RECCTN,PTR,IM,FARIDX,LASTSG
        COMMON /ARRCTN/ SOUCTN, OBSCTN,RECCTN,PTR,IM,FARIDX,LASTSG
        REAL            PI,RADIAN,ZO,XR1,YR1,XR2,YR2
        COMMON /CONSTN/ PI,RADIAN,ZO,XR1,YR1,XR2,YR2
        INTEGER         INPUTF, MESSGE, REPORT, TERMIN
        COMMON /IOUNIT/ INPUTF, MESSGE, REPORT, TERMIN

   ----------------------------------------------------------------------
          END OF COMMON
   ----------------------------------------------------------------------

        INTEGER ENDPTR,FLAG,KODE
        REAL     SARC  ,ARC ,SPACIN ,COMPEN,DOTPEN,EXPN

   ----------------------------------------
        ENDPTR=PTR+DOTNUM
      CHECK IF THE ARRAY IS BIG ENOUGH TO HANDLE THESE NEW POINTS
        IF (ENDPTR.GT.SOUMAX) GO TO 100
        COMPEN=0.0
        DOTPEN=0.0
        IF (LASTSG.EQ.1) DOTPEN=0.5
   ----------------------------------------

        IF (CABS(VOLT).EQ.0.0) GO TO 30

        IF (FLAG.EQ.0) GO TO 10
          XB(1)=XB1
          XS(1)=XB1
          YB(1)=YB1
          YS(1)=YB1
          VOLTGE(1)=VOLT
          IMPEDC(1)=CMPLX(0.0,0.0)
          PTR=PTR+1
          ENDPTR=ENDPTR+1
          COMPEN=-0.5
          DOTPEN=0.5
```

```
      10 CONTINUE

           SPACIN=SQRT(((XB2-XB1)/(DOTNUM+DOTPEN))**2
     *               +((YB2-YB1)/(DOTNUM+DOTPEN))**2)
           DO 20 I = PTR,ENDPTR
           XB(I)=XB1+((XB2-XB1)/(DOTNUM+DOTPEN))*(I-PTR+0.5-COMPEN)
           XS(I)=XB1+((XB2-XB1)/(DOTNUM+DOTPEN))*(I-PTR+0.5-COMPEN)
           YB(I)=YB1+((YB2-YB1)/(DOTNUM+DOTPEN))*(I-PTR+0.5-COMPEN)
           YS(I)=YB1+((YB2-YB1)/(DOTNUM+DOTPEN))*(I-PTR+0.5-COMPEN)
           DIS(I)=SQRT((XB2-XB(I))**2+(YB2-YB(I))**2)
           DSQ(I)=SPACIN
           MID=I-1
           VOLTGE(MID)=VOLT
           IMPEDC(MID)=CMPLX(0.0,0.0)
      20   CONTINUE

         PTR=ENDPTR
         GO TO 999


       THE PRESENT SEGMENT IS NOT A SOURCE SEGMENT


      30 IF (FLAG.EQ.0) GO TO 35
           XB(1)=XB1
           XS(1)=XB1
           YB(1)=YB1
           YS(1)=YB1
           VOLTGE(1)=CMPLX(0.0,0.0)
           IMPEDC(1)=IMP
           PTR=PTR+1
           ENDPTR=ENDPTR+1
           COMPEN=-0.5
           DOTPEN=0.5

      35 CONTINUE

           SPACIN=SQRT(((XB2-XB1)/(DOTNUM+DOTPEN))**2
     *               +((YB2-YB1)/(DOTNUM+DOTPEN))**2)
         DO 40 I = PTR,ENDPTR
           XB(I)=XB1+((XB2-XB1)/(DOTNUM+DOTPEN))*(I-PTR+0.5-COMPEN)
           XS(I)=XB1+((XB2-XB1)/(DOTNUM+DOTPEN))*(I-PTR+0.5-COMPEN)
           YB(I)=YB1+((YB2-YB1)/(DOTNUM+DOTPEN))*(I-PTR+0.5-COMPEN)
           YS(I)=YB1+((YB2-YB1)/(DOTNUM+DOTPEN))*(I-PTR+0.5-COMPEN)
           DSQ(I)=SPACIN
           MID=I-1
           VOLTGE(MID)=CMPLX(0.0,0.0)
           IF (IM.LT.0) GO TO 36
           SARC=(XR2-XB(I))**2+(YR2-YB(I))**2
           GO TO 37
      36   SARC=(XR1-XB(I))**2+(YR1-YB(I))**2
      37   ARC=(XR2-XR1)**2+(YR2-YR1)**2
           DIS(I)=SQRT(SARC)
           IF(CABS(IMP).EQ.0.0.AND.IM.GT.0)
     *     DIS(I)=SQRT((XB2-XB(I))**2+(YB2-YB(I))**2)
           IF(CABS(IMP).EQ.0.0.AND.IM.LT.0)
     *     DIS(I)=SQRT((XB1-XB(I))**2+(YB1-YB(I))**2)
           EXPN=[illegible](FLOAT(IM)/10.0)
           IF (IM.NE.0) GO TO 38
           IMPEDC(MID)=IMP
           GO TO 40
      38   IMPEDC(MID)=IMP*((SARC/ARC)**EXPN)
      40   CONTINUE
           PTR=ENDPTR
         GO TO 999

     100 WRITE(MESSGE,110) SOUMAX
     110 FORMAT(1H ,'*ERROR* ARRAY SIZE NEEDS TO BE INCREASED,',
```

```
     *        'CURRENT SIZE :',I8)
      KODE=-1
  999 RETURN
      END
      SUBROUTINE DISTAN(I)

*****************************************************************

      THIS SUBROUTINE CALCULATES THE DISTANCE BETWEEN A SOURCE
      POINT AND A OBSERVATION POINT. THIS PROCESS IS DONE FOR
      ALL SOURCE POINTS RELATIVE TO ALL OBSERVATION POINTS.

      I : varies from 1 to OBSCTN

*****************************************************************

      REAL              XS      ,YS      ,DIS      ,DSQ
      COMMON /SOURCE/ XS(100),YS(100),DIS(100),DSQ(100)
      REAL              XB      ,YB
      COMMON /OBSERV/ XB(100),YB(100)
      REAL              DS          ,DSS          ,THETA1,THETA2,INC
      COMMON /DISTNS/ DS(100,15),DSS(100,15),THETA1,THETA2,INC
      INTEGER                                              DOTNUM,CURTYP
      REAL              XS1,YS1,XS2,YS2,XB1,YB1,XB2,YB2
      COMMON /VARIAB/ XS1,YS1,XS2,YS2,XB1,YB1,XB2,YB2,DOTNUM,CURTYP
      COMPLEX*8         GAA     ,GA      ,GAAP     ,GAP
      COMMON /FOUIIS/ GAA(15),GA(15),GAAP(15),GAP(15)
      COMPLEX*8         G1,G2,G3,G4,G5,G6,G7,G8,GB     ,GBB
      COMMON /FOUIES/ G1,G2,G3,G4,G5,G6,G7,G8,GB(15),GBB(15)
      INTEGER           FOUIIN
      REAL                      FK,FRQNCY,MEW,EPSILN,WAVE,DTR,BETA
      COMMON /VARIAC/ FOUIIN,FK,FRQNCY,MEW,EPSILN,WAVE,DTR,BETA(15)
      COMPLEX*8         VOLTGE      ,IMPEDC      ,CURENT
      COMMON /VARIAD/ VOLTGE(100),IMPEDC(100),CURENT(100)
      COMPLEX*8         IMAGI
      COMMON /CNSTAN/ IMAGI
      COMPLEX*8         VOLT,IMP
      COMMON /INPUT/  VOLT,IMP
      COMPLEX*8         Z
      COMMON /OUTPUT/ Z(99,99)
      INTEGER           SOUMAX, OBSMAX
      COMMON /MAXIMN/ SOUMAX, OBSMAX
      INTEGER           SOUCTN, OBSCTN,RECCTN,PTR,IM,FARIDX,LASTSG
      COMMON /ARRCTN/ SOUCTN, OBSCTN,RECCTN,PTR,IM,FARIDX,LASTSG
      REAL              PI,RADIAN,ZO,XR1,YR1,XR2,YR2
      COMMON /CONSTN/ PI,RADIAN,ZO,XR1,YR1,XR2,YR2
      INTEGER           INPUTF, MESSGE, REPORT, TERMIN
      COMMON /IOUNIT/ INPUTF, MESSGE, REPORT, TERMIN

-------------------------------------------------------------------
        END OF COMMON
-------------------------------------------------------------------


      THE OBSERVATION POINTS AND THE SOURCE POINTS ARE DEFINED AS :

        +-----+-----+-----+-----+-----  ...
        0     1     2     3     4
      XS(1) XS(2) XS(3) XS(4) XS(5)          SOUCTN        = 4
      XB(1) XB(2) XB(3) XB(4) XB(5)          OBSCTN        = 4
                                             USEFUL POINTS = 3

      INTEGER I,J
      REAL RQPH,RQMH
      REAL ZQPH,ZQMH
      REAL RNPH,RNMH,RNP1,RNM1,RNPQ,RNMQ
      REAL ZNPH,ZNMH,ZNP1,ZNM1,ZNPQ,ZNMQ

```

```
           IEND=SOUCTN

           RQPH=(XB(I)+XB(I+1))*0.5
           ZQPH=(YB(I)+YB(I+1))*0.5
           RQMH=(XB(I)+XB(I-1))*0.5
           ZQMH=(YB(I)+YB(I-1))*0.5

           DO 50 J = 2, IEND

           RNM1=XS(J-1)
           ZNM1=YS(J-1)
           RNP1=XS(J+1)
           ZNP1=YS(J+1)
           RNPH=(XS(J)+XS(J+1))*0.5
           ZNPH=(YS(J)+YS(J+1))*0.5
           RNMH=(XS(J)+XS(J-1))*0.5
           ZNMH=(YS(J)+YS(J-1))*0.5
           RNPQ=(XS(J)*0.75+XS(J+1)*0.25)
           ZNPQ=(YS(J)*0.75+YS(J+1)*0.25)
           RNMQ=(XS(J)*0.75+XS(J-1)*0.25)
           ZNMQ=(YS(J)*0.75+YS(J-1)*0.25)


             DS(J,1)   =SQRT((RQPH-XS(J))**2+
     *                       (ZQPH-YS(J))**2)
             DS(J,2)   =SQRT((RQPH-RNM1)**2+
     *                       (ZQPH-ZNM1)**2)
             DS(J,3)   =SQRT((RQPH-RNMH)**2+
     *                       (ZQPH-ZNMH)**2)
             DS(J,4)   =SQRT((RQPH-RNP1)**2+
     *                       (ZQPH-ZNP1)**2)
             DS(J,5)   =SQRT((RQPH-RNPH)**2+
     *                       (ZQPH-ZNPH)**2)
             DS(J,6)   =SQRT((RQMH-RNMH)**2+
     *                       (ZQMH-ZNMH)**2)
             DS(J,7)   =SQRT((RQMH-RNM1)**2+
     *                       (ZQMH-ZNM1)**2)
             DS(J,8)   =SQRT((RQMH-XS(J))**2+
     *                       (ZQMH-YS(J))**2)
             DS(J,9)   =SQRT((RQMH-RNP1)**2+
     *                       (ZQMH-ZNP1)**2)
             DS(J,10)  =SQRT((RQMH-RNPH)**2+
     *                       (ZQMH-ZNPH)**2)
             DS(J,11)  =SQRT((XB(I)-XS(J))**2+
     *                       (YB(I)-YS(J))**2)
             DS(J,12)  =SQRT((XB(I)-RNMH)**2+
     *                       (YB(I)-ZNMH)**2)
             DS(J,13)  =SQRT((XB(I)-RNMQ)**2+
     *                       (YB(I)-ZNMQ)**2)
             DS(J,14)  =SQRT((XB(I)-RNPH)**2+
     *                       (YB(I)-ZNPH)**2)
             DS(J,15)  =SQRT((XB(I)-RNPQ)**2+
     *                       (YB(I)-ZNPQ)**2)
             DSS(J,1)  =SQRT((RQPH+XS(J))**2+
     *                       (ZQPH-YS(J))**2)
             DSS(J,2)  =SQRT((RQPH+RNM1)**2+
     *                       (ZQPH-ZNM1)**2)
             DSS(J,3)  =SQRT((RQPH+RNMH)**2+
     *                       (ZQPH-ZNMH)**2)
             DSS(J,4)  =SQRT((RQPH+RNP1)**2+
     *                       (ZQPH-ZNP1)**2)
             DSS(J,5)  =SQRT((RQPH+RNPH)**2+
     *                       (ZQPH-ZNPH)**2)
             DSS(J,6)  =SQRT((RQMH+RNMH)**2+
     *                       (ZQMH-ZNMH)**2)
             DSS(J,7)  =SQRT((RQMH+RNM1)**2+
     *                       (ZQMH-ZNM1)**2)
             DSS(J,8)  =SQRT(([illegible]H+XS(J))**2+
```

```
     *                  (ZQMH-YS(J))**2)
        DSS(J,9) =SQRT((RQMH+RNP1)**2+
     *                  (ZQMH-ZNP1)**2)
        DSS(J,10)=SQRT((RQMH+RNPH)**2+
     *                  (ZQMH-ZNPH)**2)
        DSS(J,11)=SQRT((XB(I)+XS(J))**2+
     *                  (YB(I)-YS(J))**2)
        DSS(J,12)=SQRT((XB(I)+RNMH)**2+
     *                  (YB(I)-ZNMH)**2)
        DSS(J,13)=SQRT((XB(I)+RNMQ)**2+
     *                  (YB(I)-ZNMQ)**2)
        DSS(J,14)=SQRT((XB(I)+RNPH)**2+
     *                  (YB(I)-ZNPH)**2)
        DSS(J,15)=SQRT((XB(I)+RNPQ)**2+
     *                  (YB(I)-ZNPQ)**2)
   50 CONTINUE
      RETURN
      END
      SUBROUTINE COMPUT

****************************************************************

      This subroutine computes the impedance and the
      current for the defined point on the "body".
      (Body of Revolution)

****************************************************************

      REAL            XS      ,YS      ,DIS      ,DSQ
      COMMON /SOURCE/ XS(100),YS(100),DIS(100),DSQ(100)
      REAL            XB      ,YB
      COMMON /OBSERV/ XB(100),YB(100)
      REAL            DS          ,DSS          ,THETA1,THETA2,INC
      COMMON /DISTNS/ DS(100,15),DSS(100,15),THETA1,THETA2,INC
      INTEGER                                          DOTNUM,CURTYP
      REAL            XS1,YS1,XS2,YS2,XB1,YB1,XB2,YB2
      COMMON /VARIAB/ XS1,YS1,XS2,YS2,XB1,YB1,XB2,YB2,DOTNUM,CURTYP
      COMPLEX*8       GAA     ,GA      ,GAAP     ,GAP
      COMMON /FOUIIS/ GAA(15),GA(15),GAAP(15),GAP(15)
      COMPLEX*8       G1,G2,G3,G4,G5,G6,G7,G8,GB     ,GBB
      COMMON /FOUIES/ G1,G2,G3,G4,G5,G6,G7,G8,GB(15),GBB(15)
      INTEGER         FOUIIN
      REAL                     FK,FRQNCY,MEW,EPSILN,WAVE,DTR,BETA
      COMMON /VARIAC/ FOUIIN,FK,FRQNCY,MEW,EPSILN,WAVE,DTR,BETA(15)
      COMPLEX*8       VOLTGE      ,IMPEDC      ,CURENT
      COMMON /VARIAD/ VOLTGE(100),IMPEDC(100),CURENT(100)
      COMPLEX*8       IMAGI
      COMMON /CNSTAN/ IMAGI
      COMPLEX*8       VOLT,IMP
      COMMON /INPUT/  VOLT,IMP
      COMPLEX*8       Z
      COMMON /OUTPUT/ Z(99,99)
      INTEGER         SOUMAX, OBSMAX
      COMMON /MAXIMN/ SOUMAX, OBSMAX
      INTEGER         SOUCTN, OBSCTN,RECCTN,PTR,IM,FARIDX,LASTSG
      COMMON /ARRCTN/ SOUCTN, OBSCTN,RECCTN,PTR,IM,FARIDX,LASTSG
      REAL            PI,RADIAN,ZO,XR1,YR1,XR2,YR2
      COMMON /CONSTN/ PI,RADIAN,ZO,XR1,YR1,XR2,YR2
      INTEGER         INPUTF, MESSGE, REPORT, TERMIN
      COMMON /IOUNIT/ INPUTF, MESSGE, REPORT, TERMIN

-------------------------------------------------------------------
        END OF COMMON
-------------------------------------------------------------------

      COMPLEX*8  EQ1  ,EQ2  ,EQ3   ,EQTNA,EQTNB,EQTNC,EQTND
      INTEGER I,J,M
      REAL XBMID,YBMID,XSMID,YSMID,DXYB1,DXYB2,DXYS1,DXYS2
```

```
      REAL LAMB1,LAMB2,LAMS1,LAMS2,XBMM,YBMM,DISMM,DSQMM
      REAL SIN1 ,SIN2 ,COS1 ,COS2 ,TSIN ,TCOS



      IEND=SOUCTN
      M = FOUIIN


        DO 100 I = 2, IEND
          CALL DISTAN(I)
          DO  80 J = 2, IEND
          CALL GREENS(I,J,M)
          XBMID=XB(I)-XB(I-1)
          YBMID=YB(I)-YB(I-1)
          XSMID=XS(J)-XS(J-1)
          YSMID=YS(J)-YS(J-1)
          DXYB1=SQRT(XBMID**2+YBMID**2)
          DXYS1=SQRT(XSMID**2+YSMID**2)
        IF (YB(I).EQ.YB(I-1)) GO TO 5
          LAMB1=ATAN(XBMID/YBMID)
          GO TO 6
 5        LAMB1=90.0*DTR
 6      IF (YS(J).EQ.YS(J-1)) GO TO 10
          LAMS1=ATAN(XSMID/YSMID)
          GO TO 15
10        LAMS1=90.0*DTR
15        XBMID=XB(I+1)-XB(I)
          YBMID=YB(I+1)-YB(I)
          XSMID=XS(J+1)-XS(J)
          YSMID=YS(J+1)-YS(J)
          DXYB2=SQRT(XBMID**2+YBMID**2)
          DXYS2=SQRT(XSMID**2+YSMID**2)
        IF (YB(I+1).EQ.YB(I)) GO TO 20
          LAMB2=ATAN(XBMID/YBMID)
          GO TO 23
20        LAMB2=90.0*DTR
23      IF (YS(J+1).EQ.YS(J)) GO TO 25
          LAMS2=ATAN(XSMID/YSMID)
          GO TO 30
25        LAMS2=90.0*DTR
30        SIN1=DXYB1*SIN(LAMB1)
          SIN2=DXYB2*SIN(LAMB2)
          COS1=DXYB1*COS(LAMB1)
          COS2=DXYB2*COS(LAMB2)
          TSIN=(SIN1+SIN2)/2.0
          TCOS=(COS1+COS2)/2.0


          EQTNA=TSIN*SIN(LAMS1)*G7
          EQTNB=TSIN*SIN(LAMS2)*G8
          EQTNC=2*TCOS*COS(LAMS1)*G5
          EQTND=2*TCOS*COS(LAMS2)*G6


          EQ1=FK*0.5*(EQTNA+EQTNB+EQTNC+EQTND)*IMAGI
          EQ2=(G1-G2)*IMAGI/(FK*DXYS1)
          EQ3=(G4-G3)*IMAGI/(FK*DXYS2)


          Z(I-1,J-1)=ZO*(EQ1+EQ2+EQ3)/(PI*PI*2.0)+SIN(LAMB1)*
     *    (IMPEDC(J-1)/PI)
80        CONTINUE
100     CONTINUE


       CALL MULTPY
       FRQNCY=FRQNCY/(1.0E6)
```

```
      WRITE(MESSGE,101) FOUIIN
  101 FORMAT(1H ,'MODE NUMBER = ',I2)
      WRITE (MESSGE,102)WAVE,FRQNCY
  102 FORMAT(1H ,'THE RESULTS FOR WAVELENGTH = ',F7.2,'  CM ',4X,
     &'FREQUENCY = ',F7.2,'MHZ')
      WRITE(MESSGE,103)
  103 FORMAT(/)
      IF (FARIDX.EQ.1) GO TO 999
      WRITE(MESSGE,104)
  104 FORMAT(8X,'DISTANCE',25X,'IMPEDANCE',10X,'CURRENT')
      WRITE(MESSGE,105)
  105 FORMAT(/)
      WRITE(MESSGE,106)
  106 FORMAT(5X,'RHO',7X,'Z',8X,'DIS',5X,'DSQ',5X,'RS',6X,'XS',7X,'MAG',
     *7X,'PHASE')
      IIND=SOUCTN-1
      DO 110 MM=1,IIND
      AMP=CABS(CURENT(MM))
      PHASE=RADIAN*ATAN2(AIMAG(CURENT(MM)),REAL(CURENT(MM)))
      DSQMM=DSQ(MM+1)/WAVE
      WRITE(MESSGE,107) XB(MM+1),YB(MM+1),DIS(MM+1),DSQMM,
     *IMPEDC(MM),AMP,PHASE
  107 FORMAT(1H ,3F9.4,F8.4,F10.4,F8.4,E11.4,F8.2)
  110 CONTINUE


  999 RETURN
      END
      SUBROUTINE GREENS(I,J,M)

*****************************************************

      M : varies from 1 to FOUIIN

*****************************************************

      REAL            XS     ,YS     ,DIS     ,DSQ
      COMMON /SOURCE/ XS(100),YS(100),DIS(100),DSQ(100)
      REAL            XB     ,YB
      COMMON /OBSERV/ XB(100),YB(100)
      REAL            DS         ,DSS         ,THETA1,THETA2,INC
      COMMON /DISTNS/ DS(100,15),DSS(100,15),THETA1,THETA2,INC
      INTEGER                                         DOTNUM,CURTYP
      REAL            XS1,YS1,XS2,YS2,XB1,YB1,XB2,YB2
      COMMON /VARIAB/ XS1,YS1,XS2,YS2,XB1,YB1,XB2,YB2,DOTNUM,CURTYP
      COMPLEX*8       GAA    ,GA    ,GAAP    ,GAP
      COMMON /FOUIIS/ GAA(15),GA(15),GAAP(15),GAP(15)
      COMPLEX*8       G1,G2,G3,G4,G5,G6,G7,G8,GB     ,GBB
      COMMON /FOUIES/ G1,G2,G3,G4,G5,G6,G7,G8,GB(15),GBB(15)
      INTEGER         FOUIIN
      REAL                   FK,FRQNCY,MEW,EPSILN,WAVE,DTR,BETA
      COMMON /VARIAC/ FOUIIN,FK,FRQNCY,MEW,EPSILN,WAVE,DTR,BETA(15)
      COMPLEX*8       VOLTGE     ,IMPEDC     ,CURENT
      COMMON /VARIAD/ VOLTGE(100),IMPEDC(100),CURENT(100)
      COMPLEX*8       IMAGI
      COMMON /CNSTAN/ IMAGI
      COMPLEX*8       VOLT,IMP
      COMMON /INPUT/  VOLT,IMP
      COMPLEX*8       Z
      COMMON /OUTPUT/ Z(99,99)
      INTEGER         SOUMAX, OBSMAX
      COMMON /MAXIMN/ SOUMAX, OBSMAX
      INTEGER         SOUCTN, OBSCTN,RECCTN,PTR,IM,FARIDX,LASTSG
      COMMON /ARRCTN/ SOUCTN, OBSCTN,RECCTN,PTR,IM,FARIDX,LASTSG
      REAL            PI,RADIAN,ZO,XR1,YR1,XR2,YR2
      COMMON /CONSTN/ PI,RADIAN,ZO,XR1,YR1,XR2,YR2
```

```
      INTEGER         INPUTF, MESSGE, REPORT, TERMIN
      COMMON /IOUNIT/ INPUTF, MESSGE, REPORT, TERMIN

-------------------------------------------------------------------
        END OF COMMON
-------------------------------------------------------------------

      COMPLEX*8 DASC,DSFK,DASC1,DSFK1
      INTEGER   I,J,K,M
      INTEGER   FLAG1,FLAG8,FLAG11
      REAL      TNNM1,TNP1N,TNNMH,TNPHN
      REAL      GG1,GG2,GG3(8),GG4(14),PK,ELTKP
      REAL      RQ1,RQMH1,RQPH1,X,H,DT(15),TMPDS,TMPCS,TMPSN,TMPDV,TMPX
      REAL      RHN,RHNM1,RHNP1,RHNMH,RHNPH,RHNMQ,RHNPQ,TMPXX

************************************************************

      RQ1  =XB(I)
      RQMH1=(XB(I)+XB(I-1))*0.5
      RQPH1=(XB(I)+XB(I+1))*0.5
      RHN  =XS(J)
      RHNM1=XS(J-1)
      RHNP1=XS(J+1)
      RHNMH=(XS(J)+XS(J-1))*0.5
      RHNMQ=XS(J)*0.75+XS(J-1)*0.25
      RHNPH=(XS(J)+XS(J+1))*0.5
      RHNPQ=XS(J)*0.75+XS(J+1)*0.25

      DT(1) =2.0*(RQPH1*RHN)
      DT(2) =2.0*(RQPH1*RHNM1)
      DT(3) =2.0*(RQPH1*RHNMH)
      DT(4) =2.0*(RQPH1*RHNP1)
      DT(5) =2.0*(RQPH1*RHNPH)
      DT(6) =2.0*(RQMH1*RHNMH)
      DT(7) =2.0*(RQMH1*RHNM1)
      DT(8) =2.0*(RQMH1*RHN)
      DT(9) =2.0*(RQMH1*RHNP1)
      DT(10)=2.0*(RQMH1*RHNPH)
      DT(11)=2.0*(RQ1*RHN)
      DT(12)=2.0*(RQ1*RHNMH)
      DT(13)=2.0*(RQ1*RHNMQ)
      DT(14)=2.0*(RQ1*RHNPH)
      DT(15)=2.0*(RQ1*RHNPQ)

      ITIME=(XS(J)*15.0)/WAVE
      ITIME=(ITIME*3)+1
      IF (ITIME.LT.4) ITIME=4
      H=PI/(ITIME-1)
      DO 100 K = 1, 15
          GA(K)=CMPLX(0.0,0.0)
          GB(K)=CMPLX(0.0,0.0)
          TMPDS=DS(J,K)**2
          GAA(K)=CMPLX(0.0,0.0)
          GBB(K)=CMPLX(0.0,0.0)

------------------------------------------------------------

      X=0.0
      DO 35 K1 = 1, ITIME

      USING FOUR POINTS SIMPSON INTEGRATION

      IFAC=3
      ICK =(K1-1)/3
      ICK =K1-(ICK*3+1)
      IF (ICK.EQ.0) IFAC=2
      IF (K1.EQ.1.OR.K1.EQ.ITIME) IFAC=1
```

```
      TMPX=COS(X)
      TMPXX=ABS(TMPX-1.0)
      --------------------
      IF (DS(J,K).LE.1.0E-5.AND.TMPXX.LE.1.0E-5) GO TO 20
      TMPDV=SQRT(TMPDS-DT(K)*(TMPX-1.0))
      TMPCS=COS(FK*TMPDV)
      TMPSN=-SIN(FK*TMPDV)
      DSFK=CMPLX(TMPCS,TMPSN)/(TMPDV*FK)
      GA(K)=GA(K)+(DSFK*IFAC)
      DSFK1=(CMPLX(TMPCS,TMPSN)-1.0)/(TMPDV*FK)
      GB(K)=GB(K)+(DSFK1*IFAC)
      -------------------
   20 IF (K.LE.10) GO TO 30
      IF (DS(J,K).LE.1.0E-5.AND.TMPXX.LE.1.0E-5) GO TO 30
      DASC=DSFK*TMPX
      GAA(K)=GAA(K)+(DASC*IFAC)
      DASC1=(DSFK*TMPX)-(1.0/(TMPDV*FK))
      GBB(K)=GBB(K)+(DASC1*IFAC)
      -------------------
   30 X=X+H
   35 CONTINUE
      GAA(K)=GAA(K)*H*0.75
      GBB(K)=GBB(K)*H*0.75
      GA(K) =GA(K)*H*0.375
      GB(K) =GB(K)*H*0.375
  100 CONTINUE
************************************************************
      TNNM1=SQRT((XS(J)-XS(J-1))**2+(YS(J)-YS(J-1))**2)
      TNP1N=SQRT((XS(J+1)-XS(J))**2+(YS(J+1)-YS(J))**2)
      TNNMH=SQRT((0.5*(XS(J)-XS(J-1)))**2+(0.5*(YS(J)-YS(J-1)))**2)
      TNPHN=SQRT((0.5*(XS(J)-XS(J+1)))**2+(0.5*(YS(J)-YS(J+1)))**2)
      BETA(1) =2*SQRT(RQPH1*RHN)   /DSS(J,1)
      BETA(2) =2*SQRT(RQPH1*RHNM1)/DSS(J,2)
      BETA(3) =2*SQRT(RQPH1*RHNMH)/DSS(J,3)
      BETA(4) =2*SQRT(RQPH1*RHNP1)/DSS(J,4)
      BETA(5) =2*SQRT(RQPH1*RHNPH)/DSS(J,5)
      BETA(6) =2*SQRT(RQMH1*RHNMH)/DSS(J,6)
      BETA(7) =2*SQRT(RQMH1*RHNM1)/DSS(J,7)
      BETA(8) =2*SQRT(RQMH1*RHN)   /DSS(J,8)
      BETA(9) =2*SQRT(RQMH1*RHNP1)/DSS(J,9)
      BETA(10)=2*SQRT(RQMH1*RHNPH)/DSS(J,10)
      BETA(11)=2*SQRT(RQ1*RHN)     /DSS(J,11)
      BETA(12)=2*SQRT(RQ1*RHNMH)   /DSS(J,12)
      BETA(13)=2*SQRT(RQ1*RHNMQ)   /DSS(J,13)
      BETA(14)=2*SQRT(RQ1*RHNPH)   /DSS(J,14)
      BETA(15)=2*SQRT(RQ1*RHNPQ)   /DSS(J,15)
C
C     Check if log function can be performed
C
       GG4(1)=0.0
       IF(DS(J,1).NE.0.0)  GG4(1)=DS(J,1)*ALOG(FK*DS(J,1))
       GG4(2)=0.0
       IF(DS(J,2).NE.0.0)  GG4(2)=DS(J,2)*ALOG(FK*DS(J,2))
       GG4(4)=0.0
       IF(DS(J,4).NE.0.0)  GG4(4)=DS(J,4)*ALOG(FK*DS(J,4))
       GG4(7)=0.0
       IF(DS(J,7).NE.0.0)  GG4(7)=DS(J,7)*ALOG(FK*DS(J,7))
       GG4(8)=0.0
       IF(DS(J,8).NE.0.0)  GG4(8)=DS(J,8)*ALOG(FK*DS(J,8))
       GG4(9)=0.0
       IF(DS(J,9).NE.0.0)  GG4(9)=DS(J,9)*ALOG(FK*DS(J,9))
```

```
          GG4(11)=0.0
          IF(DS(J,11).NE.0.0) GG4(11)=DS(J,11)*ALOG(FK*DS(J,11))
          GG4(12)=0.0
          IF(DS(J,12).NE.0.0) GG4(12)=DS(J,12)*ALOG(FK*DS(J,12))
          GG4(14)=0.0
          IF(DS(J,14).NE.0.0) GG4(14)=DS(J,14)*ALOG(FK*DS(J,14))


        GG3(1)=(TNNM1-GG4(1)-GG4(2))
        GG3(2)=(TNNM1-GG4(7)-GG4(8))
        GG3(3)=(TNP1N-GG4(1)-GG4(4))
        GG3(4)=(TNP1N-GG4(8)-GG4(9))
        GG3(5)=(TNNMH-GG4(11)-GG4(12))
        GG3(6)=(TNPHN-GG4(11)-GG4(14))
        GG3(7)=(TNNMH-GG4(11)-GG4(12))
        GG3(8)=(TNPHN-GG4(11)-GG4(14))

      DS must be positive, all 15 entries must have valid value


      If an entry of DS array does meet the condition below,
      then, it will be processed by using direct calculation.
      Otherwise, use the approximation method.
      *** i.e. If the observation point is within the source
          region --- use approximation ***

        FLAG1=0
        FLAG8=0
        FLAG11=0

      Flags are down, which means that GA1, GA8, GA11 have
      not been approximated yet.

      ***********************************************

      ---------   Calculate "G1"
        IF ((DS(J,1).GT.1.0E-5).AND.(DS(J,2).GT.1.0E-5)
     *                          .AND.(DS(J,3).GT.1.0E-5)) GO TO 106

        FLAG1=1
        CALL APPRMX(J,1,RQ1,RQMH1,RQPH1)
        CALL APPRMX(J,2,RQ1,RQMH1,RQPH1)
        CALL APPRMX(J,3,RQ1,RQMH1,RQPH1)
   102 G1=(GAP(1)+GAP(2)+4.0*GAP(3))*(TNNM1*FK/6.0)+GG3(1)*2.0/RQPH1
        GO TO 110
   106 G1=(GA(1)+GA(2)+4.0*GA(3))*(TNNM1*FK/6.0)


      ***********************************************

      ---------   Calculate "G2"
   110 IF ((DS(J,8).GT.1.0E-5).AND.(DS(J,7).GT.1.0E-5)
     *                          .AND.(DS(J,6).GT.1.0E-5)) GO TO 116

        FLAG8=1
        CALL APPRMX(J,8,RQ1,RQMH1,RQPH1)
        CALL APPRMX(J,7,RQ1,RQMH1,RQPH1)
        CALL APPRMX(J,6,RQ1,RQMH1,RQPH1)
   112 G2=(GAP(8)+GAP(7)+4.0*GAP(6))*(TNNM1*FK/6.0)+GG3(2)*2.0/RQMH1
        GO TO 120
   116 G2=(GA(8)+GA(7)+4.0*GA(6))*(TNNM1*FK/6.0)


      ***********************************************

      ---------   Calculate "G3"
   120 IF ((DS(J,1).GT.1.0E-5).AND.(DS(J,4).GT.1.0E-5)
     *                          .AND.(DS(J,5).GT.1.0E-5)) GO TO 126
```

```
      IF (FLAG1.EQ.0)
     *CALL APPRMX(J,1,RQ1,RQMH1,RQPH1)
      CALL APPRMX(J,4,RQ1,RQMH1,RQPH1)
      CALL APPRMX(J,5,RQ1,RQMH1,RQPH1)
  124 G3=(GAP(1)+GAP(4)+4.0*GAP(5))*(TNP1N*FK/6.0)+GG3(3)*2.0/RQPH1
      GO TO 130
  126 G3=(GA(1)+GA(4)+4.0*GA(5))*(TNP1N*FK/6.0)


*********************************************

---------   Calculate "G4"
  130 IF ((DS(J,8).GT.1.0E-5).AND.(DS(J,9).GT.1.0E-5)
     *                        .AND.(DS(J,10).GT.1.0E-5)) GO TO 136

      IF (FLAG8.EQ.0)
     *CALL APPRMX(J,8,RQ1,RQMH1,RQPH1)
      CALL APPRMX(J,9,RQ1,RQMH1,RQPH1)
      CALL APPRMX(J,10,RQ1,RQMH1,RQPH1)
  134 G4=(GAP(8)+GAP(9)+4.0*GAP(10))*(TNP1N*FK/6.0)+GG3(4)*2.0/RQMH1
      GO TO 141
  136 G4=(GA(8)+GA(9)+4.0*GA(10))*(TNP1N*FK/6.0)


*********************************************

---------   Calculate "G5", "G7"
  141 IF (DS(J,11).GT.1.0E-5.AND.DS(J,12).GT.1.0E-5
     *                       .AND.DS(J,13).GT.1.0E-5) GO TO 146


      FLAG11=1
      CALL APPRMX(J,11,RQ1,RQMH1,RQPH1)
      CALL APPRMX(J,12,RQ1,RQMH1,RQPH1)
      CALL APPRMX(J,13,RQ1,RQMH1,RQPH1)
  142 G5=(GAP(11)+GAP(12)+4*GAP(13))*(TNNMH*FK/6.0)+GG3(5)*2.0/RQ1
      G7=(GAAP(11)+GAAP(12)+4*GAAP(13))*(TNNMH*FK/6.0)+GG3(7)*2.0/RQ1
      GO TO 151
  146 G5=(GA(11)+GA(12)+4*GA(13))*(TNNMH*FK/6.0)
      G7=(GAA(11)+GAA(12)+4*GAA(13))*(TNNMH*FK/6.0)


*********************************************

---------   Calculate "G6", "G8"
  151 IF (DS(J,11).GT.1.0E-5.AND.DS(J,14).GT.1.0E-5
     *                       .AND.DS(J,15).GT.1.0E-5) GO TO 156

      IF (FLAG11.EQ.0)
     *CALL APPRMX(J,11,RQ1,RQMH1,RQPH1)
      CALL APPRMX(J,14,RQ1,RQMH1,RQPH1)
      CALL APPRMX(J,15,RQ1,RQMH1,RQPH1)
  154 G6=(GAP(11)+GAP(14)+4*GAP(15))*(TNPHN*FK/6.0)+GG3(6)*2.0/RQ1
      G8=(GAAP(11)+GAAP(14)+4*GAAP(15))*(TNPHN*FK/6.0)+GG3(8)*2.0/RQ1
      GO TO 161
  156 G6=(GA(11)+GA(14)+4*GA(15))*(TNPHN*FK/6.0)
      G8=(GAA(11)+GAA(14)+4*GAA(15))*(TNPHN*FK/6.0)




*********************************************

  161 RETURN
      END
      SUBROUTINE MULTPY
```

```
      ****************************************************

          THIS SUBROUTINE SOLVES THE EQUATION FOR THE
          MATRICES [Z][J]=[E]

      ****************************************************

          REAL              XS      ,YS      ,DIS      ,DSQ
          COMMON /SOURCE/   XS(100),YS(100),DIS(100),DSQ(100)
          REAL              XB      ,YB
          COMMON /OBSERV/   XB(100),YB(100)
          REAL              DS            ,DSS            ,THETA1,THETA2,INC
          COMMON /DISTNS/   DS(100,15),DSS(100,15),THETA1,THETA2,INC
          INTEGER                                               DOTNUM,CURTYP
          REAL              XS1,YS1,XS2,YS2,XB1,YB1,XB2,YB2
          COMMON /VARIAB/   XS1,YS1,XS2,YS2,XB1,YB1,XB2,YB2,DOTNUM,CURTYP
          COMPLEX*8         GAA     ,GA      ,GAAP     ,GAP
          COMMON /FOUIIS/   GAA(15),GA(15),GAAP(15),GAP(15)
          COMPLEX*8         G1,G2,G3,G4,G5,G6,G7,G8,GB      ,GBB
          COMMON /FOUIES/   G1,G2,G3,G4,G5,G6,G7,G8,GB(15),GBB(15)
          INTEGER           FOUIIN
          REAL                     FK,FRQNCY,MEW,EPSILN,WAVE,DTR,BETA
          COMMON /VARIAC/   FOUIIN,FK,FRQNCY,MEW,EPSILN,WAVE,DTR,BETA(15)
          COMPLEX*8         VOLTGE      ,IMPEDC      ,CURENT
          COMMON /VARIAD/   VOLTGE(100),IMPEDC(100),CURENT(100)
          COMPLEX*8         IMAGI
          COMMON /CNSTAN/   IMAGI
          COMPLEX*8         VOLT,IMP
          COMMON /INPUT/    VOLT,IMP
          COMPLEX*8         Z
          COMMON /OUTPUT/   Z(99,99)
          INTEGER           SOUMAX, OBSMAX
          COMMON /MAXIMN/   SOUMAX, OBSMAX
          INTEGER           SOUCTN, OBSCTN,RECCTN,PTR,IM,FARIDX,LASTSG
          COMMON /ARRCTN/   SOUCTN, OBSCTN,RECCTN,PTR,IM,FARIDX,LASTSG
          REAL              PI,RADIAN,ZO,XR1,YR1,XR2,YR2
          COMMON /CONSTN/   PI,RADIAN,ZO,XR1,YR1,XR2,YR2
          INTEGER           INPUTF, MESSGE, REPORT, TERMIN
          COMMON /IOUNIT/   INPUTF, MESSGE, REPORT, TERMIN

      ----------------------------------------------------------------
             END OF COMMON
      ----------------------------------------------------------------

          COMPLEX*8 TEMPRA,TEMPRB,P
          INTEGER   JDX,JP1,JP2,I1

          N=SOUCTN-1
          IF (N.GT.1) GO TO 10
          CURENT(1)=VOLTGE(1)/Z(1,1)
          GO TO 110

       10 NM1=N-1

          DO 80 I=1,NM1
          IP1=I+1
          IF (CABS(Z(I,I)).NE.0.0) GO TO 50
          DO 20 J=IP1,N
          JDX=J
          IF (CABS(Z(J,I)).NE.0.0) GO TO 30
       20 CONTINUE
          WRITE (MESSGE,25) I
       25 FORMAT(1H ,'Z MATRIX AT ',I3,' ROW HAS ALL ZEROS')
          GO TO 110
       30 CONTINUE
          DO 40 K=1,N
          TEMPRA  =Z(JDX,K)
          Z(JDX,K)=Z(I,K)
```

```
   40 Z(I,K)  =TEMPRA
      TEMPRB  =VOLTGE(JDX)
      VOLTGE(JDX)=VOLTGE(I)
      VOLTGE(I)=TEMPRB

   50 CONTINUE
      DO 70 JP1=IP1,N
      P=Z(JP1,I)/Z(I,I)
      DO 60 K=IP1,N
      Z(JP1,K)=Z(JP1,K)-P*Z(I,K)
   60 CONTINUE
      VOLTGE(JP1)=VOLTGE(JP1)-P*VOLTGE(I)
   70 CONTINUE
   80 CONTINUE

      CURENT(N)=VOLTGE(N)/Z(N,N)
      I1=NM1+1
   85 I1=I1-1
      IF (I1.LT.1) GO TO 110
      IP1=I1+1
      DO 90 JP2=IP1,N
      VOLTGE(I1)=VOLTGE(I1)-Z(I1,JP2)*CURENT(JP2)
   90 CONTINUE
      CURENT(I1)=VOLTGE(I1)/Z(I1,I1)
      GO TO 85

  110 RETURN
      END
      SUBROUTINE ELTK(PK,ELTKP)

*****************************************************************

         THIS SUBROUTINE COMPUTES THE ELLIPTICAL FUNCTION
         OF THE FIRST KIND K(M)
         WHERE M1=1-M
         K(M)¬A0+A1*M1+A2*M1**2+A3*M1**3+A4*M1**4-
             (B0+B1*M1+B2*M1**2+B3*M1**3+B4*M1**4)*ALOG(M1)
         FOR MAGNITUDE(ERROR) .LE. 2.0E-8

*****************************************************************

      REAL ELTKP,PK
      DATA A0,A1,A2,A3,A4,B0,B1,B2,B3,B4/
     $    1.38629436112,  .09666344259,   .03590092383,   .03742563713,
     $      .01451196212,  .5,            .12498593597,   .06880248576,
     $      .03328355346,  .00441787012/

      -------------------------------------

      A=A0+A1*PK
      B=B0+B1*PK
      IF (PK.LT.1.E-18) GO TO 10
      A=A+A2*(PK**2)
      B=B+B2*(PK**2)
      IF (PK.LT.1.E-12) GO TO 10
      A=A+A3*(PK**3)
      B=B+B3*(PK**3)
      IF (PK.LT.1.E-9) GO TO 10
      A=A+A4*(PK**4)
      B=B+B4*(PK**4)
   10 CONTINUE
      ELTKP=A-B*ALOG(PK)

      -------------------------------------

      RETURN
      END
      SUBROUTINE APPRMX(J,KK,RQ1,RQMH1,RQPH1)
```

```
C
C     *****************************************************
C
C          Calculating the GAP value using the approximation.
C          Calling routine --- GREENS
C
C     *****************************************************
C
          REAL            XS       ,YS      ,DIS      ,DSQ
          COMMON /SOURCE/ XS(100),YS(100),DIS(100),DSQ(100)
          REAL            XB      ,YB
          COMMON /OBSERV/ XB(100),YB(100)
          REAL            DS          ,DSS          ,THETA1,THETA2,INC
          COMMON /DISTNS/ DS(100,15),DSS(100,15),THETA1,THETA2,INC
          INTEGER                                          DOTNUM,CURTYP
          REAL            XS1,YS1,XS2,YS2,XB1,YB1,XB2,YB2
          COMMON /VARIAB/ XS1,YS1,XS2,YS2,XB1,YB1,XB2,YB2,DOTNUM,CURTYP
          COMPLEX*8       GAA     ,GA     ,GAAP     ,GAP
          COMMON /FOUIIS/ GAA(15),GA(15),GAAP(15),GAP(15)
          COMPLEX*8       G1,G2,G3,G4,G5,G6,G7,G8,GB     ,GBB
          COMMON /FOUIES/ G1,G2,G3,G4,G5,G6,G7,G8,GB(15),GBB(15)
          INTEGER         FOUIIN
          REAL                   FK,FRQNCY,MEW,EPSILN,WAVE,DTR,BETA
          COMMON /VARIAC/ FOUIIN,FK,FRQNCY,MEW,EPSILN,WAVE,DTR,BETA(15)
          COMPLEX*8       VOLTGE      ,IMPEDC      ,CURENT
          COMMON /VARIAD/ VOLTGE(100),IMPEDC(100),CURENT(100)
          COMPLEX*8       IMAGI
          COMMON /CNSTAN/ IMAGI
          COMPLEX*8       VOLT,IMP
          COMMON /INPUT/  VOLT,IMP
          COMPLEX*8       Z
          COMMON /OUTPUT/ Z(99,99)
          INTEGER         SOUMAX, OBSMAX
          COMMON /MAXIMN/ SOUMAX, OBSMAX
          INTEGER         SOUCTN, OBSCTN,RECCTN,PTR,IM,FARIDX,LASTSG
          COMMON /ARRCTN/ SOUCTN, OBSCTN,RECCTN,PTR,IM,FARIDX,LASTSG
          REAL            PI,RADIAN,ZO,XR1,YR1,XR2,YR2
          COMMON /CONSTN/ PI,RADIAN,ZO,XR1,YR1,XR2,YR2
          INTEGER         INPUTF, MESSGE, REPORT, TERMIN
          COMMON /IOUNIT/ INPUTF, MESSGE, REPORT, TERMIN
C
C     ----------------------------------------------------------------
C            END OF COMMON
C     ----------------------------------------------------------------
C
          INTEGER J,KK
          REAL    RQ1,RQMH1,RQPH1
          REAL    GG1,GG2,PK

          GG1=0.0
          GG2=0.0
C
C
C     ************************************
C
          PK=1-BETA(KK)
          IF (KK.GT.5) GO TO 20
C
C     ************************************
C
          IF(DS(J,KK).GT.1.0E-5.AND.PK.GT.0) GO TO 15
          GG1=ALOG(4.0)*0.5/(RQPH1*FK)
          GG2=ALOG(FK*DSS(J,KK))*0.5/(RQPH1*FK)
          GO TO 40
       15 CALL ELTK(PK,ELTKP)
          GG1=ELTKP/(FK*DSS(J,KK))
          GG2=ALOG(FK*DS(J,KK))*0.5/(RQPH1*FK)
          GO TO 40
```

```
      *************************************

        20 IF (KK.GT.10) GO TO 30

      *************************************

           IF(DS(J,KK).GT.1.0E-5.AND.PK.GT.0) GO TO 25
           GG1=ALOG(4.0)*0.5/(RQMH1*FK)
           GG2=ALOG(FK*DSS(J,KK))*0.5/(RQMH1*FK)
           GO TO 40

        25 CALL ELTK(PK,ELTKP)
           GG1=ELTKP/(FK*DSS(J,KK))
           GG2=ALOG(FK*DS(J,KK))*0.5/(RQMH1*FK)
           GO TO 40
      *************************************

        30 IF(DS(J,KK).GT.1.0E-5.AND.PK.GT.0) GO TO 33
           GG1=ALOG(4.0)*0.5/(RQ1*FK)
           GG2=ALOG(FK*DSS(J,KK))*0.5/(RQ1*FK)
           GO TO 35
        33 CALL ELTK(PK,ELTKP)
           GG1=ELTKP/(FK*DSS(J,KK))
           GG2=ALOG(FK*DS(J,KK))*0.5/(RQ1*FK)
        35 GAAP(KK)=((GG1+GG2)*4.0+GBB(KK))
        40 GAP(KK)=((GG1+GG2)*4.0+GB(KK))

           -------------------------------

           RETURN
           END
           SUBROUTINE FARFLD
      *****************************************************************

           This routine is used to calculate the far field pattern.

      *****************************************************************

           REAL             XS      ,YS      ,DIS      ,DSQ
           COMMON /SOURCE/  XS(100),YS(100),DIS(100),DSQ(100)
           REAL             XB      ,YB
           COMMON /OBSERV/  XB(100),YB(100)
           REAL             DS          ,DSS          ,THETA1,THETA2,INC
           COMMON /DISTNS/  DS(100,15),DSS(100,15),THETA1,THETA2,INC
           INTEGER                                            DOTNUM,CURTYP
           REAL             XS1,YS1,XS2,YS2,XB1,YB1,XB2,YB2
           COMMON /VARIAB/  XS1,YS1,XS2,YS2,XB1,YB1,XB2,YB2,DOTNUM,CURTYP
           COMPLEX*8        GAA     ,GA     ,GAAP     ,GAP
           COMMON /FOUIIS/  GAA(15),GA(15),GAAP(15),GAP(15)
           COMPLEX*8        G1,G2,G3,G4,G5,G6,G7,G8,GB     ,GBB
           COMMON /FOUIES/  G1,G2,G3,G4,G5,G6,G7,G8,GB(15),GBB(15)
           INTEGER          FOUIIN
           REAL                    FK,FRQNCY,MEW,EPSILN,WAVE,DTR,BETA
           COMMON /VARIAC/  FOUIIN,FK,FRQNCY,MEW,EPSILN,WAVE,DTR,BETA(15)
           COMPLEX*8        VOLTGE      ,IMPEDC      ,CURENT
           COMMON /VARIAD/  VOLTGE(100),IMPEDC(100),CURENT(100)
           COMPLEX*8        IMAGI
           COMMON /CONSTAN/ IMAGI
           COMPLEX*8        VOLT,IMP
           COMMON /INPUT/   VOLT,IMP
           COMPLEX*8        Z
           COMMON /OUTPUT/  Z(99,99)
           INTEGER          SOUMAX, OBSMAX
           COMMON /MAXIMN/  SOUMAX, OBSMAX
           INTEGER          SOUCTN, OBSCTN,RECCTN,PTR,IM,FARIDX,LASTSG
           COMMON /ARRCTN/  SOUCTN, OBSCTN,RECCTN,PTR,IM,FARIDX,LASTSG
           REAL             PI,RADIAN,ZO,XR1,YR1,XR2,YR2
           COMMON /CONSTN/  PI,RADIAN,ZO,XR1,YR1,XR2,YR2
```

```
      INTEGER          INPUTF, MESSGE, REPORT, TERMIN
      COMMON /IOUNIT/  INPUTF, MESSGE, REPORT, TERMIN

-----------------------------------------------------------------------
         END OF COMMON
-----------------------------------------------------------------------

      COMPLEX*8 BZ1  ,BZO  ,FUNCTN
      COMPLEX*8 EQTNA,EQTNB,EQTNC ,EQTND
      COMPLEX*8 FELD ,EQ1
      REAL RFB   ,KPS  ,X     ,A     ,B     ,H
      REAL THETA,XSMID,YSMID,DXYS1,DXYS2
      REAL LAMF ,LAMS1,LAMS2
      REAL SIN1 ,COS1 ,REALP1,REALP2

      ---------------------------------------------

      IF (THETA1.LE.0.0.AND.THETA2.LE.0.0) GO TO 990
      WRITE(MESSGE,1)
    1 FORMAT(1H ,/,1H ,/)
      WRITE(MESSGE,5)
    5 FORMAT(1H ,15X,'Far Field',/,1H ,3X,'Theta',8X,'(Mag)',9X,'Phase')
      THETA=THETA1
      RFB = 10.0 * WAVE
   20 BZO=CMPLX(0.0,0.0)
      BZ1=CMPLX(0.0,0.0)
      FELD=CMPLX(0.0,0.0)

      DO 100 J = 2, SOUCTN

      XSMID=XS(J)-XS(J-1)
      YSMID=YS(J)-YS(J-1)
      DXYS1=SQRT(XSMID**2+YSMID**2)
      LAMF =DTR*THETA
      IF (YS(J).EQ.YS(J-1)) GO TO 30
      LAMS1=ATAN(XSMID/YSMID)
      GO TO 35

   30 LAMS1=90*DTR
   35 XSMID=XS(J+1)-XS(J)
      YSMID=YS(J+1)-YS(J)
      DXYS2=SQRT(XSMID**2+YSMID**2)
      IF (YS(J+1).EQ.YS(J)) GO TO 40
      LAMS2=ATAN(XSMID/YSMID)
      GO TO 45

   40 LAMS2=90*DTR
   45 SIN1 =SIN(LAMF)
      COS1 =COS(LAMF)


      KPS=FK*XS(J)*SIN(LAMF)
      A=0.0
      B=PI*2.0
      H=PI*2.0/30.0
      X=A
      IF (LAMS1.EQ.(90.0*DTR)) GO TO 55
      BZO=((CMPLX(COS(KPS*COS(A)),SIN(KPS*COS(A))))+
     *     (CMPLX(COS(KPS*COS(B)),SIN(KPS*COS(B)))))/2.0
      DO 50 K = 1, 29
      X=X+H
      BZO=BZO+(CMPLX(COS(KPS*COS(X)),SIN(KPS*COS(X))))
   50 CONTINUE
      BZO=BZO*H
      GO TO 70


   55 BZ1=(CMPLX(COS(KPS*COS(A)+A),SIN(KPS*COS(A)+A))+
```

```
     *      CMPLX(COS(KPS*COS(B)+B),SIN(KPS*COS(B)+B)))/2.0
      DO 60 K = 1, 29
      X=X+H
      FUNCTN=CMPLX(COS(KPS*COS(X)+X),SIN(KPS*COS(X)+X))
      BZ1=BZ1+FUNCTN
   60 CONTINUE
      BZ1=BZ1*H*IMAGI

      ----------------------------------------------------

   70   EQTNA=COS1*SIN(LAMS1)*DXYS1*BZ1*IMAGI
        EQTNB=COS1*SIN(LAMS2)*DXYS2*BZ1*IMAGI
        EQTNC=SIN1*COS(LAMS1)*DXYS1*BZO*(CMPLX(COS(FK*YS(J)*COS(LAMF)),
     *  SIN(FK*YS(J)*COS(LAMF))))
        EQTND=SIN1*COS(LAMS2)*DXYS2*BZO*(CMPLX(COS(FK*YS(J)*COS(LAMF)),
     *  SIN(FK*YS(J)*COS(LAMF))))

   90   EQ1=(FK*ZO*0.5*IMAGI)*(EQTNA+EQTNB-EQTNC-EQTND)/
     *        RFB
        FELD=(EQ1*CURENT(J-1))/(PI*PI*4.0)+FELD
  100 CONTINUE

      AMP=CABS(FELD)
      REALP1=AIMAG(FELD)
      REALP2= REAL(FELD)
      IF (REALP2.NE.0.0)  GO TO 120
      PHASE=0.0
      GO TO 140
  120 PHASE=RADIAN*ATAN2(REALP1,REALP2)
  140 WRITE(MESSGE,110) THETA,AMP,PHASE
  110 FORMAT(1H ,2X,F7.2,3X,E12.4,5X,F7.2)

      THETA=THETA+INC
      IF(THETA.LE.THETA2) GO TO 20
  990 RETURN
      END
```

Appendix B. Singularity Analysis of Self Terms for the Geometry of Revolution

When an observation point falls within the source segment, the integrals described in Eq.(3.28) may have singular integrands. A brief procedure of evaluating the integrals is shown here. A more detailed analysis can be found in reference [30].

Throughout this section, we employ the coordinate parameter valid for

$$t_{j-1} \leqq t \leqq t_j$$

$$z = z_{j-1} + \ell \cos\gamma_j \tag{B.1a}$$

$$r = r_{j-1} + \ell \sin\gamma_j \tag{B.1b}$$

$$0 \leqq \ell \leqq \Delta t_j$$

Where

$$\ell = t - t_{j-1}$$

For self terms, we can apply equations

$$(z - z') = (\ell - \ell') \cos\gamma_j \tag{B.2a}$$

$$(r - r') = (\ell - \ell') \sin\gamma_j \tag{B.2b}$$

For the self term, the M integral may be written as

$$M = \int_{\ell_1}^{\ell_2} \int_{-\pi}^{\pi} \frac{e^{-jkR}}{R} \cos(m\alpha)\, d\alpha\, d\ell' \qquad \text{(B.3a)}$$

and

$$R = [(r - r')^2 + 2rr' (1 - \cos\alpha) + (z - z')^2]^{1/2} \qquad \text{(B.3b)}$$

As $t \to t'$ and $\alpha \to 0$, $R \to 0$, the integrand of (B.3a) is cleary singular. Then we can define

$$M = I_1 + I_2 \qquad \text{(B.4)}$$

where

$$I_1 = \int_{\ell_1}^{\ell_2} \int_{-\pi}^{\pi} \left[\frac{e^{-jkR}}{R} \cos(m\alpha) - \frac{1}{R}\right] d\alpha\, d\ell' \qquad \text{(B.5a)}$$

$$I_2 = \int_{\ell_1}^{\ell_2} \int_{-\pi}^{\pi} \frac{1}{R}\, d\alpha\, d\ell' \qquad \text{(B.5b)}$$

Since the integrand I_1 is no longer singular, I_2 may be evaluated numer:cally with a single change of variable.

$$I_2 = 4 \int_{\ell_1}^{\ell_2} \frac{1}{R_2} K(u)\, d\ell' \qquad \text{(B.6)}$$

where

$$R_2 = [(r + r')^2 + (z - z')^2]^{\frac{1}{2}} \tag{B.7}$$

and K(u) is the complete elliptical integral of the first kind defined by

$$K(u) = \int_0^{\pi} \frac{1}{[1 - u^2 \sin^2\phi]^{\frac{1}{2}}} \, d\phi \tag{B.8}$$

with

$$u = \frac{2\,(r\,r')^{\frac{1}{2}}}{R_2} \tag{B.9}$$

The integrand of Eq.(B.6) is still singular. However, near the singularity at t = t', it varies as

$$\frac{1}{R_2} K(u) \xrightarrow[t \to t']{} \frac{1}{2r} \, [(\ln(4) + \ln(R_2) - \ln(R_1)] \tag{B.10}$$

where

$$R_1 = [(r - r')^2 + (z - z')^2]^{\frac{1}{2}} \tag{B.11}$$

At this point, only the last term is singular, we can add and subtract the singular term in Eq.(B.6) to obtain

$$I_2 = I_2' + I_2'' \tag{B.12}$$

where

$$I'_2 = 4 \int_{\ell_1}^{\ell_2} [\frac{1}{R_2} K(u) + \frac{1}{2\pi} \ln(R_1)] \, d\ell' \qquad (B.13)$$

$$I''_2 = -\frac{2}{\pi} \int_{\ell_1}^{\ell_2} \ln(R_1) \, d\ell' \qquad (B.14)$$

Now, the integral I'_2 does not have a singular integrand, so the integral I''_2 can be evaluated analytically by the parameterization of Eq.(B.1) as follows

$$I''_2 = -\frac{2}{\pi} \int_{\ell_1}^{\ell_2} \ln |\ell - \ell'| \, d\ell'$$

$$= \frac{2}{\pi} [(\ell_2 - \ell_1) - (\ell_2 - \ell) \ln(\ell_2 - \ell)$$

$$- (\ell - \ell_1) \ln(\ell - \ell_1)] \qquad (B.15)$$

The integrals I_1, I'_2 and I''_2 can thus be integrated numerically, and the M integral can be evaluated by

$$M = I_1 + I'_2 + I''_2 \qquad (B.16)$$

REFERENCES

REFERENCES

1. Meier, A.S. and Summers, W.P., (1948), " Measured impedance of vertical antennas over finite ground planes," Proc. IRE, vol. 36, 609-626.

2. Bardeen, J., (1930), "The diffraction of a circularly symmetrical electromagnetic wave by a coaxial cylinder disc of infinite conductivity," Phys. Rev. 36, 1482-1488.

3. Leitner, A. and Spence, R.D., (1950), "Effect of a circular ground plane on antenna radiation," J. Appl. Phys., vol. 21, 1001-1006.

4. Storer, J.E., (1951), "The impedance of an antenna over a large circular screen," J. Appl. Phys., vol. 22, 1058-1066.

5. Storer,J.E., (1952), "The radiation pattern of an antenna over circular ground screen," J. Appl. Phys., vol. 23, 588-593.

6. Hahn, R.F. and Fikioris, J.G., (1973), "Impedance and radiation pattern of antennas above flat disc," IEEE Trans. Antennas Propagat., AP-21, 97-100.

7. Thiele, G.A. and Newhouse, T.A., (1975), "A hybrid technique for combining moment methods with the geometrical theory of diffraction," IEEE Trans.

Antennas Propagat., AP-21, 62-69.

8. Thiele, G.A. and Newhouse, T.A., (1974), "A hybrid technique for combining moment methods with the geometrical theory of diffraction." U.R.S.I. Symposium on E.M. Wave Theory, IEE Conf. Pub. 114, 117-119.

9. Green, H.E., (1969), "Impedance of a monopole on the base of a large cone," IEEE Trans. Antennas Propagat., AP-17, 703-706.

10. Awadalla, K.H., (1978), "Wire antennas on finite ground planes: Application in mobile communications," Ph.D Dissertation, Dept. of Elect. Eng., University of Birmingham, England.

11. Awadalla, K.H. and Maclean, T.S.M., (1978), "Input impedance of a monopole antenna at the center of a finite ground plane," IEEE Trans. Antennas Propagat., AP-26, 244-248.

12. Awadalla, K.H. and Maclean, T.S.M., (1979), "Monopole antenna at center of circular ground plane: input impedance and radiation pattern," IEEE Trans. Antennas Propagat., AP-27, 151-153.

13. Griffin, D.W., (1982), "Monopole antenna method of diagnosing the effectiveness of ground plane edge scattering techniques," IEEE APS Symposium Digest, Antennas Propagat., vol.1, 223-225.

14. Liepa, V.V., Knott, E.G. and Senior, T.B.A., (1971), "Plates and edges," IEEE Trans. Antennas Propagat., AP-19, 788-789.

15. Liepa, V.V., Knott, E.G. and Senior, T.B.A., (1974), "Scattering from two-dimensional bodies with absorber sheets," Air Force Avionics Laboratory Technical Report. AFALTR-74-119., University of Michigan Radiation Laboratory Report No. 011764-2-T.

16. Senior, T.B.A. and Liepa, V.V., (July, 1984), "Backscattering from Tapered Resistive Strips," IEEE Trans. Antennas Propagat., AP-32, 747-751.

17. Naor, M., (1981), "Scattering by resistive plates," Ph.D dissertation, Dept. of Elect. and Comp. Eng., University of Michigan.

18. Harrington, R.F., (1968), "Field Computation by Moment Methods", Macmillan Company.

19. Harrington, R.F. and Mautz, J.R., (1975), "An impedance sheet approximation for thin dielectric shells," IEEE Trans. Antennas Propagat., AP-23, 531-534

20. Kantorovich, L. and Krylov, V., (1964), "Approximate Methods of higher analysis," C.D.Benster, trans. New York: Wiley, Ch.4.

21. Jones, D.S., (1956), "A critique of the variational method in scattering antennas," IRE Trans. on Antennas and Propagat., AP-4, 297-301.

22. Jones, D.S., (1974), "Numerical methods for antennas problems," IEEE 121, 573-582.

23. Andreasen, M.G., (1965), "Scattering from Bodies of Revolution," IEEE Trans. on Antennas and Propagat., AP-13, 303-310.

24. Mautz, J.R. and Harrington, R.F., (1969), "Radiation and Scattering from Bodies of Revolution," Appl. Sci. Res., vol. 20, 405-435.

25. Harrington, R.F. and Mautz, J.R., (1971), "Radiation and Scattering from Loaded Bodies of Revolution," Appl. Sci. Res., vol. 26, 209-217.

26. Harrington, R.F. and Mautz, J.R., (1972), "Green's Functions for Surfaces of Revolution," Radio Science, vol. 7, 603-611.

27. Mautz, J.R. and Harrington, R.F., (1979), "A Combined Solution for Radiation and Scattering from a Perfectly Conducting Body," IEEE Trans. Antennas Propagat., AP-27, 445-454.

28. Oshiro, F.K. and Mitzner, K.M. (1967), "Digital Computer Solution of Three-Dimensional Scattering Problems," IEEE International Symposium Digest, Ann Arbor, Michigan, 257-263.

29. Uslenghi, P.L.E., (1970), "Computation of Surface Currents on Bodies of Revolution," Alta Frequenza, vol. 39, no. 8, 1-12.

30. Glisson, A.W. and Wilton, D.R., (1980), "Simple and Efficient Numerical Methods for Problems of Electromagnetic Radiation and Scattering from Surfaces," IEEE Trans. Antennas Propagat., AP-28, 593-603.

31 Glisson, A.W. and Wilton, D.R., (1979), "Simple and Efficient Numerical Techniques for Revolution," Technical Report for RADC Contract No. F30602-78-C-0120, University of Mississippi.

32 Kimura Hiroshige, (1983), "Study of Electromagnetic Scattering by Half Sheet with Cylindrical Tip," Ph.D. Dissertation, Dept. of Elect. and Comp. Eng., University of Michigan.

33. Ramo, S., Whinnery, J.R. and Van Duzer, T., (1965), "Field and Waves in Communication Electronics," John Wiley & Sons.

34. Abramowitz, M., and Stegan, I.A., (1964), "Handbook of Mathematical Functions," National Bureau of Standards, Government Printing Office.

35. Stratton, J.A., (1941), "Electromagnetic Theory," McGraw-Hill Book Company.

36. Tai, C.T., (1971), "Dyadic Green's Function in Electromagnetic Theory," International Textbook Company.

37. Kraus, J.D. and Carver, K.R., (1973), "Electromagnetics," McGraw-Hill Book Company.

38. Stutzman, W.L. and Thiele, G.A., (1981), "Antenna Theory and Design," John Willy & Son.

39. Adam, S.F., (1969), "Microwave Theory and Applications," Prentice-Hall, Inc.

40. Application note 117-1, (1970), "Microwave Network Analyzer Applications," Hewlett-Packard Company.